Optimal Inspection and Maintenance Strategies for Structural Systems

Sommer, A. M.

Publication date:
1993

Document Version
Publisher's PDF, also known as Version of record

INSTITUTTET FOR BYGNINGSTEKNIK
DEPT. OF BUILDING TECHNOLOGY AND STRUCTURAL ENGINEERING
AALBORG UNIVERSITETSCENTER • AUC • AALBORG • DANMARK

STRUCTURAL RELIABILITY THEORY
PAPER NO. 103

Ph.D.-Thesis defended publicly at the University of Aalborg
December 14, 1992

A. M. SOMMER

OPTIMAL INSPECTION AND MAINTENANCE STRATEGIES FOR STRUCTURAL SYSTEMS

MARCH 1993

ISSN 0902-7513 R9309

The STRUCTURAL RELIABILITY THEORY papers are issued for early dissemination of research results from the Structural Reliability Group at the Department of Building Technology and Structural Engineering, University of Aalborg. These papers are generally submitted to scientific meetings, conferences or journals and should therefore not be widely distributed. Whenever possible reference should be given to the final publications (proceedings, journals, etc.) and not to the Structural Reliability Theory papers.

INSTITUTTET FOR BYGNINGSTEKNIK
DEPT. OF BUILDING TECHNOLOGY AND STRUCTURAL ENGINEERING
AALBORG UNIVERSITETSCENTER • AUC • AALBORG • DANMARK

STRUCTURAL RELIABILITY THEORY
PAPER NO. 103

Ph.D.-Thesis defended publicly at the University of Aalborg
December 14, 1992

A. M. SOMMER
OPTIMAL INSPECTION AND MAINTENANCE STRATEGIES FOR STRUCTURAL SYSTEMS
MARCH 1993 ISSN 0902-7513 R9309

ACKNOWLEDGEMENTS

The present thesis has been prepared at the Department of Building Technology and Structural Engineering, University of Aalborg, in the period from January 1989 to December 1992. The work has been a part of the research program "Marine Structures" financed by the Danish Technical Research Council.

I gratefully acknowledge my supervisor Professor Palle Thoft-Christensen for guidance during my study. I would also like to thank colleagues at the Department of Building Technology and Structural Engineering for much good advice and valuable discussions.

A stay at the University of Michigan from May to July, 1990, was sponsored by the Danish Research Academy. Special thanks to Professor Andrzej S. Nowak for his helpfulness and a fruitful collaboration in connection to chapter 4.

During the work with chapter 5 colleagues at the Department of Ocean Engineering, Technical University of Denmark, have been of valuable help for which I am very grateful.

Skilful proofreading of the manuscript has been done by Senior Secretary Kirsten Aakjær and careful preparation of most figures has been carried out by Draughtsman Norma Hornung. Their work is greatly appreciated.

Aalborg, November 1992 Anne Mette Sommer

RESUMÉ (IN DANISH)

Afhandlingens emne er optimale inspektions- og vedligeholdelsesstrategier for konstruktionssystemer. Formålet er at give en samlet oversigt over konventionelle og pålidelighedsbaserede strategier samt at vise deres anvendelse på udvalgte konstruktionstyper. Endvidere at modificere eksisterende computerprogrammer, så de udvalgte eksempler kan testes. I kapitel 1 beskrives formålet med inspektion og vedligeholdelse, og der redegøres for de vigtigste svigtårsager for forskellige typer stålkonstruktioner. Derudover er der et engelsk resumé.

I kapitel 2 er konventionelle inspektions- og vedligeholdelsesstrategier beskrevet kort for tre typer stålkonstruktioner - offshore konstruktioner, skibe og broer.

Et relativt nyt forskningsområde er optimale, pålidelighedsbaserede inspektions- og vedligeholdelsesstrategier. Det nuværende stade indenfor området er beskrevet i kapitel 3, hvor de refererede modeller er delt op i tre grupper karakteriseret ved svigtmodellen.

I kapitel 4 er en typisk ståldragerbro behandlet. Dragerne antages udsat for korrosion, og tre svigtmåder for de enkelte dragere betragtes, idet det modellerede tværsnit formindskes med tiden p.g.a. korrosionen. I kapitlet er der endvidere kort beskrevet fremgangsmåden ved bestemmelse af en optimal inspektionsstrategi m.h.t. omkostninger. For et seriesystem indeholdende de tre svigtmåder er der opstillet udtryk til beregning af svigtsandsynligheden som funktion af tiden samt reparationssandsynligheden ved hver inspektion. I et eksempel belastes en given bro med lastbiltrafik, som er målt i Michigan, og pålidelighedsindekset som funktion af tiden beregnes for hver drager. Der foreslås en inspektionsstrategi (ikke optimal) med konstante inspektionsintervaller.

I kapitel 5 betragtes et tankskib, hvis skrogtværsnit antages udsat for korrosion indvendigt. Longitudinalerne (langsgående, afstivende bjælker, svejst på skibsskroget) i skibssiden antages at kunne svigte på to måder - ved udvikling af udmattelsesrevner og ved flydning. Tankskibet i eksemplet udsættes for langtidsbølgelaster svarende til sejlruten fra Rotterdam til Den Persiske golf. Pålidelighedsindekset som funktion af tiden er beregnet for de to svigtmåder for longitudinalerne op langs skibssiden og for tre af disse longitudinaler udformes optimale inspektionsstrategier afhængigt af de enkelte longitudinalers svigtsandsynlighed - hver strategi anvendes på en undergruppe af longitudinalerne. Beregningerne udføres v.hj.a. en revideret version af programmet PRODIM.

Kapitel 6 præsenterer de programmer, der er brugt til beregningerne i kapitel 4 og 5. PROBAN-2 og PARLSENSI er pålidelighedsprogrammer, og PRODIM2 er et program til bestemmelse af optimale inspektionsstrategier. I PARLSENSI og PRODIM2 er der lavet omfattende ændringer, som er beskrevet kort.

Kapitel 7 indeholder konklusionen på afhandlingen.

Appendiks 1 supplerer kapitel 2, idet der beskrives de ikke-destruktive inspektionsteknikker, der er til rådighed ved inspektion af stålemner for revner og korrosion. Der er endvidere kort beskrevet forskellige reparationsteknikker.

I appendiks 2 er der givet en kort introduktion til pålidelighedsteori.

I appendiks 3 er inputtet til PRODIM2 beskrevet og et eksempel er givet.

I appendiks 4 er der gengivet det program, som er brugt i kapitel 4 til beregning af trafiklaster.

Det "originale" arbejde i afhandlingen ligger især i beregningerne udført i kapitel 4 og 5, idet der så vidt vides ikke før er lavet tilsvarende analyser af de ovennævnte konstruktionstyper. Den beskrevne procedure, der går ud på at spare inspektionsomkostninger ved at inspicere de forskellige komponenter i en konstruktion med forskellige intervaller, er også ny. Tidsmæssigt har ikke mindst programmeringsarbejdet beskrevet i kapitel 6 krævet sin del. Derudover kan det nævnes, at i forbindelse med beregningerne i kapitel 4 er der udfærdiget et program til beregning af trafiklasten i de enkelte dragere (se appendiks 4), og i kapitel 5 er der foretaget en ret grundig undersøgelse af objektfunktionen.

LIST OF CONTENTS

CHAPTER 1
INTRODUCTION

The aim of this thesis is to give an overview of conventional and optimal reliability-based inspection and maintenance strategies and to examine for specific structures how the cost can be reduced and/or the safety can be improved by using optimal reliability-based inspection strategies. For structures with several almost similar components it is suggested that individual inspection strategies should be determined for each component or a group of components based on the reliability of the actual component. The benefit of this procedure is assessed in connection with the structures considered. Furthermore, in relation to the calculations performed the intention is to modify an existing program for determination of optimal inspection strategies.

The main purpose of inspection and maintenance of structural systems is to prevent or delay damage or deterioration to protect people, environment, and investments made in the structure. The inspection and maintenance should be performed so that the structural system is operating as much of the time as possible and the cost is kept at a minimum and so that the safety of the structure is satisfactory.

Up till now inspection strategies have been based on experience and judgement with a few exceptions within the areas of aircraft structures and offshore structures. For some aircraft structures in the U.S. Airforce, inspections are planned when the average crack is expected to exceed a given level according to Yang, 1980, and in Pedersen et al., 1992, it is described how a reliability-based inspection strategy is used for offshore structures at the Tyra Field. However, methods are being developed to determine strategies that are optimal with regard to the expected costs and that also fulfil requirements for the reliability of the system, i.e. optimal reliability-based inspection strategies. Such strategies make it possible to include the uncertainty in loads and material parameters.

In figure 1.1 the procedure is illustrated for a simple example with constant inspection intervals and two contributions to the total costs, namely inspection cost and failure cost. Two cases are indicated by arrows. In one case the costs are minimized without any restrictions on the failure rate giving an inspection interval of 2.4 and in the other case the failure rate is restricted to be less than 0.15 giving an optimal inspection interval of 1.3.

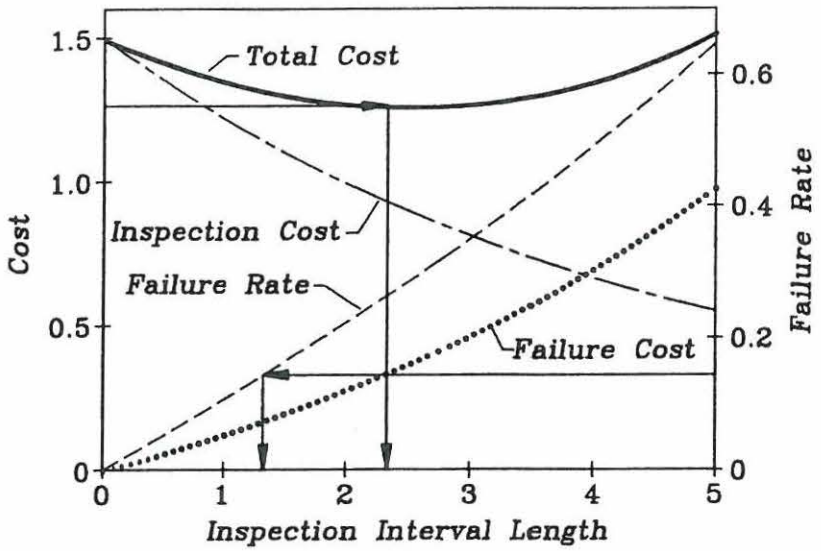

Figure 1.1 Determination of optimal constant inspection intervals (Wunderlich, 1991).

Calculation of the failure probability for a structure implies that the failure modes can be modelled in one way or another. This rises a problem because some types of failure are very difficult if not impossible to model, for instance accidents and human errors. According to Madsen et al., 1986, the most frequent reason for structural failure is human error. In Tebbett, 1987, fatigue is stated to be the cause of damage in 36% of the repair cases for offshore structures in 1982 - 1986 while the remaining causes of damage can more or less be considered as accidents or human errors. In Wunderlich, 1991, the causes of damage are split up into three contributions, see figure 1.2. The first contribution is design and construction defects and operation errors, in other words mainly human errors. These errors are normally reduced to a minimum by repair and experience after a period. The second contribution is major random external events, such as earthquakes or floods, for which the failure rate is relatively low and constant. The third contribution comes from wear failure, such as fatigue and corrosion, showing a failure rate that is increasing with time.

To the knowledge of the author, the methods that are being developed to determine optimal reliability-based inspection strategies for structural systems only include failure modes like fatigue and corrosion. In some models (see chapter 3) the failure mode is not even specified.

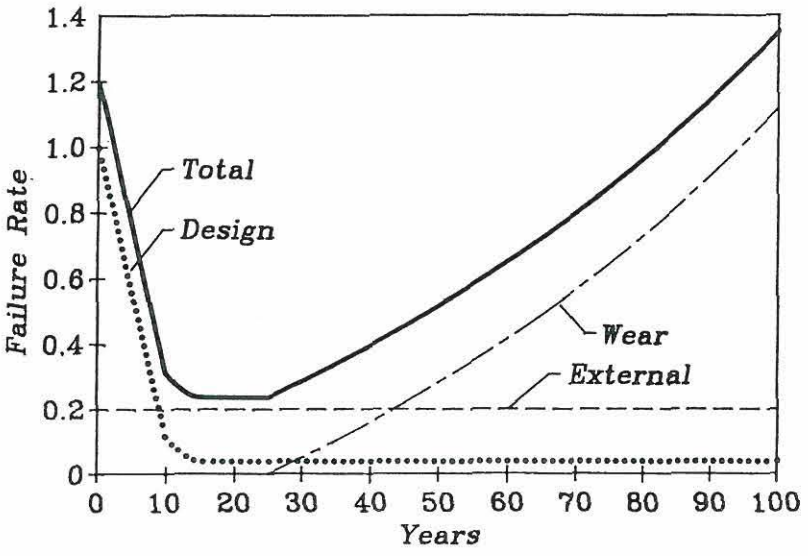

Figure 1.2 Example of failure rates (Wunderlich, 1991).

In this thesis structural systems made of steel are considered, exemplified by offshore structures, ships and bridges which represent typical as well as diverse applications of steel as a structural material. In Tebbett, 1987, several cases of repair of offshore steel structures are listed where the cause of damage is given. 61 cases of repair from the North Sea are reported up to 1981 and 39 cases from all over the world are reported from 1982 - 86, see table 1.1. An essential change after 1981 is that the number of collisions and dropped objects is considerably reduced. According to Tebbett, 1987, this suggests a significant improvement in operational practice.

Cause of damage	Number of cases	
	Up to 1981	1982 - 86
Fatigue	17 (28%)	14 (36%)
Collision	17 (28%)	5 (13%)
Dropped objects	9 (15%)	0
Design upgrading	7 (11%)	9 (23%)
Installation damage	4 (6%)	1 (2%)
Welding fault	1 (2%)	2 (5%)
Concrete construction	1 (2%)	0
Other	5 (8%)	8 (21%)
TOTAL	61	39

Table 1.1 Causes of damages (Tebbett, 1987).

According to Ferguson, 1991, fatigue cracking and corrosion are aspects of major concern with regard to inspection and maintenance of tankers. In Det Norske Veritas, 1991, it is reported that corrosion and fatigue cracking cause severe problems for bulk carriers and that corrosion developes mainly because of breakdown of the coating system or no coating system, lack of maintenance, corrosive cargo and unsatisfactory cleaning procedures and inspection routines. It is also reported that 40 - 60 % of the damages of large steel ships are fatigue cracks and that 20 - 30 % are buckling/indents. Also for steel bridges fatigue cracks and corrosion have to be inspected for.

In accordance with the above the main purpose of in-service inspection of structural components made of steel is to detect cracks, corrosion and damage caused by accidents but the latter is difficult to model. Consequently, in the examples considered in this thesis steel structures are assumed to be exposed to the development of fatigue cracks and/or corrosion.

1.1 Summary

In this section the content of the thesis is summarized. In chapter 2 conventional strategies for inspection and maintenance are described briefly for three types of steel structures - offshore structures, ships and bridges.

A relatively new research area is optimal reliability-based strategies for inspection and maintenance. The recent stage within the area is described in chapter 3, where the models refered to are divided into three groups characterized by the failure model.

In chapter 4 a typical steel girder bridge is treated. The girders are assumed to be exposed to corrosion and three failure modes are considered for each girder decreasing the modelled cross-section with time due to corrosion. Furthermore, the procedure for determining an optimal inspection strategy with regard to costs is described. For a series system including the three failure modes expressions are shown for calculation of the failure probability as a function of time and the repair probability at each inspection. In an example a bridge is loaded with truck traffic measured in Michigan and the reliability index as a function of time is calculated for each girder. An inspection strategy (not optimal) with constant inspection intervals is suggested.

In chapter 5 a tanker is considered assuming that the hull section is exposed to corrosion at internal surfaces. The longitudinals (longitudinal, stiffening beams welded on the ship hull) at the ship side are assumed to have two failure modes - the development of fatigue craks and yielding. The tanker in the example is exposed to long-term wave loads corresponding to the shipping route from Rotterdam to the Persian Gulf. The reliability index as a function of time is calculated for the two failure modes for the longitudinals up the ship side and finally, for three of these longitudinals optimal inspection strategies are determined depending on the failure probability of the longitudinals - each strategy applies to a group of the longitudinals. The calculations are made using a revised version of the program PRODIM.

Chapter 6 introduces the programs used for the calculations in chapters 4 and 5.

PROBAN-2 and PARLSENSI are reliability programs and PRODIM2 is a program for calculation of optimal inspection strategies. In PARLSENSI and PRODIM2 considerable changes have been made, which are described briefly.

Chapter 7 contains the conclusion of the thesis.

Appendix 1 supplements chapter 2 describing the non-destructive inspection techniques available for inspection of steel objects for cracks and corrosion. Furthermore, some repair techniques are listed.

In appendix 2 a short introduction to reliability theory is given.

In appendix 3 the input to PRODIM2 is described and an example is given.

In appendix 4 the program used in chapter 4 for calculation for traffic loads is shown.

The "original" work in this thesis is first and foremost the calculations performed in chapters 4 and 5. To the knowledge of the author corresponding analyses of the types of structures mentioned above have not been performed previously. The procedure whose aim is to save inspection costs by inspecting different components in a structure with different intervals is new too. Not least, the work with the programs described in chapter 6 has been time-consuming. Furthermore, it can be mentioned that in connection to the calculations in chapter 4 a program has been implemented for calculation of the traffic load in each girder (see appendix 4) and in chapter 5 a thorough examination of the objective function has been performed.

1.2 References

Det Norske Veritas (1991), *Rule Amendments*, by DSO-230, Paper Series No. 91-P013, Høvik, Norway.

Ferguson, J.M.; A.G. Gavin (1991), *Aspects of Oil Tanker Structural Inspection, Maintenance and Monitoring*, Lloyd's Register of Shipping.

Madsen, H.O.; S. Krenk; N.C. Lind (1986), *Methods of Structural Safety*, Prentice-Hall.

Pedersen, Carl; John A. Nielsen; Jens P. Riber; Henrik O. Madsen; Steen Krenk (1992), *Reliability-Based Inspection Planning for the Tyra Field*, Proceedings of OMAE 1992, Calgary, Canada, ASME, Vol. II, pp. 255-263.

Tebbett, I.E. (1987), *The Last Five Years Experience in Steel Platform Repairs*, Annual Offshore Technology Conference, Texas, OTC 5385.

Wunderlich, Walter O. (1991), *Probabilistic Methods for Maintenance*, Journal of Engineering Mechanics, Vol. 117, No. 9, ASCE.

Yang, J.N. (1980), *Statistical Estimation of Economic Life for Aircraft Structures*, Journal of Aircraft, Vol. 17, pp. 528-535.

CHAPTER 2
CONVENTIONAL STRATEGIES FOR INSPECTION AND MAINTENANCE

2.1 Introduction

Conventional strategies are based on experience rather than analytical procedures. The national authorities make regulations and rules, which have to be fulfilled when the owners of structures work out programmes for inspection and maintenance. These programmes are in general more detailed and have stricter requirements than the rules. In this chapter some of these conventional strategies for offshore structures, steel ships and bridges are described. A similar presentation is available in Sommer and Thoft-Christensen, 1990.

Several techniques are available for inspection of steel structures for e.g. cracks and corrosion which are the most important subjects for in-service inspection. An overview is given in appendix 1.

According to Offshore vedligeholdelse, 1984, there are four main types of maintenance:

1. Planned, preventive maintenance. The maintenance is performed periodically based on operating time or real time. It consists of adjustment and lubrication.
2. Planned, conditional maintenance. The maintenance is performed based on inspections or monitoring and it consists of adjustment, repair and modifying.
3. Planned, corrective maintenance. The maintenance is performed after failure, operational problems or insufficient security and it consists of adjustment, repair and modifying.
4. Unplanned, emergency maintenance. This category covers the case of unforeseen break-down or a break-down threatening the structure or operating system. Again the maintenance consists of adjustment, repair and modifying.

Corrective maintenance should only be performed for less critical components and emergency maintenance should of course be avoided. Normally the preventive or conditional maintenance is preferable according to economy and security.

2.2 Offshore Structures

In this text requirements for testing and examination of machinery and other equipment are not rendered. The classification companies Det Norske Veritas and Lloyd's Register of Shipping have made rules to set up the inspection programmes.

Det Norske Veritas

The rules apply to steel or reinforced concrete offshore structures designed to remain permanently fixed to the sea bed. In Det Norske Veritas, 1981, section 11, the requirements for periodical and special surveys are listed. A periodical survey includes:

- General visual inspection of selected parts of the structure to determine the general condition of the structure and to locate areas that should be subjected to close inspection and testing.
- Close visual inspection and non-destructive testing of selected local areas of the structure to detect possible material deterioration or incipient cracking.

The periodical inspections must be planned so that the complete structure is inspected within a period of 5 years whereas special surveys are carried out in the event of an accident or any other change in the condition or operation of the structure that may affect its safety. The requirements are visualized in figure 2.1.

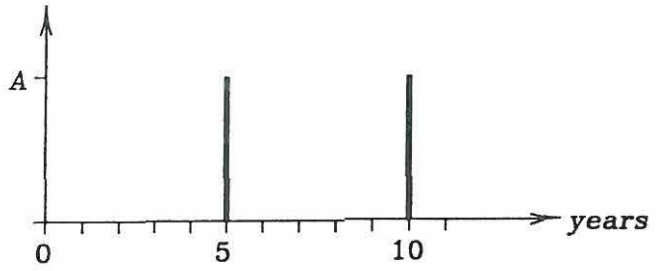

A: Visual inspection and some non-destructive testing.

Figure 2.1 Permanent offshore structures.

According to Det Norske Veritas, 1980, an inspection can be considered as one of three types. Type 1 is general visual inspection without prior cleaning, type 2 is close visual inspection with prior cleaning and type 3 is close visual inspection and non-destructive or destructive testing with prior cleaning.

Det Norske Veritas requires ND-testing of selected areas but contrary to this Dunn, 1984, states for permanent offshore structures that ND-testing is unnecessary in regular inspections as the cracks that require a repair are so big that they can be detected visually or by photos.

In section 3.5 it is described shortly how reliability-based inspection strategies have

been used for components of jacket-structures during the last couple of years. This procedure will most likely become more and more widespread as it reduces the number of inspections to be performed.

Lloyd's Register of Shipping

In Lloyd's (Mobile Offshore Units), 1984, part 1, chapter 2 it is listed which types of mobile offshore units the rules are made for:

- Ship units. Self propelled surface type units.
- Barge units. Surface type units without primary propelling machinery designed to operate in the floating condition.
- Self-elevating units. Units with sufficient buoyancy to transport drilling equipment, supplies, etc. to a desired location. The hull then lifts itself on legs to the required level above the sea surface.
- Semi-submersibles. Working platforms supported on widely spaced buoyant columns. These units are normally floating types but can be designed to rest on the sea bed.
- Support vessels. Units whose primary function is to support offshore installations and carry out maintenance, fire fighting or diving operations.

Ship and barge units also have to comply with Lloyd's (Ships), 1984.

In Lloyd's (Mobile Offshore Units), 1984, part 1, chapter 3 the Survey Regulations for mobile offshore units are stated. There are three categories of periodical surveys.

1. Annual Surveys. The general condition of the unit is examined by visual inspection. Normally it can be carried out on location or during a move. But for semi-submersibles a detailed dry examination of all bracings is required including ND-testing (Non-Destructive testing) of critical welds.
2. Docking or In-Water Surveys every 2 years. If it is possible the unit should be examined in drydock but in case docking is impractical In-Water Surveys may be accepted. The inspection includes the examinations at the Annual Survey. In addition ND-testing of important connections is performed. An In-Water Survey is to provide the same information as a Docking Survey if practicable.
3. Special Surveys every 4 years. Besides the requirements of Annual and Docking Surveys, Special Surveys include a more thorough examination of all parts of the structure. That means the structure must be made accessible by removing ceiling, lining, paint and other coverings locally.

Alternatively to Special Surveys an inspection programme based on Continuous Survey can be allowed. All parts of the unit must be inspected and tested with a maximum interval of 5 years and the Continuous Survey is to take account of inspections required at Annual and Docking Surveys.

2.3 Steel Ships

According to SSC-332, 1990, ship structures are based on a combination of "safe-life" and "fail-safe" designs. A "safe-life" design implies that the structure will not fail in its lifetime and a "fail-safe" design implies that the structure should be inspected periodically in its lifetime and that parts of the structure which develop flaws should be repaired or renewed. The design of a ship structure should be made on the following inspection related considerations; inspectability of structural elements, provision of redundant structures, identification of critically stressed parts of structures and finally, determination of standard tolerances and acceptable levels for structural deviations.

An In-Service Inspection Program should include:

- Identification of critically stressed areas.
- Significant areas due to material and/or fabrication errors during construction.
- Inspection frequencies.
- Methods and procedures for inspection.
- Tools and equipment to be used.
- Responsibilities for performance.

The classification companies Det Norske Veritas and Lloyd's Register of Shipping have made several demands on the inspection of steel ships. The requirements that have been followed until recently are described shortly below. The demands are intensified regularly and the new Unified Requirements developed by the International Association of Classification Societies (IACS) are also described. The emphasis is put on survey of the hull structure.

Det Norske Veritas

In Det Norske Veritas, 1983, part 1, chapter 2 the Periodical Survey Regulations for steel ships are stated.

1. Annual surveys. These are visual inspections to ascertain the general condition of the vessel. The surveys cover the hull above water, anchoring and mooring equipment and watertight bulkheads.
2. Intermediate surveys. The survey interval is max 2.5 years and the surveys are less comprehensive than special surveys. They are e.g. applied to oil tankers when these are older than 10 years.
3. Special periodical surveys. These are performed every 3 or 4 years (4 years for tankers). The hull and machinery are inspected. Among other things the thickness of selected plates are measured. The cargo tanks are tested from at least one side by filling the tanks with water. The requirements get stricter after 5 and 10 years.

An alternative to special periodical surveys are continuous surveys requiring that all items are surveyed with intervals not exceeding 4 or 5 years.

Lloyd's Register of Shipping

In Lloyd's (Ships), 1984, part 1 the Survey Regulations for ships are stated. The Rules apply to mercantile shipping, hovercraft, non-mercantile shipping, yachts and small craft.

1. Annual surveys. The vessel is inspected visually. For example bulkheads, all doors and openings and the anchoring and mooring equipment are examined.
2. Docking surveys. The inspection interval is 2 or 3 years. In the drydock the shell and the rudder are examined. Special attention is given to areas liable to corrosion. Every second docking survey may be replaced by an in-water survey.
3. Special surveys. These surveys take place every 4 years. Where necessary, ceiling and lining are removed for examination of the structure. Steel should be cleaned and rust removed. The requirements get stricter after 5, 10, 15 and 20 years. Cargo tank bulkheads are tested by filling alternate tanks with water. Plate thicknesses are measured.

The survey of the hull may be carried out continuously and then each part of the hull should be examined every 5 years. In figure 2.2 the requirements for the inspection of mobile offshore units and ships are visualized as they are quite similar for those of Det Norske Veritas and Lloyds.

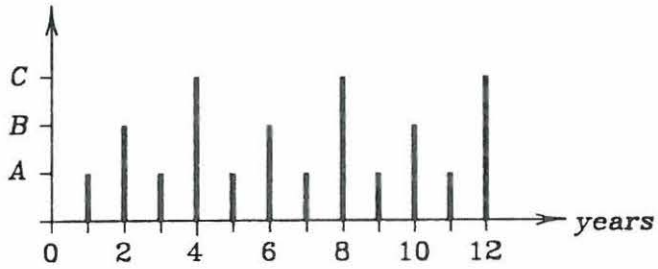

A: Annual Survey (general visual inspection).
B: Docking Survey.
C: Special Docking Survey.

Figure 2.2 Steel ships.

Enhanced Survey Programme

The fact that a number of large steel ships such as oil tankers has been involved in accidents causing loss of life and environmental pollution combined with the increasing age of the world fleet has lead to a demand for stricter requirements to the inspection of these ships. The International Association of Classification Societies (IACS) has developed unified requirements for oil tankers and bulk carriers, respectively. According to Classification News, 1993, the intention is to implement these requirements during 1993 and 1994.

There are still three types of survey but the requirements to the surveys are stricter as for instance the extent of thickness measurement of structural members is specified in detail. The alternative strategy consisting in continuous surveys will no longer be allowed. A new alternative is offered as it is recommended to base the special survey programme on analyses of the risk of structural deterioration. As mentioned before this procedure has proven to reduce the inspection cost for jacket structures. However, in this case a risk analysis does not necessarily mean reliability calculations for fatigue crack development.

In short the inspection requirements are the following.

1. Annual surveys take place every year ensuring that the hull and piping are maintained in a satisfactory condition. Examinations of ballast tanks in oil tankers or cargo holds in bulk carriers may be required depending on the age and the history of the ship.
2. The 2nd and 3rd annual survey is an intermediate survey and depending on the age of the ship it e.g. includes a close examination (including thickness measurements) of selected tanks in oil tankers and selected cargo holds in bulk carriers.
3. Special surveys take place every 5 years when the Class Certificate is renewed or confirmed. The examinations shall discover substantial corrosion, significant deformation, fractures, damages or other structural deterioration and the survey includes a dry dock examination.

In Enhanced Survey..., 1992, the guidelines for oil tankers are described in detail.

2.4 Bridges

In most countries there are guidelines for the inspection of bridges. Some of them are briefly described in this section.

There are about 575,000 bridges in the United States, of which 38% is made of steel (Kayser, 1988). AASHTO, 1983, recommends that bridges be inspected every two years and that painted and weathering steel structures are examined for corrosion and fatigue cracks. Also inspected is the condition of joints, deck, abutments and substructure and for weathering steel, the condition of the oxide film is checked as well. Normally, the inspections are visual.

In Ontario, Canada, the Ontario Highway Bridge Design Code, 1983, requires the routine inspections to be performed at intervals determined by the owner of the structure. They have to be carried out to the satisfaction of the engineer responsible for the bridge. In the Code Commentary it is stated that the policy of the Ontario Ministry of Transportation requires routine inspection every two years.

In Denmark there are about 12,000 bridges (Vejbroer, 1980). More than 90% is concrete structures and only 2-3 % is steel or composite bridges. Bridges are supervised by local road authorities while detailed visual inspections are carried out by trained inspectors. The inspection intervals are decided individually after each inspection

based on the state of the structure, age, load, environment, structural design, foundation conditions, etc. The intervals vary from 1 to 6 years and for instance, a bridge with heavy traffic would typically be inspected every three years.

According to Nowak and Absi, 1987, France has about 59,000 bridges with a span of more than 5 m. Only 5% is steel bridges. A Technical Guideline for the Inspection and Maintenance of Bridges, 1979, requires a permanent supervision by local agents, a systematic but superficial inspection every year of bridges more than 10 m long and a detailed inspection every five years of bridges more than 120 m long.

In Belgium there are about 5400 bridges with a span of at least 5 m (Nowak and Absi, 1987). About 900 of these are steel or steel-concrete bridges. Guidelines published by the Bridge Department of the Ministry of Public Works, 1978, consider three levels of inspection. Routine inspections are scheduled every year, general inspections every three years and a specialized control when a general inspection reveals the need for it. The inspections are visual and the results are shown on photos, drawings and in a report.

In Germany, the inspection of bridges is governed by the German Code DIN 1076; Engineering Structures in Connection with Roads (Nowak and Absi, 1987). The code specifies a visual inspection four times a year, a general inspection every three years, a main inspection every six years and a special survey in case of an accident or natural disaster.

A methodology for bridge monitoring suggesting three types of inspection has been proposed in Switzerland in 1987 on the initiative of the Swiss Federal Department of Transport (Nowak and Absi, 1987). Routine inspections are scheduled every 15 months, periodic inspections every five years and special inspections according to needs. Routine inspections should reveal all significant troubles and investigate the evolution of those detected earlier and periodic inspections should reveal apparent deterioration, structural cracking pattern, state of materials, deformations, state of the structure and state of the equipment.

In Italy the bridge inspection is regulated by the Ministry for Public Works Circular No. 6736/61, 1967 (Nowak and Absi, 1987). Regular inspections are carried out every three months and once a year a general and complete inspection is performed.

The review indicates that the number of inspection levels varies from one country to another. Only one type of periodic inspection is performed in Denmark, the United States and Canada, two types in France, Belgium, Switzerland and Italy and three types in Germany.

2.5 References

AASHTO (1983), *Manual for Maintenance Inspection of Bridges,* American Association of State Highway and Transportation Officials, Washington, D.C.

Classification News (1993), Published by Det Norske Veritas Classification AS, No. 1/93.

Det Norske Veritas (1983), *Rules for the Classification of Steel Ships*, Høvik, Norway.

Det Norske Veritas (1981), *Rules for the Design, Construction and Inspection of Offshore Structures*, Høvik, Norway.

Det Norske Veritas (1980), *Rules for the Design, Construction and Inspection of Offshore Structures, Appendix I, In Service Inspection*, Høvik, Norway.

Dunn, F.P. (1984), *Offshore Platform Inspection*, Proc. Int. Symp. Nov. 1983, Washington, *The Role of Design, Inspection and Redundancy in Marine Structural Reliability*, (Faulkner et al. (eds.)), pp. 199-219.

Enhanced Survey Programme for Oil Tankers, Proposed for IMO Guidelines (1992), Marine Environment Protection Committee - 33rd Session, Submitted by The International Association of Classification Societies (IACS).

Kayser, J.R. (1988), *The Effects of Corrosion on the Reliability of Steel Girder Bridges,* Ph.D. Thesis, Department of Civil Engineering, University of Michigan.

Nowak, A.S.; Absi, E. (1987), editors, *Bridge Evaluation, Repair and Rehabilitation,* Proceedings of the 1st US-European Workshop, the University of Michigan, Ann Arbor, Michigan, USA.

Lloyd's Register of Shipping, (1984) *Rules and Regulations for the Classification of Mobile Offshore Units*, London.

Lloyd's Register of Shipping, (1984) *Rules and Regulations for the Classification of Ships*, London.

Offshore vedligeholdelse (1984), Petroconsult ApS, Formidlingsrådet, Danmark.

Ontario Highway Bridge Design Code (1983), Ministry of Transportation and Communications, Ontario.

Sommer, A.M.; P.Thoft-Christensen (1990), *Inspection and Maintenance of Marine Steel Structures - State-of-the-Art*, Structural Reliability Theory, Paper no. 74, The University of Aalborg, Denmark.

SSC-332 (1990), *Guide for Ship Structural Inspections*, Ship Structure Committee, U.S. Coast Guard, Washington D.C.

Vejbroer, Vejregler for eftersyn af bygværker (1980), 8.20.2 Broteknik, Vejdirektoratet, Denmark.

CHAPTER 3
OPTIMAL RELIABILITY-BASED STRATEGIES FOR INSPECTION AND MAINTENANCE

3.1 Introduction

Optimal strategies for inspection and maintenance have been studied for about 30 years within many areas, e.g. fatigue cracks in offshore structures or aerospace structures and testing of electrical components. In Sherif and Smith, 1981, 524 references on the subject up to 1981 are summarized and in Sommer and Thoft-Christensen, 1990, the development up to 1990 is described shortly.

Models for inspection and maintenance are either deterministic or stochastic but in this thesis only stochastic models are treated. In Sherif and Smith, 1981, stochastic models are divided into two groups. In one group the time to failure is a random variable with known distribution and in the other group the distribution of the time to failure is not known.

The models developed so far describe systems that in some cases are not specified in detail and in other cases consist of a single element or a parallel system or a series system of elements. The optimization problem is usually formulated as a minimization of the expected total costs of the system where "total costs" may just include the costs that are assumed relevant with regard to the optimal inspection strategy, e.g. inspection costs. The optimization variables are usually the inspection times and for some models additional parameters (e.g. inspection qualities) and constraints are usually formulated in these optimization variables and/or in the reliability of the system.

In general an inspection strategy can be illustrated as in figure 3.1 showing the inspection times and the corresponding inspection qualities for the structural system under consideration.

In the following a summary of some recent models is presented stating the characteristic features of the models to make a comparison possible. The models are divided into three groups characterized by different failure models. In group 1 the failure mode is not specified and the system can only be in two states - the failure state or the non-failure state. In group 2 the state of the system is described by a Markov model and in group 3 a deterioration law is used describing the state of the system as continuously developing from the initial state to the failure state as the development of either fatigue cracks or corrosion is considered. Fatigue crack growth is described

by the Paris and Erdogan equation which is explained in e.g. Madsen et al., 1986, see also section 5.3.

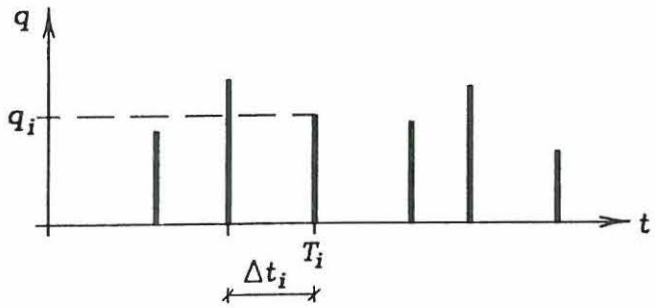

T_i - ith inspection time.
$\Delta t_i = T_i - T_{i-1}$.
q_i - inspection quality at T_i.

Figure 3.1 Inspection strategy.

3.2 Deterioration Modelled by Two States

In these models the failure mode is not specified but, except for model 1.1, the distribution of the time to failure is assumed to be known. This means that the models give a very simplified picture of the systems under consideration and they can hardly be used for realistic purposes.

Most models of this type are applied to electronical systems, see e.g. Keller, 1974, Kaio and Osaki, 1984 and 1986, Nakagawa and Yasui, 1980 and 1987, Aven, 1987, or Rodrigues Dias, 1990, but the models described below are applied to structural systems.

3.2.1 Model 1.1

This model is described in Yang and Trapp, 1975, and it deviate from the remaining models of this category as it is not the distribution of the time to failure that is known but the probability of failure during the lifetime as a function of the number of inspections. A similar model is described in Yang, 1977, but in stead of inspections, proof tests are considered.

System
The model is applied to aircraft structures and the system is assumed to consist of a fleet of airplanes.

Inspection Method
The inspection results are assumed to be correct.

Inspection Strategy
The strategy is characterized by constant inspection intervals.

Inspection Results
Detected fatigue cracks are repaired during the inspection.

Failure Probability
The probability of failure $P_F(N)$ of one airplane during its lifetime as a function of the number of inspections is known.

Optimization Problem
The objective function is the total costs of the fleet of airplanes including inspection cost and failure cost as the repair cost is assumed to be included in the inspection cost. The optimization variable is the number of inspections. A constraint is put on the failure probability $P_F(N)$ for each airplane.

Examples
A numerical example is given showing the non-dimensional relative cost (i.e. the number of airplanes is not given) as a function of the number of inspections for different ratios of the inspection cost to the failure cost.

3.2.2 Model 1.2

This model is described in Tang and Yen, 1991, and contrary to the other models the objective function is the availability of the system. The model is applied to a dam and by failure is meant that the dam is operating on unsatisfactory conditions. The failure time is a random variable and if an ageing dam is considered it is possible to let the distribution of the failure time depend on the age of the dam.

System
A system consisting of one element, i.e. a dam, is considered.

Inspection Method
The inspection method is characterized by the detectability estimated from experience.

Inspection Strategy
The strategy is characterized by constant inspection intervals.

Inspection Results
If failure is discovered the dam is repaired. The duration of repair is included in the model. The events that failure has taken place but is not detected, or that repair is not appropriate, is included and the probability of correct repair, if failure is detected, is given.

Failure Probability
The probability of failure during an inspection interval as a function of the inspection interval is known.

Optimization Problem
The objective function is the availability of the system. In Barlow and Proschan, 1975, the availability $A(t)$ of a system is defined as the probability that the system is operating at the time t. The state of the system $X(t) = 1$ if it is operating and

the state of the system $X(t) = 0$ if it is not operating.

$$A(t) = P[X(t) = 1] \tag{3.1}$$

If repair is not permitted, $A(t)$ reduces to the system reliability, i.e. the probability that the system does not fail during $[0, t]$. The optimization variable is the inspection interval and no constraints are given.

Examples
Numerical examples are given for an ageing and a non-ageing dam.

3.3 Deterioration Modelled by a Discrete Markov Process

In these models the system can be in N working states and one failure state. The lifetime of the system is divided into n duty cycles, defining a duty cycle as a repetitive period of operation in which damage can accumulate, Bogdanoff, 1978. The damage is described by the states $x_0, x_1, ..., x_N, x_{N+1}$ where x_{N+1} is the failure state. For each duty cycle the transition probabilities for going from one state to a later state is given. Furthermore, by modelling the damage accumulation process as a discrete Markov process $X(t)$, it is assumed that the conditional probability of $X(t_i) = x_j$ given $X(t_{i-1}) = x_k, ..., X(t_1) = x_l$ where $x_l \leq ... \leq x_k \leq x_j$ depends only on the latest time t_{i-1}, i.e.

$$f(X(t_i) = x_j \mid X(t_{i-1}) = x_k, ..., X(t_1) = x_l) = f(X(t_i) = x_j \mid X(t_{i-1}) = x_k) \tag{3.2}$$

where $f(X(t_i) = x_j \mid X(t_{i-1}) = x_k) = p(x_j \mid x_k)$ is called the transition probability. Markov processes are described in further detail in Madsen et al., 1986.

In models 2.1 and 2.3 described below the process under consideration is fatigue crack growth. In that case however, the assumption about the state of the system only depending on the latest of the previous states is not fulfilled. This is illustrated in figure 3.2 where the state is indicated by the crack length a. Under constant amplitude loading a duty cycle can correspond to a certain number of load cycles and obviously, the transition probability $p(a_1 \mid a_2)$ is not independent of the previous history for the experimental results shown.

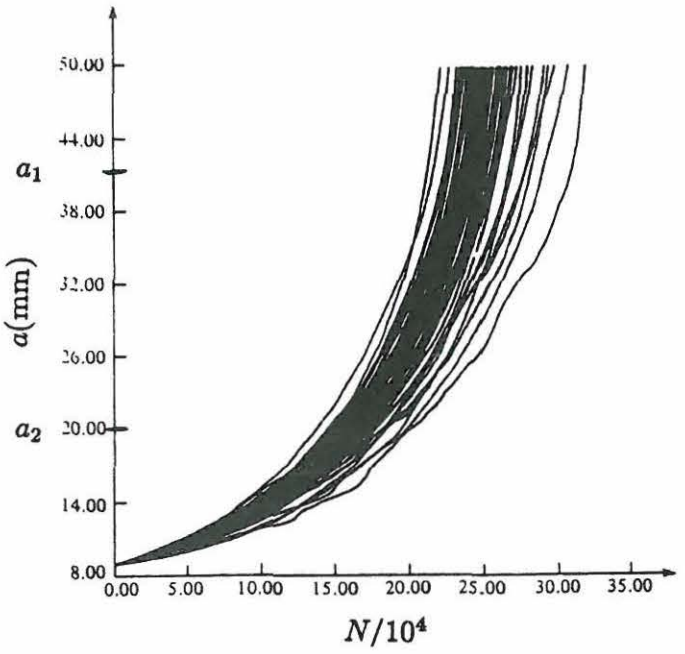

Figure 3.2 Crack length a as a function of the number of load cycles N, experimental results (Madsen et al., 1986).

3.3.1 Model 2.1

The model is described in Skjong, 1985. As an example of a failure criterion fatigue crack growth is taken and failure is defined as the excess of a critical crack size describing crack growth by the Paris and Erdogan equation.

System

An element with a single failure mode is considered.

Inspection Method

The inspection methods are characterized by the probability of detecting a crack of the size a assuming that a is greater than a lower limit a_o.

Inspection Strategy

The strategy is characterized by varying inspection intervals.

Inspection Results

Cracks greater than a critical crack size are repaired.

Failure Probability

The probability of failure before duty cycle n is given.

Optimization Problem

The total expected costs of the lifetime are minimized including inspection cost, cost of repair after inspection, failure cost and cost of repair after element failure but not structural collapse. The number of inspections in the expected lifetime of

the structure is given and the optimization variables are the inspection times and the inspection methods/qualities which can be selected among a number of given methods with known characteristics. No constraints are given on the inspection times.

Examples
A numerical example is shown in Skjong, 1985, with 30 duty cycles and two possible inspection methods.

3.3.2 Model 2.2

This model is presented in Ohnishi et al., 1986. The physical failure mode is not specified and the deterioration is assumed to be a stationary, continuous-time Markov process.

System
An unspecified system is considered.

Inspection Method
Inspection results are assumed to be correct.

Inspection strategy
Only one (the next) inspection time is calculated.

Inspection Results
One of the following decisions is possible after an inspection:
1. The time for the next inspection.
2. The system is operated without inspection until it fails.
3. The system is replaced.

Failure Probability
The probability of failure depends on the state of the system.

Optimization Problem
The objective function is the total costs including operating cost, inspection cost and replacement cost and the optimization variables are the inspection times and the decisions, i.e. the decisions are made so that the costs are minimized. No constraints are given.

Examples
None is given.

3.3.3 Model 2.3

The model is described in Fujimoto and Swilem, 1992, and it assumes fatigue to be the failure mode for each of the members included in the system.

System
A structural system consisting of several member sets is considered. All members of a set are assumed to have the same properties.

Inspection Method
Five different inspection methods are considered; no inspection, visual inspection,

mechanical inspection, visual inspection supplemented by mechanical inspection if any defects are found and, finally, mechanical inspection of a number of sample members extended to all members in case any defects are found. Each method is characterized by the probability of detecting a crack and the cost of inspection.

Inspection Strategy
The model is characterized by determining the inspection strategy sequentially considering one inspection interval at a time.

Inspection Results
Detected cracks are repaired and if a member fails it is repaired. During inspection and repair the service of the structure is suspended.

Failure Probability
The failure probability is obtained using the state vector for the structural member.

Optimization Problem
The total costs are minimized including inspection cost, repair cost, loss due to service suspension and failure cost. One inspection interval is considered at a time and the optimization is repeated at each inspection. During the optimization procedure the optimal inspection method for the present inspection and the optimal inspection interval to the next inspection are found.

Examples
Analyses of a member set and of a structure have been carried out.

3.4 Continuously Developing Deterioration

The models described here all consider a specified type of deterioration, i.e. fatigue crack growth and/or corrosion propagation in steel. Fatigue crack growth is described by the Paris and Erdogan equation and both this equation and the corrosion propagation law used in model 3.2 describes the deterioration of the system as continuously developing from the initial state to the failure state. Failure is defined as the excess of a critical limit except for model 3.4 where failure develops gradually. In this category of models the most realistic models are found.

In addition to the models described here, a model is described in Wirsching and Torng, 1990, which resembles model 3.1. A series system of fatigue failure modes is considered.

3.4.1 Model 3.1

The first description of the model is in Thoft-Christensen and Sørensen, 1987, where the reliability of the system is described by the reliability index. In Sørensen and Thoft-Christensen, 1987, the design cost is integrated in the optimization procedure and in PRODIM, 1988, a program is described using the recent stage of the model where failure is described as fatigue crack propagation. It is possible to use a 2-dimensional model including both crack depth and crack length (see PRODIM, 1988) and the effect of corrosion of the steel may be included. In Madsen et al., 1987, and

Madsen, 1989, updating through inspection is described whereas Madsen et al., 1990, present the model in short. The same is done in Madsen and Sørensen, 1990, but a detail in the description of the inspection quality is changed. In Sørensen et al., 1991, an additional decision variable is included (repair crack length limit) and an event margin for crack detection, which was included in the event margin for repair previously, is introduced. In Cramer and Friis-Hansen, 1992, a weld with multiple potential cracks and the coalescence of these is considered. In [2]Faber et al., 1992, and Sørensen et al., 1992, a number of parametric studies is performed. In [1]Faber et al., 1992, a decision strategy is described selecting which points/elements to inspect based on risk analysis. For these elements an optimal inspection strategy is calculated. The recent stage of the model is presented in the following.

System
In Thoft-Christensen and Sørensen, 1987, and Sørensen and Thoft-Christensen, 1987, structural series systems are considered and some examples with up to 8 failure elements have been shown. A structural system with one failure element characterized by one parameter is considered in PRODIM, 1988, Madsen, 1989, Madsen et al., 1990, Madsen and Sørensen, 1990, Sørensen et al., 1991, [2]Faber et al.,1992, and Sørensen et al., 1992. In Sørensen and Faber, 1991, and [1]Faber et al., 1992, a structural system including two groups of elements is considered. One group consists of vital structural elements for which failure implies global failure and the other group consists of secondary structural elements for which a sequence of elements has to fail before global failure occurs.

Inspection Method
The inspection method is characterized by an exponential function describing the probability of detecting a crack of size a.

Inspection Strategy
The strategy is characterized by varying inspection intervals

Inspection Results
The inspection times for the expected lifetime of the structure are calculated at the design stage but it is possible to recalculate the optimal inspection times after each inspection when more knowledge about the system is available. Four repair strategies are available in the model:

1. All detected cracks are repaired by welding.
2. Detected cracks smaller than a certain size are repaired by grinding, the remaining cracks are repaired by welding.
3. Detected cracks smaller than a certain size are not repaired, the remaining cracks are repaired by welding.
4. All detected cracks are repaired by replacing the element.

If failure occurs the system immediately stops functioning. If a secondary structural element fails in Sørensen and Faber, 1991, and [1]Faber et al., 1992, it can be repaired.

Failure Probability
The failure probability is calculated using the safety margin for failure and the event margins for damage detection and repair.

Optimization Problem
The total expected costs are minimized including initial cost, inspection cost, repair cost and failure cost. The optimization variables are the structural design parameter, the time interval between inspections, the inspection quality at each inspection and the repair level parameter while the total number of inspections, n, is selected beforehand to avoid a combination of integer and real valued optimization variables. By repeating the optimization for different values of n, the optimal n can be found. Constraints are given on the reliability index at the end of the lifetime and on the optimization variables. Furthermore, in [1]Faber et al., 1992, the suspension cost due to loss of production is included in the repair and failure costs, the choice of which elements to inspect is included in the optimization variables and constraints are given on each of the four contributions to the total costs.

Examples
The model has been applied to several simple examples.

3.4.2 Model 3.2

This model is described in Sørensen and Thoft-Christensen, 1988, and it is based on Thoft-Christensen and Sørensen, 1987, and Sørensen and Thoft-Christensen, 1987. It is a variant of model 3.1 but contrary to model 3.1 the failure mode has been exemplified by corrosion of reinforcement in a concrete bridge and failure is defined as the excess of the moment capacity of the structural element. Due to the corrosion effect the reinforcement area is a function of time.

System
A structural element (T-beam) in a concrete bridge.

Inspection Methods
The reliability of the inspection methods is not specified except that the inspection quality is q_1 for routine inspections and q_2 for detailed inspections. Routine inspections are assumed to be visual inspections and they will reveal whether the concrete cover is flaking off whereas detailed inspections provide an estimate of the chloride concentration variation with the depth from the concrete surface and give a picture of where corrosion occurs.

Inspection Strategy
Routine inspections are performed at fixed time intervals Δt and detailed inspections are performed at varying intervals being a multiple of Δt.

Inspection Results
Repair is carried out when corrosion is detected.

Failure Probability
The safety margin is defined from the moment capacity of the structural element and

similar to model 3.1 event margins are defined for repair after routine or detailed inspections.

Optimization Problem
The total costs are minimized including initial cost, inspection cost, repair cost and failure cost and the optimization variables are the concrete cover, the number of detailed inspections and the time intervals between detailed inspections. Constraints are given on the reliability index, the concrete cover and the summation of the inspection intervals.

Examples
A numerical example is given where the problem is solved by recalculation for different fixed values of the number of detailed inspections.

3.4.3 Model 3.3

This model is described in Fujita et al., 1990. Growth of the crack length is described by the Paris and Erdogan equation and failure is defined as crack instability considering it as a first-passage problem.

System
A metallic structure with one component is considered.

Inspection Method
The inspection method is characterized by the smallest detectable crack size and the measurement error.

Inspection Strategy
Only one inspection time is calculated.

Inspection Results
Detected cracks exceeding a critical crack length are repaired.

Failure Probability
The failure probability is updated after each inspection and it depends on whether the component is repaired or not.

Optimization Problem
The objective function is the total costs including inspection cost, repair cost and failure cost and the optimization variable is the inspection time. The model includes bounds on the inspection time. The possibility of placing a limit on the failure probability or the risk function is mentioned.

Examples
An illustrative example is shown. The different contributions to the total costs have been shown as functions of time and updated failure probabilities have been calculated for different inspection results.

3.4.4 Model 3.4

This model is described in Cramer and Hauge, 1991. It is related to model 3.1

but characteristic of the model is that it defines failure as a gradually developing process and the structure is never completely failed, i.e. not working. Fatigue crack growth is described by the Paris and Erdogan equation (one-dimensional model). The sample space is not divided into a safe set and a failure set, i.e. failure is developing continuously as a function of the crack size.

System
A structural detail with one failure mode is considered.

Inspection Method
The inspection method is characterized by the probability of detecting a crack of the size a.

Inspection Strategy
The strategy is characterized by varying inspection intervals.

Inspection Results
Cracks greater than a critical crack size are repaired.

Failure Probability
The failure probability is not included in the model since failure is assumed to develop gradually. Only the probability of detecting a crack or of repair is used.

Optimization Problem
The total expected costs of the lifetime are minimized including design cost, inspection cost, repair cost and failure cost. The number of inspections in the expected lifetime is given and the optimization variables are a design variable and inspection times. No constraints are given.

Examples
Four numerical examples are given. The number of inspections is 0 or 1.

3.5 Conclusions

In the following a survey is given of the most important properties of real life, that are not incorporated in the models.

Failure
There are several causes of failure in steel structures, e.g. crack propagation, corrosion, accidents, bigger loads than expected, errors in design and construction.

System
Structures are usually modelled by a complicated system of series and parallel elements.

Inspection Methods
The characteristics of the inspection methods are quite unpredictable regarding reliability and accuracy. In the models the duration of an inspection is assumed to be negligible but in reality it can take weeks or months for a large structure. Usually several inspection methods are used, making the characterization of the inspection even more difficult.

Inspection Results
To distinguish only between failure and non-failure is a simplification since failure can result in either system-down or the system is still functioning but with extra cost and reduced reliability, or the system is functioning without extra cost and with reduced reliability. The decision of repair is ambiguous too since the extent and cost of repair can vary a great deal as indicated in appendix 1.

Objective Function
Most models do not include all types of cost and the dependence on the variables for the different types of cost is simplified. In general the calculation of the cost will be inaccurate due to the above-mentioned approximations.

Optimization Variables
As mentioned above inspection times may be periods instead of moments of time.

All the models have disadvantages compared to reality. Only some models specify the failure mode and none of them incorporate all causes of failure in real life which of course is also not possible regarding accidents and errors. The system can in some models only be in two states - failure state or working state (type 1 models) and in most of these models the failure time is given as a random variable with a known distribution. Other models include a number of working states and one failure state (type 2 models), in other words the deterioration process is considered to be a Markov process. Finally, there are models that describe the state of the system by a deterioration law such as the Paris and Erdogan equation (models 3.1, 3.3, 3.4) or a corrosion propagation law (model 3.2). Failure is defined as the excess of a critical limit except for model 3.4 where failure develops gradually. It was found that only the models of type 3 are sufficiently realistic for practical purposes.

In most cases the structural system is reduced to one failure element (models 1.1, 1.2, 2.1, 3.1, 3.2, 3.3, 3.4) or not specified (model 2.2). Model 3.1 has also been used for small series systems and more complex systems, i.e. a series system of parallel systems. In model 2.3 a structure consisting of a number of member sets is considered. From a theoretical point of view it is easy to incorporate more complex series and/or parallel systems but the calculations and implementations quickly become very expensive and time-consuming.

As stated above sufficient knowledge about the inspection methods is not available and this makes it difficult to characterize them realistically in the models. The inspection method is in models 1.1 and 2.2 assumed to be 100% reliable but in the remaining models it is possible to include the reliability or measurement uncertainty of the inspection method which introduces inspection quality as an optimization variable (models 2.1, 2.3, 3.1).

In most models repair takes place depending on the inspection result but in model 2.2 the inspection may result in replacement.

Except for model 1.1 the failure probability in all models depends on the state of the

system, i.e. the inspection results, and only in models 1.1, 3.1 and 3.2 is it possible to place constraints on the failure probability/reliability index.

The costs included in the total costs vary a great deal in the models. Most costs are included in models 3.1, 3.2, and 3.4, namely initial, inspection, repair and failure costs. In model 1.2 the costs are not considered as the availability of the system is optimized.

Numerical examples have been implemented for all models except 2.2 and for models 3.1 and 3.3 the effect of changing some of the parameters has been studied.

Only very few real-life examples have been found where inspection planning is based on reliability calculations. According to Yang, 1980, U.S. Air Force structural integrity and durability design specifications require that the economic life of airframe components be analytically predicted and a procedure is presented where inspections are planned when the average crack, e.g. in fastener holes, is expected to exceed a given level. By economic life is meant the time until either the cost of maintenance or the cracks exceeding the economical repair crack size are getting too big. In Pedersen et al., 1992, it is described how inspection of a structural component of the offshore structures at the Tyra Field is performed when the reliability index of the component is reduced to a specified minimum level. The inspection strategy is not found by an optimization procedure since, in this case, experience has shown that the cheapest is to wait as long as possible, without violating safety demands, before inspecting a structural member. This procedure is also recommended in Underwater Inspection..., 1989. The deterioration process under consideration is fatigue described by the Paris and Erdogan equation.

Related models are developed but not described in detail here. As in Pedersen et al., 1992, in these models inspections are planned when the failure probability reaches a target level. Within the area of aircraft structures this procedure has been subject to studies for many years and some of the earliest work is described in Eggwertz, 1963, where constant intervals for the inspection of wing structures for cracks are determined. In Fujimoto et al., 1989, a structure with a number of members subjected to fatigue failure is considered. The model in Jiao, 1992, is partly based on model 3.1 but it is assumed to be optimal to inspect when the failure probability reaches the minimum acceptable level.

3.6 References

Aven, Terje (1987), *Optimal Inspection and Replacement of a Coherent System*, Microelectronics and Reliability, Vol. 27, No. 3, pp. 447-450.

Barlow, Richard E.; Frank Proschan (1975), *Statistical Theory of Reliability and Life Testing*, Holt, Rinehart and Winston, Inc., U.S.A.

Bogdanoff, J.L. (1978), *A New Cumulative Damage Model, Part I*, ASME Journal of Applied Mechanics, Vol. 45, No.2, pp. 246-250.

Cramer, Espen H.; Lars H. Hauge (1991), *A Maximum Utility Model for Structures*

Subject to Fatigue Crack Growth, Proceedings of OMAE 1991, Stavanger, Norway, ASME, Vol.II, pp. 119-125.

Cramer, E.H.; P. Friis-Hansen (1992), *Reliability-Based Optimization of Multi-Component Welded Structures*, Proceedings of OMAE 1992, Calgary, Canada, ASME, Vol. II, pp. 265-271.

Eggwertz, S. (1963), *Inspection Periods Determined from Data on Crack Development and Strength Reduction of an Aircraft Structure using Statistical Analysis*, Proceedings of ICAF Symposium of Fatigue of Aircraft Structures, pp. 345-362.

[1]Faber, M.H.; J.D. Sørensen; I. Kroon (1992), *Optimal Inspection Strategies for Offshore Structural Systems*, Proceedings of OMAE 1992, Calgary, Canada, ASME, Vol. II, pp. 145-151.

[2]Faber, M.H.; J.D. Sørensen; R. Rackwitz; P. Thoft-Christensen; Ph. Bryla (1992), *Reliability Analysis of an Offshore Structure. A Case Study - I*, Proceedings of OMAE 1992, Calgary, Canada, ASME, Vol. II, pp. 449-455.

Fujimoto, Y; H. Itagaki; S. Itoh; H. Asada; M Shinozuka (1989), *Bayesian Reliability Analysis of Structures with Multiple Components*, Proceedings of ICOSSAR '89, ASCE, U.S.A., pp. 2143-2146.

Fujimoto, Yokio; Swilem A.M. Swilem (1992), *Inspection Strategy for Deteriorating Structures Based on Sequential Cost Minimization Method*, Proceedings of OMAE 1992, Calgary, Canada, ASME, Vol. II, pp. 219-226.

Fujita, M.; G. Schall; R. Rackwitz (1990), *Adaptive Reliability-Based Inspection Strategies for Structures Subject to Fatigue*, Proceedings of ICOSSAR '89, ASCE, U.S.A., pp. 1619-1626.

Jiao, Guoyang (1992), *Reliability Analysis of Crack Growth With Inspection Planning*, Proceedings of OMAE 1992, Calgary, Canada, ASME, Vol. II, pp. 227-235.

Kaio, Naoto; Shunji Osaki (1984), *Some Remarks on Optimum Inspection Policies*, IEEE Transactions on Reliability, Vol. R-33, No. 4, pp. 277-279.

Kaio, Naoto; Shunji Osaki (1986), *Optimal Inspection Policy with Two Types of Imperfect Inspection Probabilities*, Microelectronics and Reliability, Vol. 26, No. 5, pp. 935-942.

Keller, Joseph B. (1974), *Optimum Checking Schedules for Systems Subject to Random Failure*, Management Science, Vol. 21, No. 3, pp. 256-260.

Madsen, Henrik O. (1989), *Stochastic Modelling of Fatigue Crack Growth*, ISPRA Course, Structural Reliability, Lisboa.

Madsen, H.O.; S. Krenk; N.C. Lind (1986), *Methods of Structural Safety*, Prentice-Hall.

Madsen, Henrik O.; Rolf Skjong; Andrew G. Tallin; Finn Kirkemo (1987), *Probabilistic Fatigue Crack Growth Analysis of Offshore Structures, with Reliability Updating Through Inspection*, Proceedings, Marine Structural Reliability Symposium, Arlington, SNAME, pp. 45-56.

Madsen, H.O.; J.D. Sørensen (1990), *Probability-Based Optimization of Fatigue Design, Inspection and Maintenance*, Proc. on Integrity of Offshore Structures, Glasgow, Elsevier Applied Science, p. 421.

Madsen, H.O.; J.D. Sørensen; R. Olesen (1990), *Optimal Inspection Planning for Fatigue Damage of Offshore Structures*, Proceedings of ICOSSAR '89, ASCE, U.S.A., pp. 2099-2106.

Nakagawa, T.; K. Yasui (1980), *Approximate Calculation of Optimal Inspection Times*, The Journal of the Operational Research Society, Vol. 31, No. 9, pp. 851-853.

Nakagawa, Toshio; Kazumi Yasui (1987), *Optimum Policies for a System with Imperfect Maintenance*, IEEE Transactions on Reliability, Vol. R-36, No. 5, pp. 631-633.

Ohnishi, Masamitsu; Hajime Kawai; Hisashi Mine (1986), *An Optimal Inspection and Replacement Policy for a Deteriorating System*, Journal of Applied Probability, Vol. 23, No. 4, pp. 973-988.

Pedersen, Carl; John A. Nielsen; Jens P. Riber; Henrik O. Madsen; Steen Krenk (1992), *Reliability-Based Inspection Planning for the Tyra Field*, Proceedings of OMAE 1992, Calgary, Canada, ASME, Vol. II, pp. 255-263.

PRODIM, Theoretical Manual (1988), A.S. Veritas Research Report No. 88-2029, Høvik, Norway.

Rodrigues Dias, J. (1990), *A New Approximation for the Inspection Period of Systems with Different Failure Rates*, European Journal of Operational Research, Vol. 45, No. 2-3, Elsevier Science Publishers B.V., North-Holland, pp. 219-223.

Sherif, Y.S.; M.L. Smith (1981), *Optimal Maintenance Models for Systems Subject to Failure - A Review*, Naval Research Logistics Quarterly, Vol. 28, pp. 47-74.

Skjong, Rolf (1985), *Reliability-Based Optimization of Inspection Strategies*, Proceedings of ICOSSAR '85, ASCE, U.S.A., pp. III-614-618.

Sommer, A.M.; P.Thoft-Christensen (1990), *Inspection and Maintenance of Marine Steel Structures - State-of-the-Art*, Structural Reliability Theory, Paper no. 74, The University of Aalborg, Denmark.

Sørensen, J.D.; M.H. Faber (1991), *Optimal Inspection and Repair Strategies for Structural Systems*, Proc. IFIP WG 7.5, Conference on Reliability and Optimization of Structural Systems (eds. R. Rackwitz and P. Thoft-Christensen), Springer-Verlag, Lecture Notes in Engineering, Vol. 76, pp. 383-394.

Sørensen, J.D.; M.H. Faber; R. Rackwitz; P. Thoft-Christensen (1991), *Modelling in Optimal Inspection and Repair*, Proceedings of OMAE 1991, Stavanger, Norway, ASME, Vol. II, pp. 281-288.

Sørensen, J.D.; M.H. Faber; R. Rackwitz; P. Thoft-Christensen; G. Lebas (1992), *Reliability Analysis of an Offshore Structure. A Case Study - II*, Proceedings of OMAE 1992, Calgary, Canada, ASME, Vol. II, pp. 457-463.

Sørensen, J.D.; P. Thoft-Christensen (1987), *Integrated Reliability-Based Optimal Design of Structures*, Proc. IFIP WG 7.5, Conference on Reliability and Optimization of Structural Systems (edt. P. Thoft-Christensen), Springer-Verlag, Lecture Notes in Engineering, Vol. 33, pp. 385-398.

Sørensen, J.D.; P. Thoft-Christensen (1988), *Inspection Strategies for Concrete Bridges*, Proc. IFIP WG 7.5, Conference on Reliability and Optimization of Structural Systems (edt. P. Thoft-Christensen), Springer-Verlag, Lecture Notes in Engineering, Vol. 48, pp. 325-335.

Tang, Wilson H.; Ben Chie Yen (1991), *Dam Safety Inspection Scheduling*, Journal of Hydraulic Engineering, Vol. 117, No. 2, ASCE, U.S.A., pp. 214-229.

Thoft-Christensen, P.; J.D. Sørensen (1987), *Optimal Strategy for Inspection and Repair of Structural Systems*, Civil Engineering Systems, Vol. 4, pp. 94-100.

Underwater Inspection of Steel Offshore Installations: Implementions of a New Approach (1989), MTD Ltd. Publication 89/104, London.

Wirsching, Paul H.; Yi Torng (1990), *Optimal Strategies for Design, Inspection and Repair of Fatigue-Sensitive Structural Systems Using Risk-Based Economics*, Proceedings of ICOSSAR '89, ASCE, U.S.A., pp. 2107-2114.

Yang, J.N. (1977), *Optimal Periodic Proof Test Based on Cost-Effective and Reliability Criteria*, AIAA Journal, Vol. 15, pp. 402-409.

Yang, J.N. (1980), *Statistical Estimation of Economic Life for Aircraft Structures*, Journal of Aircraft, Vol. 17, pp. 528-535.

Yang, J.N.; W.J. Trapp (1975), *Inspection Frequency Optimization for Aircraft Structures Based on Reliability Analysis*, Journal of Aircraft, Vol. 12, pp. 494-496.

CHAPTER 4
A RELIABILITY-BASED INSPECTION STRATEGY FOR STEEL GIRDER BRIDGES

4.1 Introduction

Periodical inspection of bridges is typically scheduled to take place every 2-3 years or, if two types of inspection are performed, a superficial inspection takes place every year and a more detailed inspection every 3-5 years. These conventional strategies are described in detail for a number of countries in chapter 2. Deterioration of steel structures in bridges is mainly caused by the development of corrosion and fatigue cracks and this chapter deals with inspection of corroded steel girder bridges subjected to three failure modes, namely bending, shear and bearing failure of a girder. The reliability index as a function of time is calculated for each girder in a typical highway bridge, it is examined whether some girders are more critical than others and based on this an inspection strategy is suggested. A presentation of the content of this chapter is available in Sommer et al., 1992.

4.2 Corrosion of Steel Girder Bridges

Kayser, 1988, described five of the most important forms of corrosion which are summarized here. The most common form is *general corrosion* which is uniformly distributed on the surface while *pitting corrosion* is restricted to a small area and it usually begins with an anomaly on the surface. *Crevice corrosion* occurs where different components of the structure are close making narrow spaces and *galvanic corrosion* takes place when two different metals are placed in an electrolyte and are electrically connected, as is possible at bolted or welded connections. Tensile stress will increase the rate of corrosion which is called *stress corrosion*. A combination of different forms of corrosion can often occur, for instance, the combination of pitting, crevice and stress corrosion under cyclic loading is called corrosion fatigue.

Corrosion causes loss of material thereby decreasing the load-carrying capacity of the bridge and it can cause a build-up of corrosion products which exerts pressure on adjacent elements resulting in eccentricities and stresses. It can also lock the mechanism of bearings and hinges.

Data on corrosion performance in actual steel bridges have been collected by Kayser, 1988, and as expected, corrosion occurs where water is accumulated. For steel girder bridges this happens at leaking deck joints and at the upper side of the bottom

flange. Furthermore, corrosion is influenced by the environment, i.e. the amount of moisture in the air and the presence of salt. Therefore, the geographical location is of vital importance when planning the maintenance of a steel bridge. For example, in Michigan, U.S.A., a severe corrosion was observed due to use of salt as a de-icing agent and insufficient painting. It is only in a very dry climate that paint lasts indefinitely. It has been observed that the rate of corrosion may be different for different girders. For example, in highway overpasses girders are exposed to a mixture of salt, snow and water splashed by trucks and the highest concentration of this aggressive medium is on the exterior girder while the concentration of salt and/or water decreases in the direction of traffic.

In this chapter general corrosion is considered as the most common form. Studies have shown that the corrosion propagation can be modelled, with a good approximation, by an exponential function (see Albrecht and Naeemi, 1984)

$$C(t) = At^B \tag{4.1}$$

where $C(t)$ is the average corrosion penetration in microns (10^{-6} m), t is the time in years and A, B are stochastic parameters to be determined from regression analysis of experimental data. In this expression, however, only the statistical uncertainty is included as the residual is neglected and furthermore, A and B are described by separate distribution functions - not a joint distribution function.

The parameters A and B have been determined in Kayser, 1988, based on field tests by Albrecht and Naeemi, 1984, and for carbon steel and weathering steel the mean values, the coefficients of variation and the coefficients of correlation for A and B are given in table 4.1. It shows, as expected, that the parameters for weathering steel are smaller than for carbon steel since corrosion develops slower in weathering steel after the first year and it also shows that in most cases the parameters are lowest in rural environment and highest in urban environment. It should be stated that the determination of A and B involves a considerable uncertainty.

Type of steel		Carbon		Weathering	
Corrosion parameter		A	B	A	B
Rural env.	Mean value, μ	34.0	0.650	33.3	0.498
	Coeff. of variation, $\frac{\sigma}{\mu}$	0.09	0.10	0.34	0.09
	Coeff. of correlation, ρ_{AB}	not available		-0.05	
Urban env.	Mean value, μ	80.2	0.593	50.7	0.567
	Coeff. of variation, $\frac{\sigma}{\mu}$	0.42	0.40	0.30	0.37
	Coeff. of correlation, ρ_{AB}	0.68		0.19	
Marine env.	Mean value, μ	70.6	0.789	40.2	0.557
	Coeff. of variation, $\frac{\sigma}{\mu}$	0.66	0.49	0.22	0.10
	Coeff. of correlation, ρ_{AB}	-0.31		-0.45	

Table 4.1 Statistical parameters for A and B (from Kayser, 1988).

To illustrate the problem a simple-span steel girder bridge is considered and the observed general corrosion pattern is shown in figure 4.1a. The mid-section of the girder, where corrosion takes place only at the bottom of the web and on the upper side of the flange, is mainly subjected to bending but the bending capacity depends on the cross-section of the flanges and not so much on the web. Therefore, the corroded cross-section is modelled in the same way at mid-section and at the supports where shear forces dominate. The modelled corroded cross-section is shown in figure 4.1b.

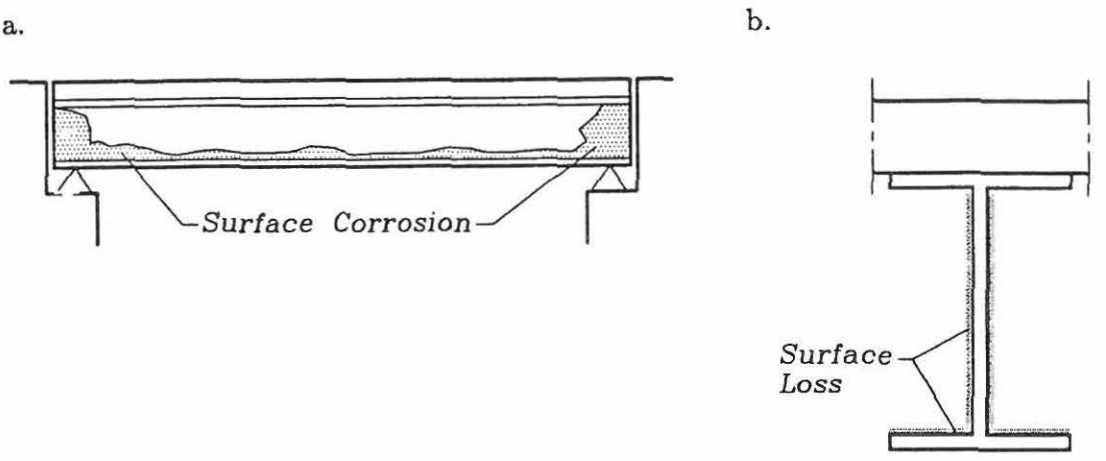

Figure 4.1 Corrosion of a steel girder (Kayser, 1988).

4.3 Failure Modes

Three failure modes are considered namely bending failure, shear failure and bearing failure[1] and calculating the corresponding failure probability is a time-variant reliability problem. The load is represented by the bending moment at the mid-section or by the shear force at the supports. In the calculations the traffic load is conservatively represented by the maximum 75 year truck troughout the lifetime. It would be more realistic to base the reliability analyses on a first-passage problem, see figure 4.1a, modelling the traffic load as a stochastic process but this is not used in the example.

[1] Bearing failure applies to compression in short components (the stiffened web) at the supports.

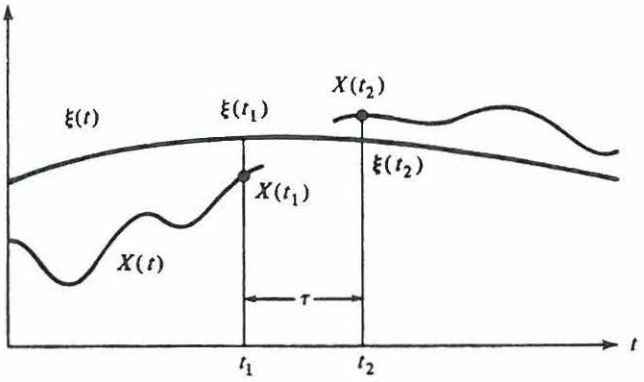

Figure 4.1a First-passage problem (Madsen et al., 1986).

For bending failure, for instance, the barrier $\xi(t)$ is the nominal moment strength as a function of time minus the dead load moment, i.e. $M_n(t) - M_D$, while the stochastic load process $X(t)$ is the midspan moment. Assuming that the barrier crossings are independent, the failure probability can be calculated as (see Madsen et al., 1986)

$$P_F(t) = 1 - F_{X(0)}(\xi(0))exp \mid - \int_0^t \nu^+(\xi(\tau))d\tau \mid \tag{4.1a}$$

where $\nu^+(\xi(\tau))$ is the upcrossing rate. It is assumed that $F_{X(0)}(\xi(0)) = P(X(0) < \xi(0)) \simeq 1$, i.e. no failure at $t = 0$. The upcrossing rate can be calculated by Rice's formula

$$\nu^+(\xi(t)) = \int_{\xi}^{\infty} f_{X\dot{X}}(\xi(t), \dot{x})(\dot{x} - \dot{\xi})d\dot{x} \tag{4.1b}$$

The traffic load moment is a discrete process. One approach is to model the midspan moment as a square-wave filtered Poisson process. A stochastic process

$$X(t) = \sum_{i=1}^{N(t)} w(t, \tau_i, S_i) \tag{4.1c}$$

is called a filtered Poisson process when $N(t)$ is a Poisson process, $\{S_i\}$ is a sequence of identically distributed and independent random variables and $w(t, \tau, s)$ is the response function defined to be zero for $t < \tau$. S_i is the magnitude of the signal taking place at τ_i. $w(t, \tau_i, s)$ represents the value at time t of a signal of magnitude s originating at time τ_i and $X(t)$ represents the value at time t of the sum of signals arising from the events occuring in the interval [0,t]. For the bridge under consideration S_i represents the traffic load and w represents the response of the bridge to the traffic load.

According to Madsen et al., 1986, the upcrossing rate is

$$\nu^+(\xi(t)) = \mu(t)(1 - F_S(\xi(t)) \tag{4.1d}$$

where $\mu(t)$ is the intensity of the Poisson process $N(t)$. In other words $\mu(t)$ expresses the number of "truck events" per time unit.

The calculations are rather complicated and they are not described in further detail here. For a Gaussian process the calculation procedure is explained in section 5.4.

The bending, shear and bearing capacities are calculated from material and corrosion parameters and corrosion as a function of time t is included in the calculation by using the reduced values of the web thickness t_w and bottom flange thickness t_f, where

$$t_w(t) = t_{w0} - 2C(t), \qquad t_w \geq 0 \tag{4.2}$$

$$t_f(t) = t_{f0} - C(t), \qquad t_f \geq 0 \tag{4.3}$$

t_{w0} is the initial web thickness (mm), t_{f0} is the initial flange thickness (mm), t is the time in years and $C(t)$ is the average corrosion penetration (mm). The top flange thickness is assumed constant with time and equal to t_{f0}.

4.3.1 Bending Failure

The effective slab width is assumed according to AASHTO, 1989, as shown in figure 4.2. Neglecting the effect of reinforcement in the slab the nominal bending moment strength M_n is calculated based on plastic stress distribution in the composite section (Salmon, 1990) and it is assumed that the web slenderness ratio, λ, fulfils the following requirement according to Load and Resistance Factor Design (Salmon, 1990)

$$\lambda = \frac{h_c}{t_w} \leq \lambda_p = \frac{640}{\sqrt{f_{yf}}} \tag{4.4}$$

where h_c is the unsupported web depth, t_w is the thickness of the web, λ_p is the maximum slenderness ratio and f_{yf} is the yield stress of the flange in ksi (1 ksi = 6.895 N/mm^2). If this requirement is not fulfilled the calculations must be based on superposition of elastic stresses.

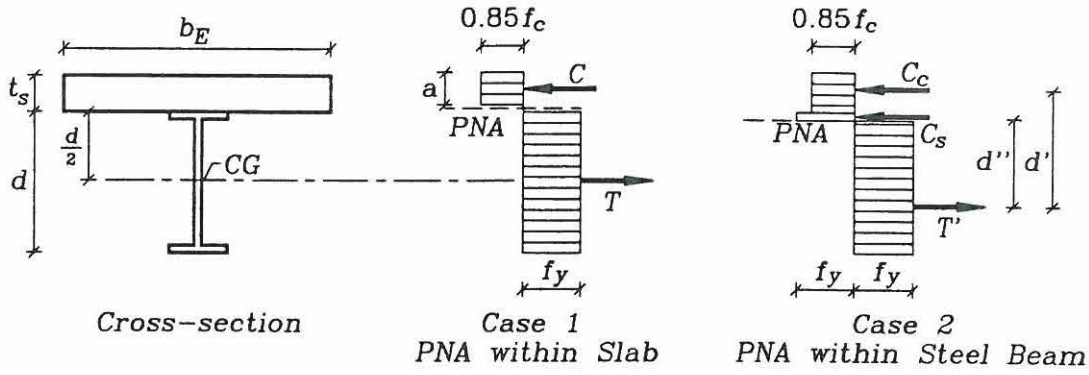

Figure 4.2 Plastic stress distribution at nominal moment strength (Salmon, 1990).

There are two cases depending on whether the plastic neutral axis (PNA) is in the slab or in the steel section. In figure 4.2 the cross-section and the stress distribution are shown.

Case 1. PNA within Slab
The distance a in figure 4.2 becomes

$$a = \frac{A_s f_y}{0.85 f_c b_E}, \qquad a \leq t_s \tag{4.5}$$

where A_s is the steel section area, f_y is the yield stress of the steel, f_c is the specified 28-day compressive strength of the concrete and b_E is the effective width of the slab. The nominal bending moment strength M_n is

$$M_n = A_s f_y \left(\frac{d}{2} + t_s - \frac{a}{2} \right) \tag{4.6}$$

Case 2. PNA within Steel Beam
The compressive force in the concrete slab is

$$C_c = 0.85 f_c b_E t_s \tag{4.7}$$

where t_s is the slab thickness. The compressive force in the steel is,

$$C_s = \frac{A_s f_y - 0.85 f_c b_E t_s}{2} \tag{4.8}$$

and the tensile force in steel is

$$T' = A_s f_y - C_s \tag{4.9}$$

Knowing C_c, C_s and T', the PNA and the distances d' and d'' (see figure 4.2) can be found. The nominal bending moment capacity is

$$M_n = C_c d' + C_s d'' \tag{4.10}$$

A safety margin for bending failure is

$$M_{F1}(t) = Z_1 M_n(t) - M_D - M_L \tag{4.11}$$

where Z_1 is a variable modelling the uncertainty in estimating the moment capacity. $M_n(t)$ is the nominal moment strength at the time t (including the effect of corrosion), M_D is the dead load moment and M_L is the live load moment due to the maximum 75 year truck.

4.3.2 Shear Failure

Shear forces are carried mainly by the web, the critical stress is calculated according to

plate buckling theory (Salmon, 1990) and the web panel is modelled as a rectangular plate in pure shear with simply supported edges as shown in figure 4.3.

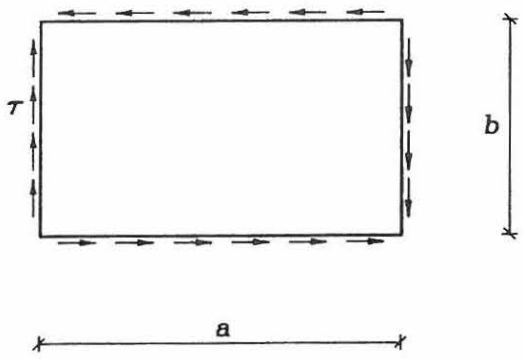

Figure 4.3 Web panel.

The elastic buckling shear stress is

$$\tau_{el} = k\frac{\pi^2 E}{12(1-\nu^2)\left(\frac{b}{t_w}\right)^2} \tag{4.12}$$

where $k = 5.34 + 4.0\left(\frac{b}{a}\right)^2$ is the plate boundary coefficient (pure shear, simply supported). E is the modulus of elasticity, ν is Poison's ratio, b is the shortest dimension of the plate (equal to $d - 2t_f$), a is the longest dimension of the plate and t_w is the thickness of the plate. The critical shear stress, τ_{cr}, depends on the size of C_v which is defined as

$$C_v = \frac{\tau_{el}}{\tau_y} \tag{4.13}$$

where $\tau_y = \frac{1}{\sqrt{3}} f_y$ is the shear yield stress.
For elastic buckling, i.e. $C_v \leq 0.8$,

$$\tau_{cr} = \tau_{el} \tag{4.14}$$

for inelastic buckling, i.e. $0.8 \leq C_v \leq 1.0$,

$$\tau_{cr} = \sqrt{0.8\tau_y \tau_{el}} \tag{4.15}$$

and in case of plastic buckling, i.e. $1.0 \leq C_v$,

$$\tau_{cr} = \tau_y \tag{4.16}$$

The shear force capacity is

$$V_{sh} = \tau_{cr}(d - 2t_f)t_w \tag{4.17}$$

A safety margin for shear failure is

$$M_{F2}(t) = Z_2 V_{sh}(t) - V_D - V_L \tag{4.18}$$

where Z_2 is a variable modelling the uncertainty in estimating the shear capacity. $V_{sh}(t)$ is the nominal shear strength at the time t, V_D is the dead load shear and V_L is the live load shear due to the maximum 75 year truck.

4.3.3 Bearing Failure

Calculation of the shear capacity at the supports depends on whether a stiffener is present or not. A stiffened web is calculated by considering the web as a compression member and an unstiffened web is calculated by using plate buckling theory. However, the plate boundary coefficients are not available for plates with one free edge subjected to shear. According to AASHTO, 1989, stiffening of the web over end bearings is required for all plate girders but for rolled girders it is required only when the nominal shear load exceeds 75% of the allowable shear. Here, a stiffened web is considered, see figure 4.4. The effective width of the web is equal to no more than 18 times the web thickness (AASHTO, 1989) and the calculation of the stiffened web is performed as described by Salmon, 1990.

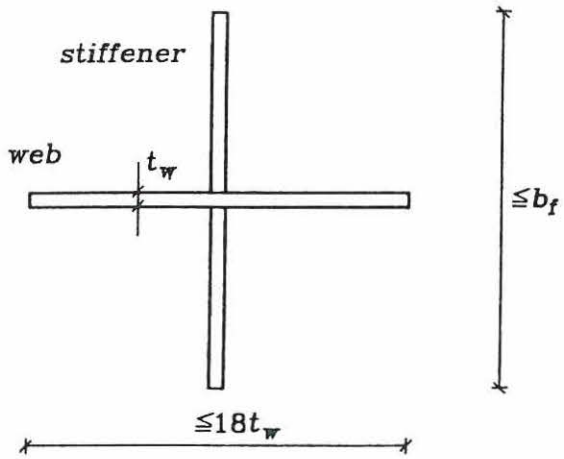

Figure 4.4 Stiffened web.

The elastic critical stress (Euler-stress) is

$$F_{el} = \frac{\pi^2 E}{(Kd/r)^2} \tag{4.19}$$

where K is the effective length factor (K=0.75 according to Salmon, 1990), d is the depth of web, $r = \sqrt{\frac{I}{A}}$ is the minimum radius of gyration. The critical stress, F_{cr}, depends on the slenderness parameter, λ_c, defined as

$$\lambda_c = \sqrt{\frac{f_y}{F_{el}}} \tag{4.20}$$

For the elastic region, i.e. $\lambda_c \geq \sqrt{2}$,

$$F_{cr} = F_{el} \tag{4.21}$$

For the inelastic region the SSRC parabolic equation has been used by AISC since 1960, $\lambda_c \leq \sqrt{2}$,

$$F_{cr} = f_y\left(1 - \frac{f_y}{4\pi^2 E}\left(\frac{Kd}{r}\right)^2\right) = f_y\left(1 - \frac{\lambda_c^2}{4}\right) \tag{4.22}$$

The bearing capacity is

$$V_{be} = F_{cr}A_s \tag{4.23}$$

where A_s is the cross-sectional area of the effective web and stiffener, see figure 4.4.

A safety margin for bearing failure is

$$M_{F3}(t) = Z_3 V_{be}(t) - V_D - V_L \tag{4.24}$$

where Z_3 is a variable modelling the uncertainty in estimating the capacity of the stiffened web. $V_{be}(t)$ is the nominal bearing strength at the time t.

4.4 Inspection Strategy

It is assumed that inspections are performed at constant time intervals Δt since the inspection authorities will often prefer constant inspection intervals to facilitate the planning. An inspection strategy is formulated so that the girder(s) with the largest failure probability are checked more frequently than others. This may not save much money for a highway bridge of the type considered here but for structures with a larger number of almost equal components the procedure can be valuable. If two different intervals are considered, the strategy can be illustrated as shown in figure 4.5, i.e. one group of girders G_B is checked at all inspections and a second group G_A is checked at longer intervals. T is the lifetime of the bridge, T_i are the inspection times, Δt is the inspection interval for girder group G_B and $n\Delta t$ is the inspection interval for girder group G_A. Each girder is considered separately when calculating the inspection strategy and then the shortest inspection interval found in G_A and G_B, respectively, will be used for the whole group G_A or G_B.

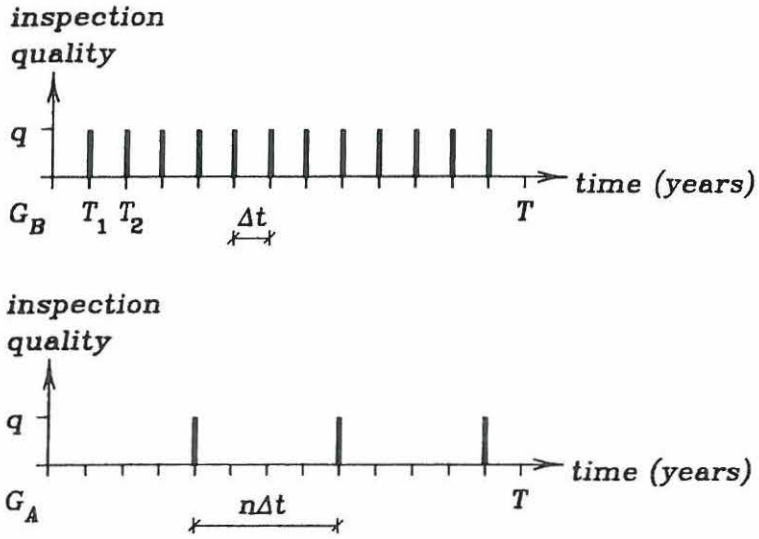

Figure 4.5 Inspection strategies for girder groups G_A and G_B.

A condition to determine when repair is to be performed in a girder after an inspection is formulated. It is assumed, that the web thickness is constant in the girder and that if the measured web thickness t_w is smaller than the critical value $t_{w,cr}$ then the girder must be repaired. The event margin for repair at the time t is

$$H(t) = Z_R t_w(t) - t_{w,cr} = Z_R(t_{w0} - 2C(t)) - t_{w,cr} \tag{4.25}$$

where Z_R is a variable modelling the uncertainty in estimating the web thickness. The possible decisions after each inspection in the lifetime of the bridge can be presented in the form of an event tree, as shown in figure 4.6. T_i is the time of inspection no. "i".

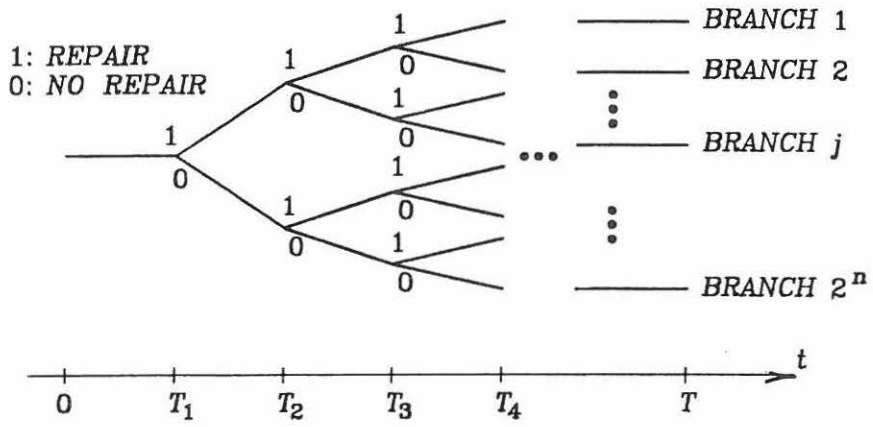

Figure 4.6 Event tree for the inspection strategy (PRODIM, 1988).

4.5 Reliability of Steel Girder Bridges

Failure of a girder is modelled by a series system with three elements corresponding to the three failure modes (bending, shear and bearing failure) and the failure probability for the series system is shown below for the first three inspection intervals. This series system for each girder should not be confused with the structural series system with elements corresponding to failure of each of the girders which is not considered here. The superscripts ^{1} and ^{0} indicate that repair has been performed or not performed after earlier inspections, respectively. $\Delta P_{FS}(T_i, t)$ denotes the probability of failure in the time interval from T_i to t.

For $0 \leq t \leq T_1$:

$$P_{FS}(t) = P\big(M_{F1}(t) \leq 0 \bigcup M_{F2}(t) \leq 0 \bigcup M_{F3}(t) \leq 0\big) \tag{4.26}$$

For $T_1 < t \leq T_2$:

$$\begin{aligned} P_{FS}(t) &= P_{FS}(T_1) + \Delta P_{FS}(T_1, t) \\ &= P_{FS}(T_1) + \Delta P^0_{FS}(T_1, t) + \Delta P^1_{FS}(T_1, t) \\ &= P_{FS}(T_1) \\ &+P\big(M_{F1}(T_1) > 0 \bigcap M_{F2}(T_1) > 0 \bigcap M_{F3}(T_1) > 0 \bigcap H > 0 \\ &\bigcap \big(M^0_{F1}(t) \leq 0 \bigcup M^0_{F2}(t) \leq 0 \bigcup M^0_{F3}(t) \leq 0\big)\big) \\ &+P\big(M_{F1}(T_1) > 0 \bigcap M_{F2}(T_1) > 0 \bigcap M_{F3}(T_1) > 0 \bigcap H \leq 0 \\ &\bigcap \big(M^1_{F1}(t) \leq 0 \bigcup M^1_{F2}(t) \leq 0 \bigcup M^1_{F3}(t) \leq 0\big)\big) \end{aligned} \tag{4.27}$$

For $T_2 < t \leq T_3$:

$$\begin{aligned} P_{FS}(t) &= P_{FS}(T_2) + \Delta P_{FS}(T_2, t) \\ &= P_{FS}(T_2) + \Delta P^{00}_{FS}(T_2, t) + \Delta P^{01}_{FS}(T_2, t) + \Delta P^{10}_{FS}(T_2, t) + \Delta P^{11}_{FS}(T_2, t) \\ &= P_{FS}(T_2) \\ &+P\big(M_{F1}(T_1) > 0 \bigcap M_{F2}(T_1) > 0 \bigcap M_{F3}(T_1) > 0 \bigcap H > 0 \\ &\bigcap M^0_{F1}(T_2) > 0 \bigcap M^0_{F2}(T_2) > 0 \bigcap M^0_{F3}(T_2) > 0 \bigcap H^0 > 0 \\ &\bigcap \big(M^{00}_{F1}(t) \leq 0 \bigcup M^{00}_{F2}(t) \leq 0 \bigcup M^{00}_{F3}(t) \leq 0\big)\big) \\ &+P\big(M_{F1}(T_1) > 0 \bigcap M_{F2}(T_1) > 0 \bigcap M_{F3}(T_1) > 0 \bigcap H > 0 \\ &\bigcap M^0_{F1}(T_2) > 0 \bigcap M^0_{F2}(T_2) > 0 \bigcap M^0_{F3}(T_2) > 0 \bigcap H^0 \leq 0 \\ &\bigcap \big(M^{01}_{F1}(t) \leq 0 \bigcup M^{01}_{F2}(t) \leq 0 \bigcup M^{01}_{F3}(t) \leq 0\big)\big) \\ &+P\big(M_{F1}(T_1) > 0 \bigcap M_{F2}(T_1) > 0 \bigcap M_{F3}(T_1) > 0 \bigcap H \leq 0 \\ &\bigcap M^1_{F1}(T_2) > 0 \bigcap M^1_{F2}(T_2) > 0 \bigcap M^1_{F3}(T_2) > 0 \bigcap H^1 > 0 \\ &\bigcap \big(M^{10}_{F1}(t) \leq 0 \bigcup M^{10}_{F2}(t) \leq 0 \bigcup M^{10}_{F3}(t) \leq 0\big)\big) \\ &+P\big(M_{F1}(T_1) > 0 \bigcap M_{F2}(T_1) > 0 \bigcap M_{F3}(T_1) > 0 \bigcap H \leq 0 \\ &\bigcap M^1_{F1}(T_2) > 0 \bigcap M^1_{F2}(T_2) > 0 \bigcap M^1_{F3}(T_2) > 0 \bigcap H^1 \leq 0 \\ &\bigcap \big(M^{11}_{F1}(t) \leq 0 \bigcup M^{11}_{F2}(t) \leq 0 \bigcup M^{11}_{F3}(t) \leq 0\big)\big) \end{aligned} \tag{4.28}$$

R_i is the number of repairs for a girder at inspection time T_i. R_i is equal to zero or one as not more than one repair can take place at one inspection, therefore, the expected value of R_i, $E_S[R_i]$, is the same as the probability of repair. $E_S[R_i]$ for the first three inspections is calculated as

$$E_S[R_1] = P\big(M_{F1}(T_1) > 0 \bigcap M_{F2}(T_1) > 0 \bigcap M_{F3}(T_1) > 0 \bigcap H \leq 0\big) \tag{4.29}$$

$$\begin{aligned} E_S[R_2] &= E_S[R_2^0] + E_S[R_2^1] \\ &= P\big(M_{F1}(T_1) > 0 \bigcap M_{F2}(T_1) > 0 \bigcap M_{F3}(T_1) > 0 \bigcap H > 0 \\ &\bigcap M_{F1}^0(T_2) > 0 \bigcap M_{F2}^0(T_2) > 0 \bigcap M_{F3}^0(T_2) > 0 \bigcap H^0 \leq 0\big) \\ &+P\big(M_{F1}(T_1) > 0 \bigcap M_{F2}(T_1) > 0 \bigcap M_{F3}(T_1) > 0 \bigcap H \leq 0 \\ &\bigcap M_{F1}^1(T_2) > 0 \bigcap M_{F2}^1(T_2) > 0 \bigcap M_{F3}^1(T_2) > 0 \bigcap H^1 \leq 0\big) \end{aligned} \tag{4.30}$$

$$\begin{aligned} E_S[R_3] &= E_S[R_3^{00}] + E_S[R_3^{01}] + E_S[R_3^{10}] + E_S[R_3^{11}] \\ &= P\big(M_{F1}(T_1) > 0 \bigcap M_{F2}(T_1) > 0 \bigcap M_{F3}(T_1) > 0 \bigcap H > 0 \\ &\bigcap M_{F1}^0(T_2) > 0 \bigcap M_{F2}^0(T_2) > 0 \bigcap M_{F3}^0(T_2) > 0 \bigcap H^0 > 0 \\ &\bigcap M_{F1}^{00}(T_3) > 0 \bigcap M_{F2}^{00}(T_3) > 0 \bigcap M_{F3}^{00}(T_3) > 0 \bigcap H^{00} \leq 0\big) \\ &+P\big(M_{F1}(T_1) > 0 \bigcap M_{F2}(T_1) > 0 \bigcap M_{F3}(T_1) > 0 \bigcap H > 0 \\ &\bigcap M_{F1}^0(T_2) > 0 \bigcap M_{F2}^0(T_2) > 0 \bigcap M_{F3}^0(T_2) > 0 \bigcap H^0 \leq 0 \\ &\bigcap M_{F1}^{01}(T_3) > 0 \bigcap M_{F2}^{01}(T_3) > 0 \bigcap M_{F3}^{01}(T_3) > 0 \bigcap H^{01} \leq 0\big) \\ &+P\big(M_{F1}(T_1) > 0 \bigcap M_{F2}(T_1) > 0 \bigcap M_{F3}(T_1) > 0 \bigcap H \leq 0 \\ &\bigcap M_{F1}^1(T_2) > 0 \bigcap M_{F2}^1(T_2) > 0 \bigcap M_{F3}^1(T_2) > 0 \bigcap H^1 > 0 \\ &\bigcap M_{F1}^{10}(T_3) > 0 \bigcap M_{F2}^{10}(T_3) > 0 \bigcap M_{F3}^{10}(T_3) > 0 \bigcap H^{10} \leq 0\big) \\ &+P\big(M_{F1}(T_1) > 0 \bigcap M_{F2}(T_1) > 0 \bigcap M_{F3}(T_1) > 0 \bigcap H \leq 0 \\ &\bigcap M_{F1}^1(T_2) > 0 \bigcap M_{F2}^1(T_2) > 0 \bigcap M_{F3}^1(T_2) > 0 \bigcap H^1 \leq 0 \\ &\bigcap M_{F1}^{11}(T_3) > 0 \bigcap M_{F2}^{11}(T_3) > 0 \bigcap M_{F3}^{11}(T_3) > 0 \bigcap H^{11} \leq 0\big) \end{aligned} \tag{4.31}$$

These expressions are extensions of the expressions used in model 3.1 described in chapter 3. In model 3.1 failure and repair probabilities are given for a system consisting of one element, see e.g. PRODIM, 1988.

An optimal inspection strategy with regard to costs can be calculated for each girder using the objective function (the expected costs) and the calculation procedure as described in chapter 5. The probabilities shown above are used to calculated the expected costs. However, in the example it has been chosen to suggest an inspection strategy based on the failure probabilities alone without including the effect of inspections.

To be able to interpret the result of a reliability analysis, a requirement to the reliability of the structural system has to be set. A constant reliability level throughout the lifetime can be obtained by a constant failure rate defining the failure rate as the

probability density function for the time to failure

$$f_T(t) = \frac{dF_T(t)}{dt} = \frac{P(t \leq T \leq t + dt)}{dt} \tag{4.32}$$

where T is the time to failure (see Madsen et al., 1986). From a user's point of view it would be natural to set constraints on the failure rate for the structure. However, for the owner of the structure the important issue is the expected failure cost rather than the safety in itself and since the expected failure cost depends on the accumulated failure probability during the lifetime a constraint is normally set on the failure probability/the reliability index at the end of the lifetime. The failure rate and the failure probability are related as follows

$$P_F(t) = F_T(t) = \int_0^t f_T(t)dt \tag{4.33}$$

It shows that a constant failure rate during the lifetime gives a increasing failure probability (with a constant slope). In other words to obtain a certain maximum failure rate during the lifetime, the requirement to the failure probability should be a function of time being stricter at the beginning of the lifetime than at the end of the lifetime.

4.6 Example

A typical highway steel girder bridge designed according to AASHTO, 1989, is considered. However, the bridge is assumed not to be protected against corrosion. The bridge has a simple span of 24.4m and two lanes with traffic in the same direction and the cross-section is shown in figure 4.7. The material parameters, corrosion parameters and the model uncertainty variables are assumed to be log-normally distributed and the mean values and standard deviations are shown in table 4.2. The corrosion parameters are chosen corresponding to carbon steel in a marine environment but no correlation between A and B is assumed due to the very uncertain estimation of the coefficient of correlation (see table 4.1). The observations referred to in Albrecht and Naeemi, 1984, are made onshore nearby the coast. The truncation of A and B is chosen in accordance with Albrecht and Naeemi, 1984. For the model uncertainty variables the values used in Sørensen and Thoft-Christensen, 1988, are used but as they are not justified by any analyses they could just as well be neglected.

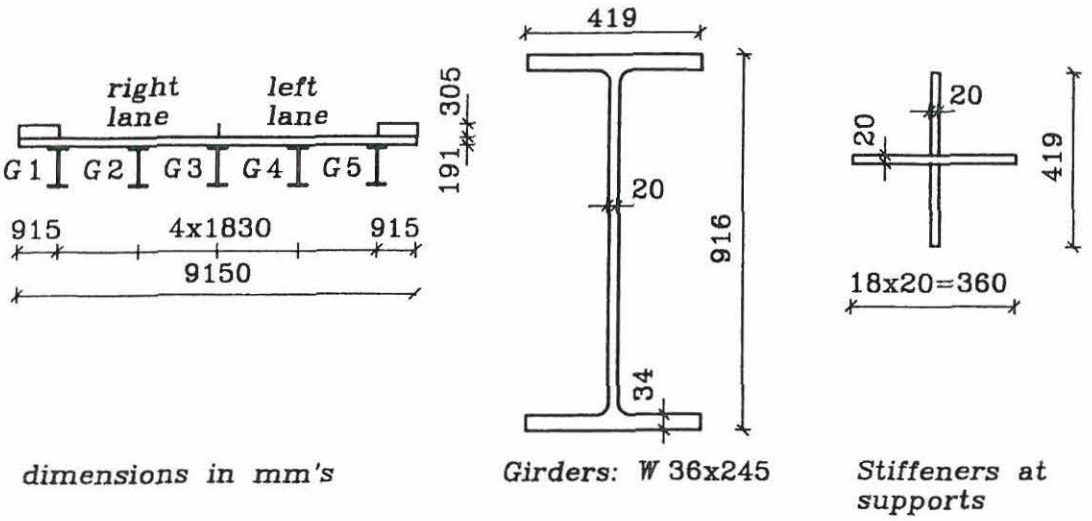

Figure 4.7 Bridge cross-section.

	μ	σ
Modulus of elasticity for steel, E	$2.1 \cdot 10^5 \text{N/mm}^2$	$2.1 \cdot 10^4 \text{N/mm}^2$
Yield stress in steel, f_y	248 N/mm^2	25 N/mm^2
Compr. strength in concrete, f_c	21 N/mm^2	4 N/mm^2
Corrosion parameter, A	$71 \cdot 10^{-3}$mm	$47 \cdot 10^{-3}$mm
$A < 200 \cdot 10^{-3}$mm		
Corrosion parameter, B	0.79	0.39
$B < 1.5$		
Model uncertainty variable, Z_1	1.0	0.10
Model uncertainty variable, Z_2	1.0	0.10
Model uncertainty variable, Z_3	1.0	0.10

Table 4.2 Values used in calculations (log-normal distributions).

The lifetime T is chosen as 75 years and the minimum reliability index $\beta^{\min} = 4.0$ at the end of the lifetime. The reliability index is defined in appendix 2.

A deterministic analysis using mean values of the material parameters showed that for each girder the nominal moment capacity is $M_n = 5249$ kNm, prior to any corrosion, the shear force capacity is $V_{sh} = 2428$ kN and the bearing capacity is $V_{be} = 3755$ kN. In the probabilistic analysis M_n, V_{sh} and V_{be} are calculated using the statistical parameters shown in table 4.2.

Dead Load

The dead load D is assumed to be normally distributed and the means and coefficients of variation of dead load are given in table 4.3.

	μ	σ
Interior girders (G2, G3, G4):		
Midspan moment, M_D	929 kNm	93 kNm
Shear load, V_D	152 kN	15 kN
Exterior girders (G1, G5):		
Midspan moment, M_D	1428 kNm	143 kNm
Shear load, V_D	234 kN	23 kN

Table 4.3 Dead load (normal distributions).

Traffic Load

Based on measurements of heavy truck traffic midspan moment distributions for bridges with simple spans have been calculated in Nowak, 1992. The moment-distributions are approximately log-normal. For a two lane bridge with a simple span of 24.4 m the mean maximum 75 year static live load is 5075 kNm. The live load L includes a static and dynamic component, the latter is 10% of the static live load. Therefore, the live load is 5583 kNm and the standard deviation is 1005 kNm (18% of the mean).

The distributions of transverse truck position within each lane were considered by Nowak et al., 1990, for a two lane bridge. The distributions are based on visual observations on interstate highway I-94 in Southeastern Michigan. Furthermore, it was observed that in 66% of the cases a truck was in the right lane, in 33% of the cases a truck was in the left lane and in 1% of the cases there were trucks in both lanes.

Hong, 1990, calculated the influence lines for midspan cross-sections with girders spaced at 1.2 to 3.0 m and bridge spans of 9, 18, 27 and 36m. The influence lines show the effect of the truck position across the bridge so knowing the midspan moment of the bridge and the corresponding truck position the moment in each girder can be found.

Based on these observations and calculations, the probability density function for the moment has been calculated for each girder as shown in figure 4.8, using the following procedure. The log-normally distributed live load moment, M_L, is discretized using increments of 250 kNm. First, the truck in the right lane is considered and the moment distribution for each girder is calculated for the various M_L values. Then similar calculations are made for the truck in the left lane and for two trucks side-by-side. The calculations are performed using the program shown in appendix 4 and for each case, the mean and standard deviation of M_L are shown in table 4.4.

	μ (kNm)	σ (kNm)
Girder G1:		
Truck in right lane	1772	425
Truck in left lane	431	144
Truck in both lanes	2066	473
Girder G2:		
Truck in right lane	1815	330
Truck in left lane	758	176
Truck in both lanes	2446	456
Girder G3:		
Truck in right lane	1357	261
Truck in left lane	1318	247
Truck in both lanes	2550	474
Girder G4:		
Truck in right lane	841	192
Truck in left lane	1833	333
Truck in both lanes	2549	475
Girder G5:		
Truck in right lane	497	135
Truck in left lane	1853	400
Truck in both lanes	2218	466

Table 4.4 Midspan moment M_L for live load (log-normal distributions).

The resulting density functions (see figure 4.8) are determined as

$$f^i_{M_L}(m_L) = 0.66 f^{i,R}_{M_L}(m_L) + 0.33 f^{i,L}_{M_L}(m_L) + 0.01 f^{i,RL}_{M_L}(m_L) \qquad (4.34)$$

where f_{M_L} is the probability density function for the live load moment and i is the girder number. Superscript R indicates a truck in the right lane, L a truck in the left lane and RL two trucks side-by-side.

The shear load at supports is calculated by assuming that the traffic load is uniformly distributed determining the load intensity from the midspan moments M_L. This is a conservative assumption and gives

$$V_L = \frac{4M_L}{l} = \frac{M_L}{6.1} \quad (m^{-1}) \qquad (4.35)$$

where l is the span length.

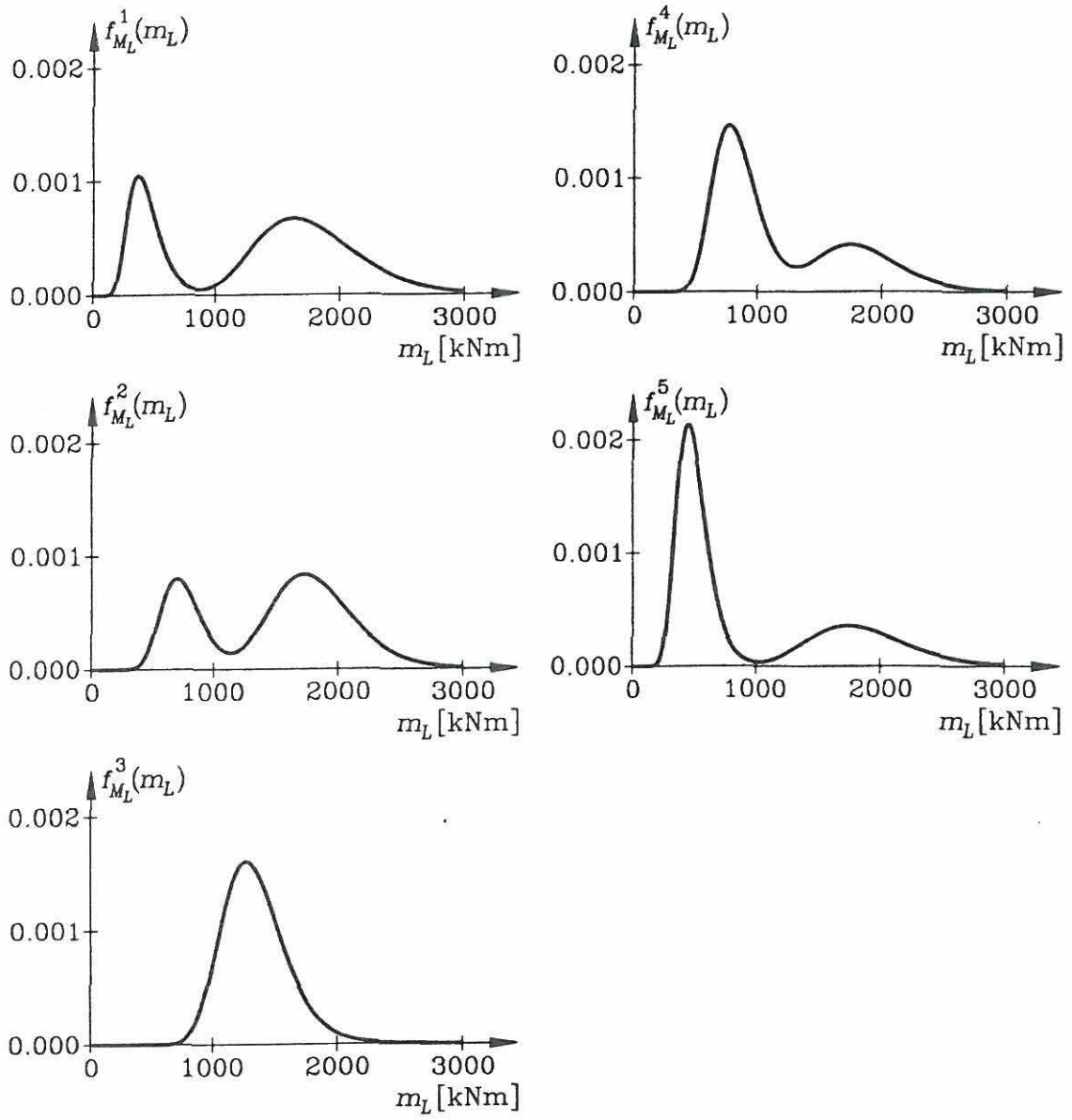

Figure 4.8 Probability density functions for midspan moments in girders $G1 - G5$.

Results

The reliability analyses were performed by the First Order Reliability Method (see appendix 2) using PROBAN-2 which is briefly described in chapter 6. Without inspection and repair, the reliability indices vary with time as shown in figure 4.9. The calculations show that the system reliability index is always close to the smallest of the element reliability indices, therefore, the system reliability index is not indicated in figure 4.9. It is interesting to observe that bending failure is the dominant failure mode for all girders in the first 10 years and after that shear failure becomes the dominant failure mode. This is in accordance with the corrosion model (see figure

4.1) as the web, which influences the shear capacity more than the bending capacity, is corroded on both sides.

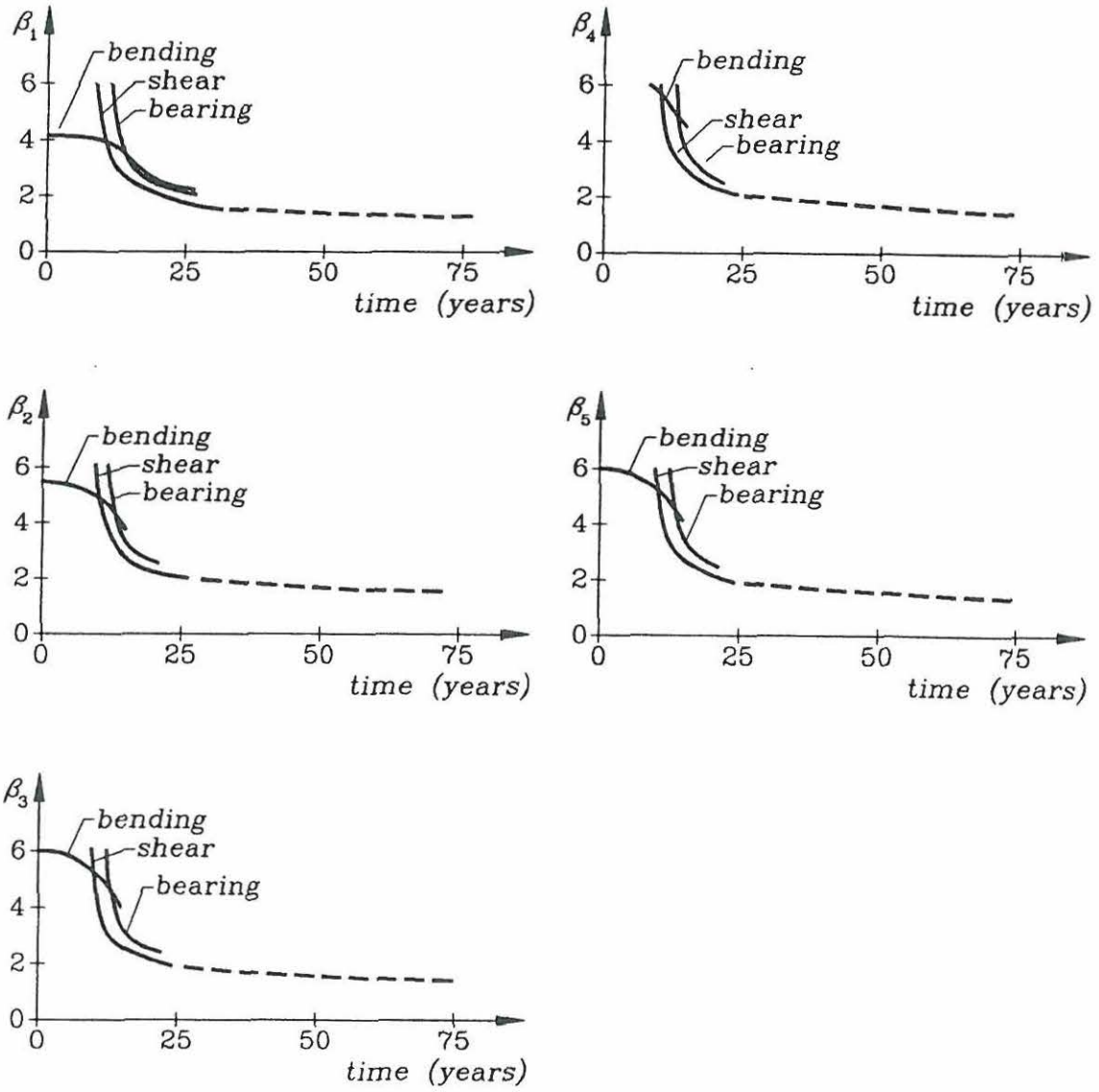

Figure 4.9 Reliability indices for girders $G1 - G5$.

It has not been possible to explain why the curves flatten out after 10-15 years and why the reliability index does not become negative until after 1000 years but it has been observed that the outcome of the corrosion parameters increases during the first 10-15 years and thereafter decreases, i.e. the outcome is biggest when the curves are steepest. This means that the reliability indices shown in figure 4.9 are probably only realistic for the first 10-15 years.

Sensitivity analyses showed that during the first 10 years the traffic load and the model uncertainty variables have the biggest influence on the reliability index. Afterwards, the corrosion parameters become most important and after 20 years it is

mainly the corrosion parameter B that influences the reliability index.

The analyses show that the reliability index for all girders decreases to $\beta^{min} = 4$ after 10 years even though the reliability index prior to corrosion is varying from 4.2 for girder $G1$ to 6.6 for girder $G4$. So for this bridge there is no reason for inspecting the girders with different intervals as suggested in section 4.4. From a designers point of view it is satisfactory to note that the girders are utilized to the same degree after the first 10 years.

Based on this, a reliability-based inspection strategy with an inspection interval of 8 years is suggested in figure 4.10. Using this strategy though, is no guarantee that the reliability index will not decrease to less than 4 during the lifetime. An improved reliability-based strategy could be found by updating the reliability after each inspection under the conservative assumption that no repairs are performed. As mentioned before an optimal inspection strategy could be found using the procedure described in chapter 5 and the expressions in section 4.5 and assuming a constant inspection interval the optimal solution would probably be an interval of between 5 and 10 years.

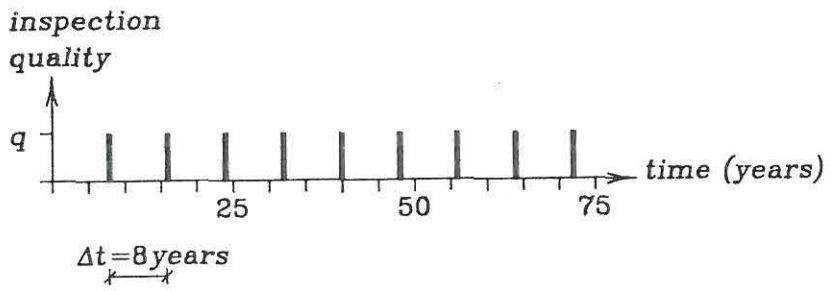

Figure 4.10 Inspection strategy.

4.7 Conclusions

Calculations are made for a bridge which is not protected against corrosion so the level of the reliability indices is probably not realistic. The live load modelling is simplified by assuming only one or two trucks on the bridge at a time. Highway bridges are typically inspected every 2 - 5 years which is more often than suggested here but if the reliability was updated after each inspection and fatigue was included in the calculations the inspection interval would possibly be found to be less than 8 years.

The procedure suggested whose aim is to inspect girders with different intervals based on the individual reliability indices turned out not to be relevant for the highway steel girder bridge considered since the reliability index reduces to the minimum reliability index at the same time for all girders. However, reliability calculations of the girders one at a time can be of value to the inspector indicating which girders are exposed to the greatest failure risk. The savings by not inspecting all girders at each inspection may be insignificant for a highway bridge.

The calculations can be improved in the following ways:

- The calculations can be refined by using different corrosion parameters in the girders. As mentioned at the beginning of this chapter, the first girder in the traffic direction will develop more corrosion due to salt and water splashed by the traffic. This has not been done due to the very uncertain estimation of the corrosion parameters.
- It is possible to include corrosion protection of the girders by assuming that the paint will last for a number of years after which the corrosion will start.
- Furthermore, analysis of the whole structural system could be made including the effect of redistribution of forces through the concrete slab. Then also the effect of redistribution of the load due to different corrosion in the girders could be included.
- As mentioned before it would be more realistic to consider the reliability problem as a first-passage problem which would probably increase the value of the reliability indices.

4.8 References

AASHTO (1989), *Standard Specifications for Highway Bridges,* American Association of State Highway and Transportation Officials, Washington D.C., 14th ed.

Albrecht, P.; A.H. Naeemi (1984), *Performance of Weathering Steel in Bridges,* Report 272, NCHRP, Transportation Research Board, Washington.

Hong, Y.K. (1990), *Live Load Models for Girder Bridges,* Ph.D. Thesis, Department of Civil Engineering, University of Michigan, Ann Arbor, MI, U.S.A.

Kayser, J.R. (1988), *The Effects of Corrosion on the Reliability of Steel Girder Bridges,* Ph.D. Thesis, Department of Civil Engineering, University of Michigan, Ann Arbor, MI, U.S.A.

Madsen, H.O.; S. Krenk; N.C. Lind (1986), *Methods of Structural Safety,* Prentice-Hall.

Nowak, A.S. (1992), *Calibration of LRFD Bridge Design Code*, Report submitted to NCHRP, Department of Civil Engineering, University of Michigan, Ann Arbor, MI, U.S.A.

Nowak, A.S.; Y.K. Hong; E.S. Hwang (1990), *Calculation of Load and Resistance Factors for OHBDC 1990,* Report UMCE 90-06, Department of Civil Engineering, University of Michigan, Ann Arbor, MI, U.S.A.

PRODIM, Theoretical Manual (1988), A.S. Veritas Research Report No. 88-2029, Høvik, Norway.

Salmon, C.G.; J.E. Johnson (1990), *Steel Structures, Design and Behaviour,* Harper & Row, New York, 3rd ed.

Sommer, A.M.; A.S. Nowak; P. Thoft-Christensen (1992), *Probability-Based Bridge Inspection Strategy*, Submitted to Journal of Structural Engineering, ASCE, U.S.A.

Sørensen, J.D.; P. Thoft-Christensen (1988), *Inspection Strategies for Concrete Bridges*, Proc. IFIP WG 7.5, Conference on Reliability and Optimization of Structural Systems (edt. P. Thoft-Christensen), Springer-Verlag, Lecture Notes in Engineering, Vol. 48, pp. 325-335.

CHAPTER 5
AN OPTIMAL INSPECTION STRATEGY FOR THE LONGITUDINALS IN A TANKER

5.1 Introduction

According to Løseth et al., 1992, the use of high-tensile steel in ship hulls has increased during the last decade having both positive and negative effects. On the one hand the steel weight and thereby the investment is reduced but on the other hand the repair cost is increased due to corrosion and fatigue cracks because the fatigue strength of high-tensile steel is almost the same as for mild steel so with reduced dimensions fatigue failure becomes more critical.

As described in chapter 2, steel ships are traditionally subject to inspections at short time intervals. Typically the ship hull will be inspected visually each year and examined carefully every 4 years. In this chapter optimal inspection strategies for the side longitudinals[1] in a tanker are considered. Longitudinals serve two purposes, firstly they stiffen the plates to which they are welded thereby reducing the deformations of the plates and secondly they contribute to the section modulus of the ship hull thereby reducing the stresses originating from the hull bending moment. The longitudinals can only be regarded as part of the hull cross-section if the connections between longitudinals and transverse structural elements such as bulkheads are designed so that the longitudinals can be regarded as being continuous. In figure 5.1 an example how to make a watertight connection between a longitudinal and a bulkhead is shown. In this case the longitudinal has an L-shaped cross-section and a corresponding slot is burned into the bulkhead. The example shows a longitudinal at the bottom of a ship hull.

Two kinds of deterioration of the longitudinals are described in this chapter - corrosion and fatigue cracks which are both important subjects to inspection. The reliability index as a function of time is calculated for two failure modes - yielding and fatigue, and an optimal inspection strategy is determined based on the yielding failure mode.

[1] Longitudinals denote stiffening, longitudinal beams welded on the ship hull.

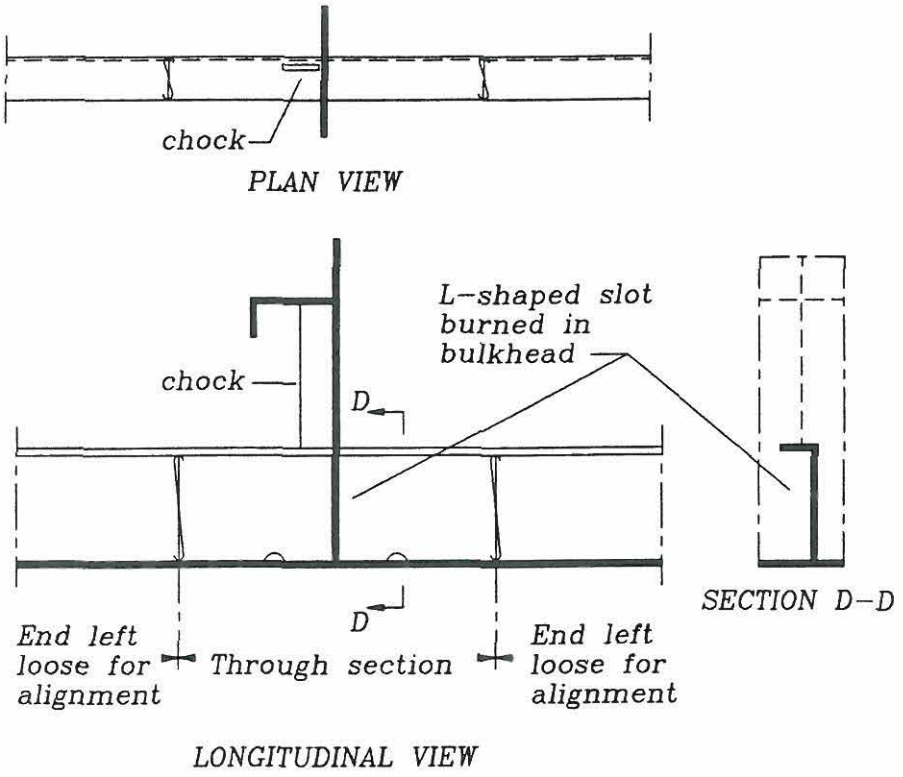

Figure 5.1 Watertight connection between longitudinal and bulkhead (Taggert et al., 1980).

5.2 Corrosion of Tankers

Corrosion is a serious problem for steel ships because of the harsh environment where the air is normally salty and humid. Since ship hulls for the most part are made of carbon steel (Recommended Practice.., 1972) the following will describe corrosion of carbon steel in a marine environment.

The most common forms of corrosion are according to Seawater Corrosion Handbook, 1979, general corrosion, galvanic corrosion, pitting and crevice corrosion. General corrosion is assumed uniformly distributed over the surface. Galvanic corrosion takes place when two different metals are placed in an electrolyte, e.g. seawater. Because of their different potentials one will function as an anode and the other as a cathode. Pitting is concentrated in a small area and it may be initiated by discrete salt particles or surface defects while crevice corrosion takes place in narrow spaces in the structure. Tensile stresses or cyclic tensile stresses will increase the rate of corrosion. In seawater the corrosion may be increased because of impingement, i.e. turbulent and bubbling water may destroy protective films or attack the metal locally, or because of cavitation, i.e. the pressure in the seawater is reduced to the vapour pressure because of high velocity, for example around a propeller. Then boiling occurs and

when the vapour bubbles collapse they may damage the metal.

In Seawater Corrosion Handbook, 1979, the corrosion in a marine environment is described in air as well as in water. In air the composition of the steel has a great effect on the rate of corrosion and the corrosion varies with the content of salt in the air. The most aggressive zone is the splash and tide zone where the metal is wet and in contact with oxygen, actually, the corrosion rate can be up to 10 times faster there than under water. In seawater the composition of the steel has no significant influence on the corrosion rate. A layer of rust protects the metal against further corrosion which means that water with a high velocity compared to the steel may increase the corrosion by removing the rust and by providing more oxygen. According to Recommended Practice.., 1972, a velocity of 10 knots may increase the rate of galvanic corrosion by 15 times compared to stagnant seawater.

Information about the rate of corrosion is rather sparse but in table 5.1 it is shown what is available about general corrosion from the references. As it appears, it is quite difficult to predict the corrosion rate because the observations are very diversified. The observations mentioned in Seawater Corrosion Handbook, 1979, and Albrecht and Naeemi, 1984, have been made near seawater on beaches and similar places. The only observations that have been made for the inside of tankers are in Condition Evaluation.., 1991, and in Løseth et al., 1992, but these observations show as much or more scattering as the remaining references.

Location	Corrosion rate (μm per year)
Seawater Corrosion Handbook, 1979:	
U.S.A., England, New Zealand, Panama	16 - 71
Kure Beach (N.C., U.S.A.)	439
Ceylon	1194
Albrecht and Naeemi, 1984:	
U.S.A, England	31 - 150
Chandler, 1985:	
Marine atmosphere	100
Splash zone	150 - 450
Low tide, seawater	100 - 150
Jansen, 1978:	
Hull, inside	200 - 300
Steel in seawater	300 - 500
Condition Evaluation.., 1991:	
Inside segregated ballast tanks	100 - 1200
Inside cargo/ballast tanks	30 - 700
Løseth et al., 1992:	
Inside tanks	50-350

Table 5.1 Corrosion of carbon steel in marine environments.

In a ship hull corrosion will take place first of all where water is caught, e.g. at the upper side of horizontal stiffeners or at the bottom of the hull. The example in figure 5.2 shows how the most severe corrosion develops in corners and where cut-outs allow water to run through.

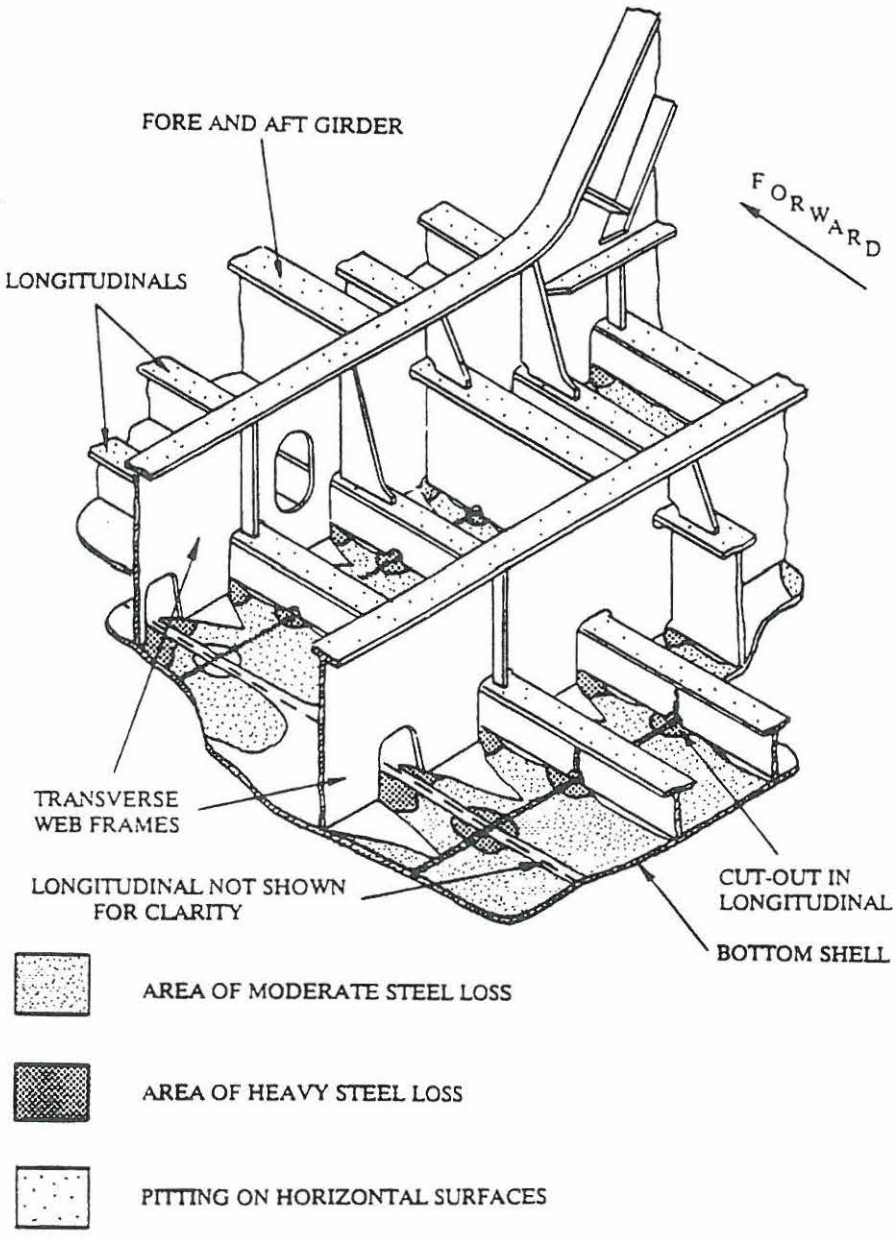

Figure 5.2 Typical wastage of bottom structure (Condition Evaluation.., 1991).

The temperature, the humidity and the salt content of the air influence the corrosion. For instance, in tankers and other large vessels the low temperature at the bottom of the hull will cause less corrosion at the bottom than at the top of the hull and in empty tanks next to tanks containing warm oil corrosion is increased. Furthermore, it has been observed that most corrosion takes place in water ballast tanks (as salt water is more aggressive than oil), some corrosion takes place in tanks for crude oil and only little corrosion takes place in tanks for oil products.

For longitudinals a so-called necking effect as illustrated in figure 5.3 can occur due to the combination of deflection caused by cyclic loading and accumulated water, mud etc.

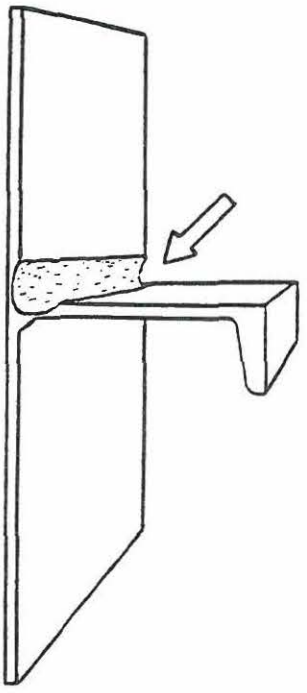

Figure 5.3 Corrosion of longitudinal in uncoated water ballast tank (Condition Evaluation.., 1991).

Corrosion Protection

Normally, the corrosion protection of a ship hull is chosen as a combination of hard coating, soft coating and sacrificial anodes (Condition Evaluation..., 1991).

Hard coating is e.g. paint, bitumastic or cement and the condition of this type of coating is described by a rating system. According to Condition Evaluation..., 1991, a good condition is characterized by only minor spot rusting, a fair condition is characterized by light rusting at 20% of the area and local breakdown at edges and weld connections, a poor condition is characterized by general rusting at 10% - 60% of the area and finally, a complete breakdown is characterized by rusting at more than 60% of the area. According to Løseth et al., 1992, epoxy coating in ballast tanks usually lasts for 8 - 13 years.

Soft coating is e.g. based on lanolin, oil or chemical reactions with the steel (Condition Evaluation..., 1991). Normally, these types of coating only lasts for two to four years and they are difficult to assess visually so they are recommended only to be used temporarily.

Areas that are immersed into water can be protected by sacrificial anodes. (cathodic protection) which are often used in combination with hard coating.

In Det Norske Veritas, 1992, two categories of corrosion protection systems characterized by different qualities and durabilities are specified. The specifications apply to hard coating of ballast tanks, oil cargo tanks and holds in newbuildings. For specification I the useful life of the coating is estimated to last 5 ± 3 years considering useful life to be until 20% of the coated surface is rusted (corresponding to a "fair" condition) and for specification II the useful life is estimated to last 10 ± 3 years. For these specifications the surface preparation, the type of coating and the maintenance requirements are specified for ballast tanks, oil cargo tanks and holds in bulk carriers/OBO. Since ballast tanks are more sensitive to corrosion than cargo tanks it is recommended that the coating in ballast tanks is combined with cathodic protection. According to Ferguson, 1991, it has been required by the classification societies since 1991 that protective coating in ballast tanks should be maintained and in Det Norske Veritas, 1992, it is specified for ballast tanks that maintenance should be carried out before 5% of the surface area is rusted.

Modelling of Corrosion

In the calculations in this chapter only general corrosion is considered since the other types of corrosion are quite difficult to model and very few observations are available. The corrosion rate is not constant with time and within the area of marine engineering the corrosion rate is traditionally modelled as a normally distributed parameter. For instance, in Løseth et al., 1992, probabilistic cost/benefit analyses of ship hulls have been performed using normally distributed corrosion rates with means of 50-350 μm per year and standard deviations of 10-80 μm per year. Furthermore, the mean corrosion rates are multiplied by a non-linear correction factor increasing from 0.3 during the first year to a maximum of 1.5. Here it has been chosen, however, to use the following model which is also used in chapter 4. In Albrecht and Naeemi, 1984, the propagation of general corrosion is approximated by an exponential function.

$$C(t) = At^B \tag{5.1}$$

where $C(t)$ is the average corrosion in microns (10^{-6} m's), t is the time in years and A and B are parameters to be determined from regression analysis of experimental data. In the calculations made later on in this chapter two sets of the corrosion parameters A and B are used. One set is based on the data in Albrecht and Naeemi, 1984, and another set is based on the data in Løseth et al., 1992. For a marine environment the mean μ, standard deviation σ and correlation coefficient ρ for the log-normally distributed parameters A and B are determined from the data in Albrecht and Naeemi, 1984, as

$\mu_A = 71$ μm per year $\quad \sigma_A = 47$ μm per year
$\mu_B = 0.79$ $\quad \sigma_B = 0.39$
$\rho_{AB} = -0.31$

By comparison to other environments and steel types it turns out that the correlation between A and B is very uncertain being positive as well as negative. Because of this the correlation is not taken into consideration in the calculations. From Løseth et al., 1992, only A is available but B is determined so that it corresponds to a correction factor of 1.5 (see above) after the lifetime which is 20 years. Both A and B are normally distributed.

$\mu_A = 200$ μm per year $\quad \sigma_A = 40$ μm per year
$\mu_B = 1.1$ $\quad \sigma_B = 0.1$

A cross-section of a tanker as shown in figure 5.4 is considered in this chapter and calculations are made for the longitudinals indicated. It is assumed that the ship hull is coated on the inside and that the coating will last for a number of years after which the corrosion propagation will start. Conservatively it is assumed here that the coating is not maintained unless a longitudinal is in such a bad state that a repair is needed. General corrosion is assumed to take place at all inner surfaces which means that the thickness of plates at the top, side and bottom will be reduced by $C(t)$ at the time t, see (5.1), and the thickness of longitudinal bulkheads and longitudinals will be reduced by $2C(t)$.

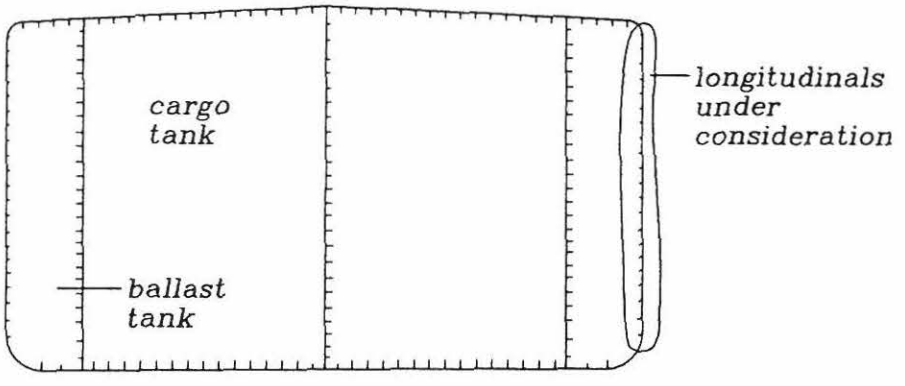

Figure 5.4 Cross-section of tanker.

5.3 Fatigue Cracks in Tankers

In SSC-318, 1983, it is stated that if the damage in ships is classified as either fatigue cracks, deformations or corrosion, surveys have shown that in ships over 200 m in length about 70% of the total damage is caused by fatigue while only about 20% of the damage is caused by fatigue in ships less than 200 m in length. Fatigue cracks propagate due to cyclic loading and, according to SSC-318, 1983, the factors that affect fatigue behaviour can be separated into three general categories namely geometry (i.e. general configuration and local geometry), loading conditions (e.g. constant amplitude cyclic loading, residual stresses, random loading and frequency

of loading) and finally, material strength. For instance, change of ship design has often caused problems due to fatigue cracking e.g. by introducing structural details with which the designer had no or little experience as described in Ferguson, 1991.

In Cracking of HTS.., 1991, the tendencies regarding fatigue cracks in tankers are listed. It has been observed that most cracks develop in the area from the load waterline (i.e. the mean water level when the oil tanks are full) to 8 m below the load waterline, that they are found mostly at the intersection of side longitudinals with the transverse bulkheads and that there are a lot of cracks in oil tanks but only a few in water ballast tanks. In agreement with this the side-structure of oil tankers is the most fatigue-prone area according to Ferguson, 1991.

In figure 5.5 an example is shown of a fracture at the connection between a longitudinal and a transverse bulkhead. Compared to figure 5.1 this connection has extra stiffening brackets but, nevertheless, a crack has developed because one bracket is too small. In figure 5.6 several different typical cracks are shown for connections between longitudinals and web frames. These connections are not watertight, which makes it possible to avoid overlapping welds and that makes the welding easier and reduces the risk of fatigue cracks. The illustration shows that cracks develop at cut-outs and other discontinuities in both welds and plates.

According to Cracking of HTS.., 1991, fatigue cracks in side longitudinals are mainly caused by cyclic loading due to wave pressure on the ship side, by relative transverse deflection between adjacent bulkheads and web frames inducing secondary stresses, by reduced scantlings in new tankers compared to old tankers due to the use of high-tensile steel, by asymmetric cross-sections of the longitudinals and by asymmetric stiffening of the connections between longitudinals and side transverses.

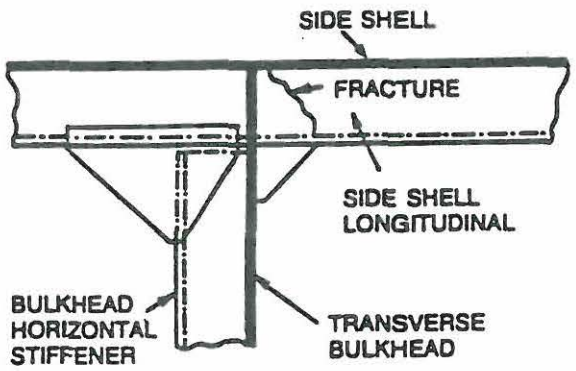

Figure 5.5 Fatigue crack in side shell longitudinal (Guidance Manual.., 1986).

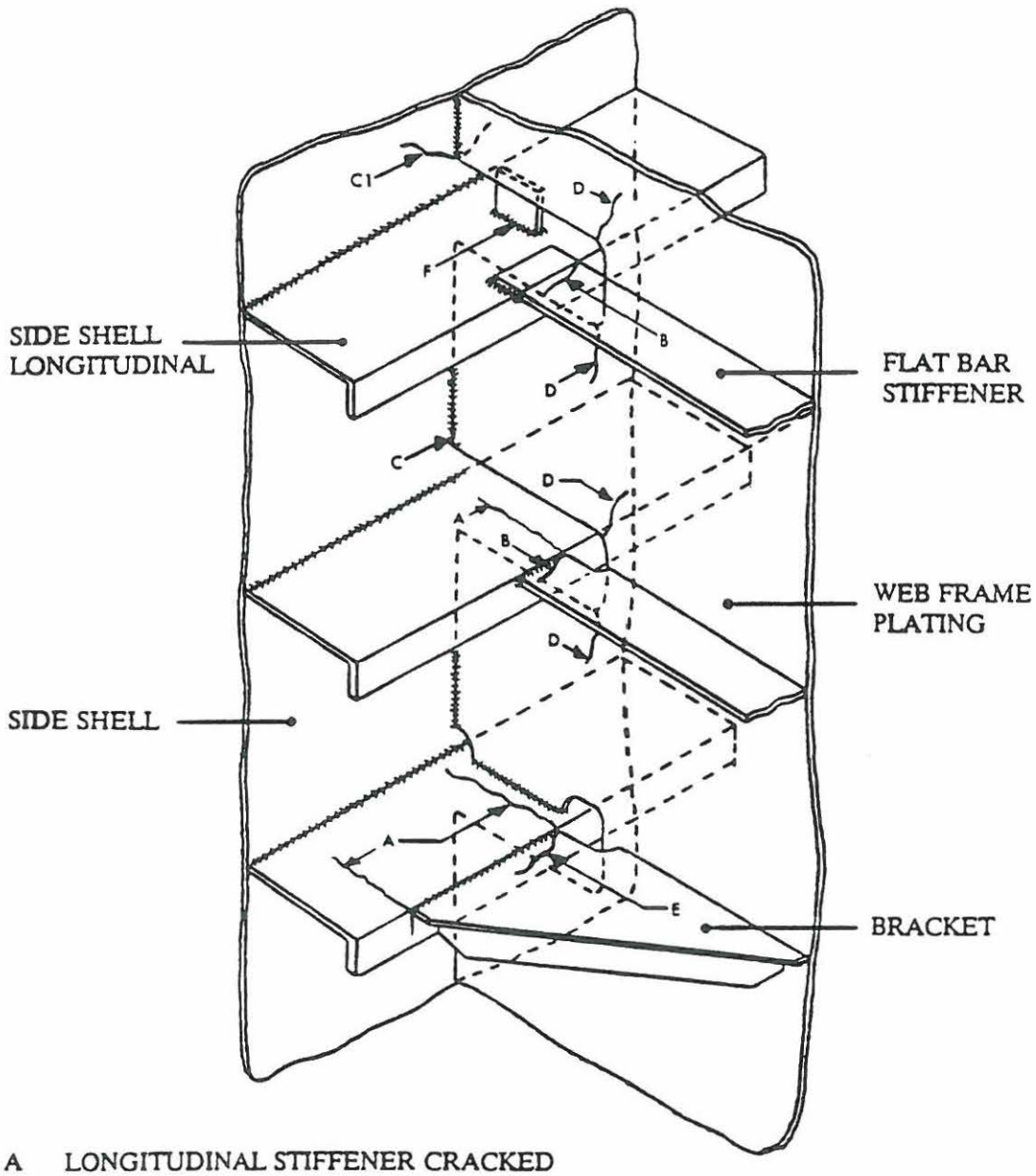

A LONGITUDINAL STIFFENER CRACKED
B FLAT BAR STIFFENER CRACKED
C SHELL PLATE TO WEB WELD CRACKED
C1 C CRACK EXTENDING INTO SHELL PLATE
D WEB FRAME CRACKED
E BRACKET CRACKED
F LUG CRACKED (TYPICAL DETAIL)

Figure 5.6 Fatigue cracks at side shell connections (Condition Evaluation.., 1991).

Modelling of Fatigue Cracks

As mentioned before most fatigue cracks are found in oil tanks and the cracks indicated in figure 5.5 and 5.6 are probably found in tankers with oil tanks at the ship side and not ballast tanks as it is the case for the tanker considered in this chapter (see figure 5.4). Considering a full oil tank at the ship side the level of the oil is higher than the mean water level at the outside of the ship, therefore, the side longitudinals are exposed to horizontal bending giving tension at the inside at the end-connections which is where cracks are observed. The stress range due to horizontal bending is calculated from the relative motion between the ship side and the water surface.

If a ballast tank is placed at the ship side the tank is empty at full cargo condition and the side longitudinals are exposed to horizontal bending giving tension at the outside at the end-connections. Therefore, it is assumed in this chapter that cracks propagate from the side shell into the longitudinals starting at cut-outs as e.g. shown in figure 5.1. It is not known to the author whether cracks have been observed or not at this position in ballast tanks.

If ballast condition is considered cracks may propagate from the inside as for oil tanks but then only a few longitudinals are exposed to fatigue as the draught is smaller. In Cracking of HTS.., 1991, it is mentioned that only a few cracks are found in water ballast tanks, but the location of the ballast tanks referred to is not described so it is not known whether the observations are typical for ballast tanks of the type considered here.

Propagation of fatigue cracks can e.g. be modelled by the Paris and Erdogan equation, see e.g. Madsen et al., 1986. The relation between the rate of crack growth per cycle and the load is based on linear elastic fracture mechanics

$$\frac{da}{dN} = C_{cra}(\Delta K)^m, \qquad \Delta K > 0 \tag{5.2}$$

where a is the crack length, N is the number of stress cycles, C_{cra} and m are material constants and ΔK is the range of the stress intensity factor.

$$\Delta K = \Delta\sigma Y(a)\sqrt{\pi a} \tag{5.3}$$

where $\Delta\sigma$ is the stress range and $Y(a)$ is the geometry function depending on the physical problem.

In the case considered here the fatigue crack problem can be simplified to the model shown in figure 5.7, i.e. the crack propagates from the edge of the longitudinal at the ship side, and the geometry function taken from Hellan, 1985, is

$$Y(a) = 1.12 - 1.39\frac{a}{h_l} + 7.3\left(\frac{a}{h_l}\right)^2 - 13\left(\frac{a}{h_l}\right)^3 + 14\left(\frac{a}{h_l}\right)^4 \tag{5.4}$$

where h_l is the width of the longitudinal.

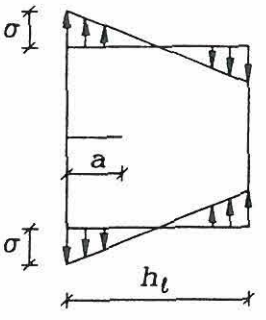

Figure 5.7 Through-crack in longitudinal.

5.4 Failure Modes

Two failure modes for the longitudinals at the ship side are considered namely yielding and fatigue cracks which both include the effect of corrosion. To describe these failure modes the load on the longitudinals is first evaluated. The longitudinals are welded to the ship side and to transverse bulkheads or web frames at certain intervals so the longitudinals are assumed fixed at the bulkheads and at the web frames even though they are only partly fixed. A conservative assumption is made in the calculations by assuming that the tanker is always at full cargo condition, i.e. the cargo tanks are full and the ballast tanks are empty. The effect of the relative deflection between adjacent bulkheads and web frames is neglected as it would require a three-dimensional finite element analysis of the ship hull to include it. Slamming at the ship side is neglected as this effect is only important at the bow, consequently, according to the Department of Ocean Engineering, Technical University of Denmark there are two main contributions to the load on the longitudinals:

1. The bending moment of the cross-section of the ship results in an axial stress in the longitudinals while the shear force results in a shear stress which is neglected.
2. The water pressure on the ship side results in a horizontal load on longitudinals underneath the water surface. Only the bending moment from this load is included in the calculations.

The total axial stress in the longitudinals then is

$$\sigma_{tot}(t) = Z_1\sigma_1(t) + Z_2\sigma_2(t) \tag{5.5}$$

where Z_1 and Z_2 are model uncertainty variables for calculating σ_1 and σ_2, respectively, σ_1 and σ_2 are the axial stress from load contributions 1 and 2, respectively.

Calculation of σ_1

$$\sigma_1(t) = \frac{M_h}{I_h(C(t))}(z_0(C(t)) - z) \tag{5.6}$$

where M_h is the bending moment in the hull around the horizontal axis (M_h is a stochastic process), I_h is the moment of inertia of the ship hull around the horizontal axis through the centre of gravity, z_0 is the vertical distance from the bottom of the ship hull to the centre of gravity, z is the vertical distance from the bottom of the ship hull to the longitudinal under consideration and C is the corrosion penetration (as a function of the time t). I_h and z_0 both depends on the dimensions of the ship cross-section so they are functions of the corrosion penetration C.

Calculation of σ_2

When calculating the stress σ_2 from the bending moment on the longitudinals some part of the ship side is included in the longitudinal cross-section, see figure 5.8. The L-shaped cross-section of the longitudinals is approximated to a rectangular cross-section.

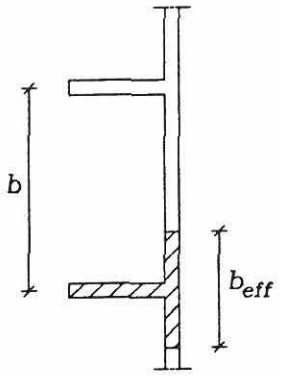

Figure 5.8 Cross-section of longitudinals.

The effective width b_{eff} (see figure 5.8) is according to Terndrup Pedersen and Jensen, 1983, assumed to be

$$b_{eff} = \min \begin{cases} b(1 - (\frac{K - L/b}{K})^3) \\ b \end{cases} \tag{5.7}$$

where b is the distance between longitudinals, K is a constant equal to 7 for a distributed load, L is the distance between moment zero points. For a fixed beam $L \simeq 0.6l$.

As mentioned earlier the corrosion takes place on inner surfaces giving the longitudinal cross-section as shown in figure 5.9.

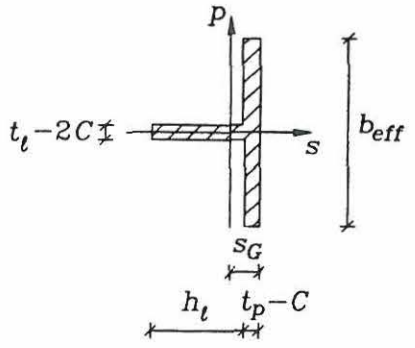

Figure 5.9 Effective cross-section of longitudinal.

The distance s_G to the centre of gravity is

$$s_G(C(t)) = \frac{(t_p - C)^2 b_{eff}/2 + h_l(t_l - 2C)(t_p - C + h_l/2)}{(t_p - C)b_{eff} + h_l(t_l - 2C)} \tag{5.8}$$

where t_p and t_l are the plate thicknesses of the ship side and the longitudinal, respectively, before corrosion has taken place.

The moment of inertia I_l around the p-axis is

$$I_l(C(t)) = \frac{1}{12}(b_{eff}(t_p - C)^3 + (t_l - 2C)h_l^3) + (t_p - C)b_{eff}(s_G - \frac{1}{2}(t_p - C))^2$$

$$+h_l(t_l - 2C)(h_l/2 + t_p - C - s_G)^2 \tag{5.9}$$

The water pressure is calculated from the depth of the water column above the longitudinal and this depth is calculated from the relative motion z_R between the ship side and the water surface, see figure 5.10. z_R is a stochastic process.

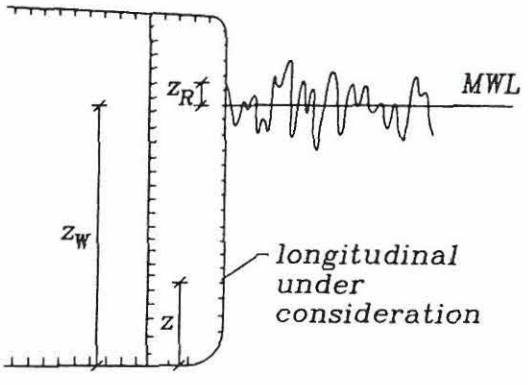

Figure 5.10 Ship side and water level.

Assuming a wave top the depth of the water column h_{top} is

$$h_{top} = \max \begin{cases} z_w + z_R - z \\ 0 \end{cases} \tag{5.10}$$

Assuming a wave trough the depth of the water column h_{trough} is

$$h_{trough} = \max \begin{cases} z_w - z_R - z \\ 0 \end{cases} \tag{5.11}$$

The expected depth h of the water column is

$$h = \frac{1}{2}(h_{top} + h_{trough}) \tag{5.12}$$

The water pressure p on the ship side is

$$p = h\rho g \tag{5.13}$$

where ρ is the density of salt water, g is the acceleration of gravity.

The line load q on a longitudinal is

$$q = pb \tag{5.14}$$

The sectional moment M_l is largest at the ends of the longitudinal, therefore, this section will be considered as regards yielding as well as fatigue failure. The sectional moment is

$$M_l = \frac{1}{12}ql^2 \tag{5.15}$$

The maximum tensile stress $\sigma_{2,t}$ is

$$\sigma_{2,t}(t) = \frac{M_l}{I_l(C(t))} s_G(C(t)) \tag{5.16}$$

The maximum compression stress $\sigma_{2,c}$ is

$$\sigma_{2,c}(t) = \frac{M_l}{I_l(C(t))}(h_l + t_p - C(t) - s_G(C(t))) \tag{5.17}$$

Yielding Failure

It is assumed that the two load contributions (the hull moment and the relative motion between the ship side and the water surface) are uncorrelated. According to the Department of Ocean Engineering, Technical University of Denmark, this is the normal procedure in ship design. In Huss, 1990, these correlation coefficients have been calculated for bottom longitudinals for another ship type (double bottom). The calculations showed negative correlations for the stresses at the bulkheads and

this indicates that the assumption of no correlation is conservative for the lowest longitudinals.

The yielding failure mode is defined as exceeding the yielding strength and the safety margin is

$$M_{F1}(t) = f_y - Z_1\sigma_1(t) - Z_2\sigma_{2,c}(t) = f_y - \sigma_{tot}(t) \tag{5.18}$$

It would be more correct to consider the longitudinals as compression members but in the example considered in section 5.8 the compression contribution σ_1 is so small compared to the bending contribution $\sigma_{2,c}$ so that it would only influence σ_{tot} by about 0.5%, i.e. the calculations are hardly influenced by this approximation.

First-Passage Problem

The model above has been used in the calculations in section 5.8 but it is not realistic as the reliability problem is in fact a first-passage problem. In section 5.8 the wave loads are based on long-term statistics but in the description below of the first-passage problem the wave loads are assumed to be modelled by extreme-value distributions based on short-term statistics and M_h and z_R are not assumed to be uncorrelated.

Considering a first-passage problem and assuming that the barrier crossings are independent, the failure probability $P_F(t)$ and the upcrossing rate $\nu^+(\xi(t))$ can be calculated as explained in chapter 4, (4.1a) and (4.1b). In this case the barrier $\xi(t)$ is equal to f_y, i.e. it is not a function of time, and the stochastic process is σ_{tot}.

Considering longitudinals below the water level only and not including the model uncertainty variables Z_1 and Z_2, σ_{tot} can be written

$$\sigma_{tot}(t) = \sigma_1(t) + \sigma_{2,c}(t) = k_1(t)M_h(t) + k_2(t)z_R(t) + k_3(t) \tag{5.18a}$$

where k_1 is determined from (5.6) and k_2 and k_3 are determined from (5.8) - (5.17). k_1, k_2 and k_3 are functions of time due to the corrosion. M_h and z_R are assumed to be ergodic and stationary Gauss-processes, which is a usual approximation for wave loads, but σ_{tot} is not stationary because of the corrosion. This makes it rather complicated to determine the upcrossing rate so below the calculation procedure is explained for the following simplified case.

$$X(t) = k_1X_1(t) + k_2X_2(t) \tag{5.18b}$$

where X, X_1 and X_2 are ergodic and stationary Gauss-processes and k_1 and k_2 are constants.

A stochastic process $X(t)$ is said to be a Gauss-process if any set of stochastic variables $X(t_i)$, $i = 1, 2,...$ has a joint Gaussian distribution function.

Assuming that $\dot{\xi} \ll \dot{X}$ (for $\xi(t) = f_y$, $\dot{\xi} = 0$), the upcrossing rate is according to Madsen, 1989

$$\nu^+(\xi(t)) = \nu_o exp\left(-\frac{1}{2}\left(\frac{\xi(t) - \mu_x}{\sigma_x}\right)^2\right) \tag{5.18c}$$

where ν_o is the upcrossing rate of the mean level.

$$\nu_o = \frac{1}{2\pi}\sqrt{\frac{\lambda_2}{\lambda_o}} \tag{5.18d}$$

The spectral moments λ_j are defined by

$$\lambda_j = \int_0^\infty \omega^j S_X(\omega) d\omega, \quad j = 0, 1, 2... \tag{5.18e}$$

where ω is the angular frequency and $S_X(\omega)$ is the spectral density. A one-sided spectrum is considered.

The spectral density of X is

$$S_X(\omega) = k_1^2 S_{X_1}(\omega) + k_2^2 S_{X_2}(\omega) + 2k_1 k_2 S_{X_1 X_2}(\omega) \tag{5.18f}$$

where $S_{X_1}(\omega)$ is the spectral density of X_1, $S_{X_2}(\omega)$ is the spectral density of X_2 and $S_{X_1 X_2}(\omega)$ is the cross spectral density of X_1 and X_2.

$$S_{X_1 X_2}(\omega) = S^Q(\omega) H_{X_1}(\omega) \overline{H_{X_2}(\omega)} \tag{5.18g}$$

where $S^Q(\omega)$ is the spectral density of the excitation process and $H_{X_1}(\omega)$ and $H_{X_2}(\omega)$ are the frequency response functions of X_1 and X_2, respectively. The bar denotes complex conjugate.

The standard deviation is calculated as

$$\sigma_X^2 = \int_0^\infty S_X(\omega) d\omega \tag{5.18h}$$

After having calculated the expected value of X the upcrossing rate can be estimated using (5.18c) and the failure probability can be calculated using (4.1a).

Fatigue Crack Failure

The stress range is determined from the axial stresses σ_1 and σ_2 and since only tensile stresses contribute to fatigue crack development the stress range contribution from the hull moment is calculated as

$$\Delta\sigma_1(t) = \sigma_1(t) - 0 \tag{5.19}$$

The stress range contribution from the water pressure $\Delta\sigma_2$ is calculated as $\sigma_{2,t}$ but instead of h, Δh is used

$$\Delta h = h_{top} - h_{trough} \tag{5.20}$$

$$\Delta q = \Delta h \rho g b \tag{5.21}$$

$$\Delta M_l = \frac{1}{12}\Delta q l^2 \tag{5.22}$$

$$\Delta\sigma_2(t) = \Delta\sigma_{2,t}(t) = \frac{\Delta M_l}{I_l(C(t))} s_G(C(t)) \tag{5.23}$$

The crack propagation is described by the Paris and Erdogan equation and by inserting (5.3) in (5.2) and separating the variables the equation is reformulated

$$\frac{da}{(Y(a)\sqrt{\pi a})^m} = C_{cra}(\Delta\sigma(t))^m dN \tag{5.24}$$

The safety margin M_{F2} is defined as exceeding a critical crack size by introducing a damage function $\Psi(a)$, see e.g. Madsen et al., 1986.

$$M_{F2}(t) = \Psi(a_c) - \Psi(a_t) \tag{5.25}$$

$$\Psi(a_c) = \int_{a_0}^{a_c} \frac{da}{(Y(a)\sqrt{\pi a})^m} \tag{5.26}$$

where a_c is the critical crack size and a_0 is the initial crack size.

$$\Psi(a_t) = \int_{a_0}^{a_t} \frac{da}{(Y(a)\sqrt{\pi a})^m} \tag{5.27}$$

where a_t is the crack size at the time t.

$\Psi(a_t)$ is rearranged using (5.24)

$$\Psi(a_t) = \int_{\nu_0 t_0}^{\nu_0 t} C_{cra}(\Delta\sigma(t))^m dN \tag{5.28}$$

where ν_0 is the number of stress cycles per time unit, t_0 is the initial time and t is the actual time. An exact calculation involves the calculation of the cross spectral density function for the two load contributions, which is rather complicated as explained above. Here it is assumed conservatively that the two load contributions are fully correlated and that the damage function is

$$\begin{aligned}\Psi(a_t) &= \int_{\nu_0 t_0}^{\nu_0 t} C_{cra}(\Delta\sigma_1(t) + \Delta\sigma_2(t))^m dN \\ &\simeq C_{cra} E[(\Delta\sigma_1(t) + \Delta\sigma_2(t))^m]\nu_0(t - t_0)\end{aligned} \tag{5.29}$$

This expression could either be calculated numerically or analytically. The assumption is made that the relation $\frac{\Delta\sigma_1}{\Delta\sigma_2} = k_\sigma$ is a constant which must be a good approximation considering $\Delta\sigma_1$ and $\Delta\sigma_2$ are assumed to be fully correlated. This relation is inserted in (5.29)

$$\begin{aligned}\Psi(a_t) &\simeq C_{cra} E[((1 + k_\sigma)\Delta\sigma_2(t))^m]\nu_0(t - t_0) \\ &= C_{cra}(1 + k_\sigma)^m E[(\Delta\sigma_2(t))^m]\nu_0(t - t_0)\end{aligned} \tag{5.30}$$

Finally, (5.30) is rearranged as

$$\Psi(a_t) \simeq C_{cra}\left((1+k_\sigma)\frac{\rho g b l^2}{12}\right)^m E\left[\frac{s_G(C(t))\Delta h^m}{I_l(C(t))}\right]\nu_0(t-t_0) \qquad (5.31a)$$

In the calculations in section 5.8, however, the following expression, which is not quite correct, is used

$$\Psi(a_t) \simeq C_{cra}\left((1+k_\sigma)\frac{s_G(C(t))\rho g b l^2}{12 I_l(C(t))}\right)^m E[\Delta h^m]\nu_0(t-t_0) \qquad (5.31b)$$

Δh is calculated from z_R and $E[\Delta h^m]$ is calculated numerically in the example.

5.5 Inspection Strategy

A procedure similar to the one described in chapter 4 is suggested for the inspection planning (see section 4.4). The different longitudinals in the ship side are subjected to different loads, they have different thicknesses and they may corrode at different speeds because of lower temperatures at the bottom of the hull than at the top. Therefore, it may be profitable to inspect the longitudinals at different time intervals. Consequently, the longitudinals are divided into two or three groups with failure probabilities of the same order in each group and in each group all the longitudinals will get the same inspection schedule calculated by minimizing the expected costs of inspection, repair and failure.

An event margin describing whether repair is performed or not after each inspection is defined assuming that repair is performed when corrosion has reduced the longitudinal thickness to a critical thickness. The event margin is

$$H(t) = Z_3(t_l - 2C) - t_{l,cr} \qquad (5.32)$$

where Z_3 is a variable modelling the uncertainty in estimating the longitudinal thickness and $t_{l,cr}$ is the critical longitudinal thickness.

5.6 Reliability of Longitudinals

Failure of a longitudinal can be modelled as a series system with two failure elements corresponding to the two failure modes. Here it is chosen to include only one element, namely yielding failure, and base the inspection strategy on that failure mode. When calculating the inspection strategy the probability of failure P_F at any time and the probability of repair at inspection times are needed. For the first three inspection intervals these probabilities are shown below (taken from PRODIM, 1988). The superscripts ^{1} and ^{0} indicate that repair has been performed or not performed after earlier inspections, respectively. $\Delta P_F(T_i, t)$ denotes the probability of failure in the time interval from T_i to t, M_F is the safety margin for the failure mode under consideration and H is the event margin for repair.

For $0 \leq t \leq T_1$:

$$P_F(t) = P(M_F(t) \leq 0) \tag{5.33}$$

For $T_1 < t \leq T_2$:

$$\begin{aligned} P_F(t) &= P_F(T_1) + \Delta P_F(T_1, t) \\ &= P_F(T_1) + \Delta P_F^0(T_1, t) + \Delta P_F^1(T_1, t) \\ &= P_F(T_1) \\ &+P(M_F(T_1) > 0 \bigcap H > 0 \bigcap M_F^0(t) \leq 0) \\ &+P(M_F(T_1) > 0 \bigcap H \leq 0 \bigcap M_F^1(t) \leq 0) \end{aligned} \tag{5.34}$$

For $T_2 < t \leq T_3$:

$$\begin{aligned} P_F(t) &= P_F(T_2) + \Delta P_F(T_2, t) \\ &= P_F(T_2) + \Delta P_F^{00}(T_2, t) + \Delta P_F^{01}(T_2, t) + \Delta P_F^{10}(T_2, t) + \Delta P_F^{11}(T_2, t) \\ &= P_F(T_2) \\ &+P(M_F(T_1) > 0 \bigcap H > 0 \bigcap M_F^0(T_2) > 0 \bigcap H^0 > 0 \bigcap M_F^{00}(t) \leq 0) \\ &+P(M_F(T_1) > 0 \bigcap H > 0 \bigcap M_F^0(T_2) > 0 \bigcap H^0 \leq 0 \bigcap M_F^{01}(t) \leq 0) \\ &+P(M_F(T_1) > 0 \bigcap H \leq 0 \bigcap M_F^1(T_2) > 0 \bigcap H^1 > 0 \bigcap M_F^{10}(t) \leq 0) \\ &+P(M_F(T_1) > 0 \bigcap H \leq 0 \bigcap M_F^1(T_2) > 0 \bigcap H^1 \leq 0 \bigcap M_F^{11}(t) \leq 0) \end{aligned} \tag{5.35}$$

R_i is the number of repairs for a girder at inspection time T_i and R_i is equal to zero or one as not more than one repair can take place at one inspection. Therefore, the expected value of R_i, $E[R_i]$, is the same as the probability of repair. $E[R_i]$ for the first three inspections is calculated as

$$E[R_1] = P(M_F(T_1) > 0 \bigcap H \leq 0) \tag{5.36}$$

$$\begin{aligned} E[R_2] &= E[R_2^0] + E[R_2^1] \\ &= P(M_F(T_1) > 0 \bigcap H > 0 \bigcap M_F^0(T_2) > 0 \bigcap H^0 \leq 0) \\ &+P(M_F(T_1) > 0 \bigcap H \leq 0 \bigcap M_F^1(T_2) > 0 \bigcap H^1 \leq 0) \end{aligned} \tag{5.37}$$

$$\begin{aligned} E[R_3] &= E[R_3^{00}] + E[R_3^{01}] + E[R_3^{10}] + E[R_3^{11}] \\ &= P(M_F(T_1) > 0 \bigcap H > 0 \bigcap M_F^0(T_2) > 0 \bigcap H^0 > 0 \bigcap M_F^{00}(T_3) > 0 \bigcap \\ &H^{00} \leq 0) \\ &+P(M_F(T_1) > 0 \bigcap H > 0 \bigcap M_F^0(T_2) > 0 \bigcap H^0 \leq 0 \bigcap M_F^{01}(T_3) > 0 \bigcap \\ &H^{01} \leq 0) \\ &+P(M_F(T_1) > 0 \bigcap H \leq 0 \bigcap M_F^1(T_2) > 0 \bigcap H^1 > 0 \bigcap M_F^{10}(T_3) > 0 \bigcap \\ &H^{10} \leq 0) \\ &+P(M_F(T_1) > 0 \bigcap H \leq 0 \bigcap M_F^1(T_2) > 0 \bigcap H^1 \leq 0 \bigcap M_F^{11}(T_3) > 0 \bigcap \\ &H^{11} \leq 0) \end{aligned} \tag{5.38}$$

5.7 Optimization Problem

The optimal inspection strategy with regard to costs is determined for the longitudinals and for each longitudinal the objective function is defined as the expected total costs in the lifetime T, i.e. the sum of the expected inspection cost, repair cost and failure cost. If failure occurs it is assumed that the longitudinal cannot be repaired. The optimization variables are the inspection intervals t_i and the number of inspections n and the optimal number of inspections is found by solving the optimization problem for different values of n. Constraints are related to the reliability index $\beta(t)$ and to the inspection intervals. The optimization problem for each longitudinal is (see PRODIM, 1988)

$$\min_{t_1,\ldots,t_n} \quad \sum_{i=1}^{n}(C_I(1-P_F(T_i))+C_R E[R_i])\frac{1}{(1+r)^{T_i}} \tag{5.39}$$

$$+\sum_{i=1}^{n+1} C_F(P_F(T_i)-P_F(T_{i-1}))\frac{1}{(1+r)^{T_i}}$$

subject to

$$\beta(T) \geq \beta^{\min}$$
$$t^{\min} \leq T - \textstyle\sum_{i=1}^{n} t_i \leq t^{\max}$$
$$t^{\min} \leq t_i \leq t^{\max}$$

where C_I is the inspection cost per inspection, C_R is the repair cost per repair and C_F is the failure cost. r is the real rate of interest, $\beta^{\min}$ is the minimum reliability index at the end of the lifetime, $t^{\min}$ is the minimum inspection interval and $t^{\max}$ is the maximum inspection interval.

As an alternative the inspection intervals can be chosen to be constants and then n is the only optimization variable. To rationalize the inspections the longitudinals can, as mentioned earlier, be divided into two or three groups using the same inspection strategy for all longitudinals in each group.

5.8 Example

Calculations have been made for a typical tanker being a 50,000 DWT crude/product carrier with the characteristics shown in table 5.2. A longitudinal section of the ship is shown in figure 5.11 and the cross-section is shown in figure 5.12. All inner surfaces of the ship hull is assumed to be protected against corrosion, i.e. coated and the coating is assumed to last for a number of years after which the corrosion starts to propagate.

Length o.a. (overall)	182.53 m
Length p.p. (between perpendiculars)	173.50 m
Width moulded at DWL	32.30 m
Depth moulded at DWL	17.80 m
Lowest draught (ballast)	6.50 m
Highest draught	13.29 m
Corresponding deadweight	50,000 t

Table 5.2 Crude/product carrier 50,000 DWT.

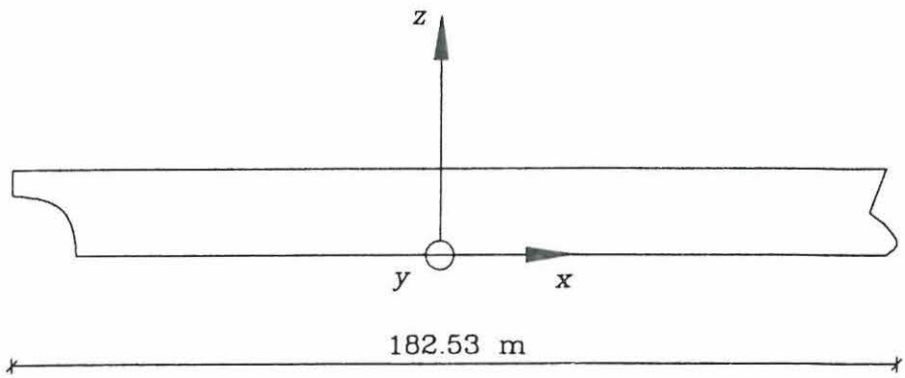

Figure 5.11 Longitudinal section.

The cross-section is modelled by panels connected at the nodal points shown in figure 5.12. Only the numbered panels are used in the model due to the symmetry of the cross-section. Each panel has a constant plate thickness and equidistant longitudinals of the same depth and thickness. In the calculations the cross-section of the longitudinals is assumed to be rectangular. The dimensions are given in table 5.3.

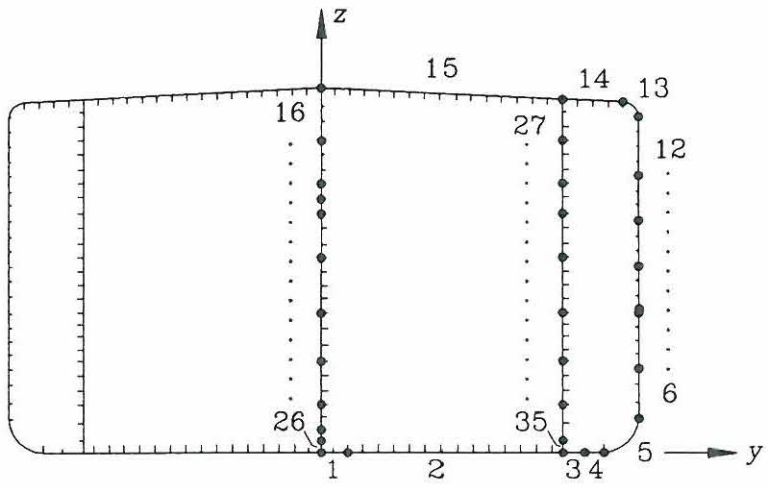

Figure 5.12 Cross-section with panel numbers.

The longitudinals are fixed at bulkheads at 16 m intervals and in between they are fixed at web frames at 4 m intervals, i.e. the length is set to 4 m. The distance between the longitudinals in the ship side is $b = 760$ mm and the effective width (see (5.7)) is

$$b_{eff} = b\left(1 - \left(\frac{K - \frac{L}{b}}{K}\right)^3\right) = 760\left(1 - \left(\frac{7 - \frac{0.6 \cdot 4000}{760}}{7}\right)^3\right) = 634 \text{ mm} \qquad (5.40)$$

The draught at full cargo condition is $z_w = 13.29$ m.

Panel	Start node		End node		Plate	Longitudinals	
no.	y (m)	z (m)	y (m)	z (m)	t_p(mm)	h_l(mm)	t_l(mm)
1	0.00	0.00	1.40	0.00	17.5	320	14.0
2	1.40	0.00	12.50	0.00	15.5	400	15.0
3	12.50	0.00	13.41	0.00	15.5	260	12.0
4	13.41	0.00	14.30	0.00	15.5	400	15.0
5	14.30	0.00	16.10	1.80	15.5	-	-
6	16.10	1.80	16.10	4.41	14.0	340	15.0
7	16.10	4.41	16.10	7.16	13.5	340	13.0
8	16.10	7.16	16.10	7.31	13.5	300	13.0
9	16.10	7.31	16.10	9.59	13.0	300	13.0
10	16.10	9.59	16.10	11.87	13.0	280	13.0
11	16.10	11.87	16.10	14.15	13.0	260	12.0
12	16.10	14.15	16.10	17.18	13.0	240	11.0
13	16.10	17.18	15.45	17.83	13.0	-	-
14	15.45	17.83	12.50	17.97	13.0	240	12.0
15	12.50	17.97	0.00	18.56	13.5	240	12.0
16	0.00	18.56	0.00	15.96	14.0	240	11.0
17	0.00	15.96	0.00	13.71	11.0	240	11.0
18	0.00	13.71	0.00	12.96	11.0	260	12.0
19	0.00	12.96	0.00	12.21	13.0	260	12.0
20	0.00	12.21	0.00	9.96	13.0	280	13.0
21	0.00	9.96	0.00	7.16	12.5	300	13.0
22	0.00	7.16	0.00	4.70	12.5	340	13.0
23	0.00	4.70	0.00	2.45	13.5	340	15.0
24	0.00	2.45	0.00	1.20	14.0	340	15.0
25	0.00	1.20	0.00	0.60	14.0	280	13.0
26	0.00	0.60	0.00	0.00	14.0	250	17.7
27	12.50	17.97	12.50	15.96	10.5	240	11.0
28	12.50	15.96	12.50	13.71	10.0	240	11.0
29	12.50	13.71	12.50	12.21	10.0	260	12.0
30	12.50	12.21	12.50	9.96	10.0	280	13.0
31	12.50	9.96	12.50	7.16	11.0	300	13.0
32	12.50	7.16	12.50	4.70	11.5	340	13.0
33	12.50	4.70	12.50	2.45	12.5	340	15.0
34	12.50	2.45	12.50	0.60	13.0	340	15.0
35	12.50	0.60	12.50	0.00	13.0	250	17.7

Table 5.3 Panel dimensions.

5.8.1 Calculation of Loads

The loads are calculated using the ISH-DESIGN programmes at the Department of Ocean Engineering, Technical University of Denmark. The calculations are made in several steps:

1. FORMDA. In this program the outer shape of the ship is modelled.
2. SHIPIN. The program is used to make plots of the ship.
3. HYDRO. Hydrostatic calculations are made for ballast condition with TRIM = 2 m (TRIM = draught abaft - draught fore) and for full cargo condition with TRIM = 0 m. These calculations give among other things the displacement of the ship and the longitudinal centre of buoyancy.
4. STRIP. The ship motions and sea loads are calculated by the Korvin-Kroukovsky strip theory. Calculations are made for ballast and full conditions at two speeds; 4 knots (min. speed at harsh weather conditions) and 16 knots (normal speed), 5 different heading-angles; 0°, 45°, 90°, 135° and 180°, and 15 different wave lengths; varying from 0.40 to 2.50 times the length p.p. The program does not include sway (movement in the y-direction), yaw (rotation about the z-axis) and roll (rotation about the x-axis). For the different speeds, heading-angles and wave lengths the frequency of encounter and the following transfer functions are calculated: Heave (movement in the z-direction) and pitch (rotation about the y-axis). The shear force and bending moment at $\frac{lengtho.a.}{4}$ abaft midship, midship and $\frac{lengtho.a.}{4}$ forward of midship. The absolute acceleration, relative motion, relative velocity and absolute motion at $\frac{lengtho.a.}{4}$ forward of midship. The vertical exciting force and pitch exciting moment.
5. STATI. This program makes stationary stochastic predictions of loads in an irregular seaway (short time statistics). A Pierson-Moskowitz wave-spectrum and short crested waves are chosen. The stochastic predictions are made from the 5 heading-angles and the 15 wave lengths used in STRIP. Calculations are made for ballast and full condition at two speeds; 4 knots and 16 knots, 5 ship courses; 0°, 45°, 90°, 135° and 180° off the wave direction, and 10 dimensionless significant wave periods. For the different speeds, ship courses and significant wave periods the dimensionless standard deviations of the following responses are calculated; shear force, bending moment and relative motion at $\frac{lengtho.a.}{4}$ forward of midship. The section at $\frac{lengtho.a.}{4}$ forward of midship is chosen as being the section with the largest load.
6. NONSTA. This program makes non-stationary stochastic predictions of loads in an irregular seaway (long-term statistics). The stochastic predictions are made from the 2 speeds and 5 ship courses used in STATI combined with the wave heights corresponding to the shipping route from Rotterdam to the Persian Golf. The wave heights are known by the program when indicating how large a part of the time is spent in different Marsden Areas. The Marsden Areas where long-term observations have been made are shown in figure 5.13.

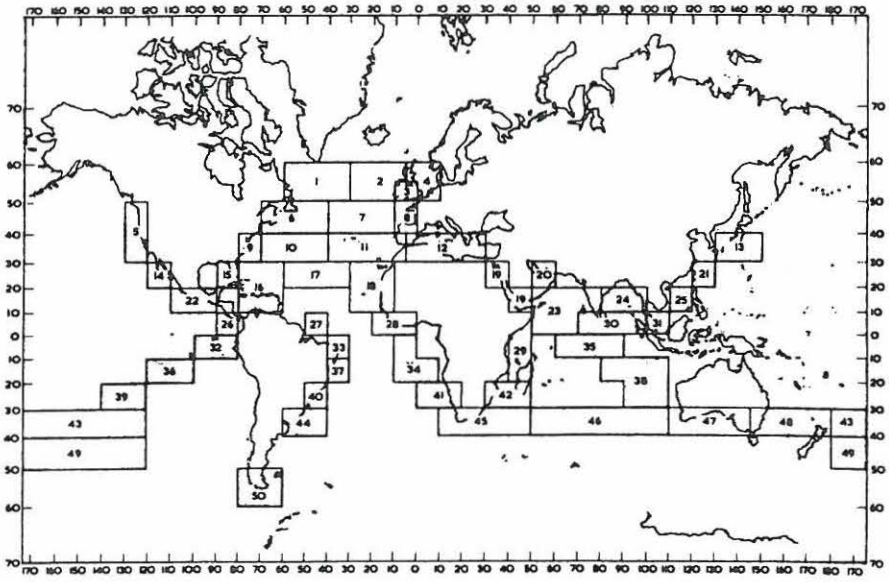

Figure 5.13 Marsden Areas (Terndrup Pedersen and Jensen, 1983).

The percentage of time spent in each Marsden Area is shown in table 5.4.

Marsden Area	Time factor (%)
4	4.3
8	8.7
11	8.7
12	26.1
19	26.1
23	8.7
20	13.0
Harbour	4.3

Table 5.4 Time spent in Marsden Areas.

For ballast and full condition the following responses are calculated; distributions for the amplitude of the shear force, the amplitude of the bending moment and the amplitude of the relative motion $\frac{lengtho.a.}{4}$ forward of midship. The calculations also show that the distributions are close to Weibull distributions and the Weibull parameters are calculated. The amplitude of the hull bending moment M_h for the full condition has the following distribution function

$$F_{M_h}(m_h) = 1 - \exp\left(-\left(\frac{m_h}{2.66 \cdot 10^7}\right)^{0.93}\right) \qquad \text{(Nm)} \qquad (5.41)$$

The axial stress σ_2 (see (5.16) and (5.17)) is calculated from the amplitude of the relative motion z_R for the full condition which has the following distribution

function

$$F_{Z_R}(z_R) = 1 - \exp\left(-\left(\frac{z_R}{0.318}\right)^{0.90}\right) \qquad \text{(m)} \qquad (5.42)$$

7. Using the cross-section shown in figure 5.12 the sectional properties, the shear stresses in each panel for a unit shear force Q_z and the axial stresses in each panel for a unit bending moment M_y are calculated by another ISH-DESIGN program. The beam theory for thin walls is used. The moment of inertia of the ship hull as a function of the corrosion penetration $I_h(C)$ and the centre of gravity of the ship hull as a function of the corrosion penetration $z_0(C)$ are found by calculating the moment of inertia and the centre of gravity for different plate thicknesses assuming that corrosion takes place on all inner surfaces of the ship hull. I_h and z_0 as a function of C are approximated to a third degree polynomial

$$I_h(C) = (-0.0026C^3 - 0.0110C^2 - 14.2270C + 139.3656) \cdot 10^{12} \qquad (\text{mm}^4) \quad (5.43)$$

$$z_0(C) = (-0.0027C^3 + 0.0021C^2 - 0.0585C + 8.3160) \cdot 10^3 \qquad (\text{mm}) \quad (5.44)$$

5.8.2 Reliability Calculations

In the reliability calculations the parameters shown in table 5.5 are used. For the model uncertainty variables the values used in Sørensen and Thoft-Christensen, 1988, are chosen which means they are chosen by judgement. To avoid numerical problems in the reliability calculations the standard deviation of the corrosion parameters is reduced compared to the statistics shown in section 5.2. The corrosion parameters are not truncated as in chapter 4, instead limits are introduced by not allowing outcomes above the limits in the reliability calculations. In some of the optimization calculations other values of the corrosion parameters A and B are used as explained later. For the initial crack size and the material parameters m and C_{cra} the values used in PROBAN-2, 1989, are chosen. The values of m and C_{cra} imply that units N and mm are used in the Paris and Erdogan equation. The critical crack size is chosen as a reasonable value compared to the depth of the side longitudinals which is 240 - 340 mm. The number of cycles per year is stated by the Department of Ocean Engineering, Technical University of Denmark. In the calculations it is assumed that the coating of the inside of the hull will last for about 9 years after which the corrosion will start to propagate, see table 5.5. A deterministic analysis using mean values of the stochastic variables shows that $\frac{\Delta\sigma_1}{\Delta\sigma_2} \simeq \frac{1.24}{4.21} = 0.29$ for the lowest longitudinal ($z = 1.800$ m) and smaller for the remaining longitudinals so $\frac{\Delta\sigma_1}{\Delta\sigma_2} = 0.29$ is used in (5.31).

The reliability index β as a function of the time t has been calculated for the two failure modes described in section 5.4 using PROBAN-2 which is briefly described in chapter 6. Results are shown in figure 5.14 for three different longitudinals. If the two failure modes are combined in a series system the system reliability index is close to the lowest element reliability index. Therefore, the system reliability index is not shown. The reliability index corresponding to yielding has the same tendency

to flatten out as a function of time as the reliability indices in chapter 4 but it does not show in figure 5.14 because the time does not exceed 20 years.

	Distrib.	μ	σ
Model uncertainty variable, Z_1	Log-normal	1.0	0.1
Model uncertainty variable, Z_2	Log-normal	1.0	0.1
Yield stress, f_y	Log-normal	353 N/mm^2	35 N/mm^2
Corrosion parameter, A $A \leq 400 \cdot 10^{-3}$ mm	Log-normal	$71 \cdot 10^{-3}$ mm	$30 \cdot 10^{-3}$ mm
Corrosion parameter, B $B \leq 1.6$	Log-normal	0.79	0.08
Density of salt water, ρ	Fixed	1025 kg/m^3	
Acc. of gravity, g	Fixed	9.82 m/s^2	
Initial crack size, a_0	Exponential	1.0 mm	0.999 mm
Critical crack size, a_c	Normal	100 mm	1 mm
Material parameter, m	Normal	3.0	0.3
Material parameter, lnC_{cra}	Normal	-29.75	0.50
Number of cycles per year, ν_0	Fixed	$5 \cdot 10^6$	
Initial time, T_0	Fixed	0 years	
Duration of coating, T_c	Normal	9 years	0.9 years

Coefficient of correlation for m and lnC_{cra} is -0.90.

Table 5.5 Parameters used in reliability calculations.

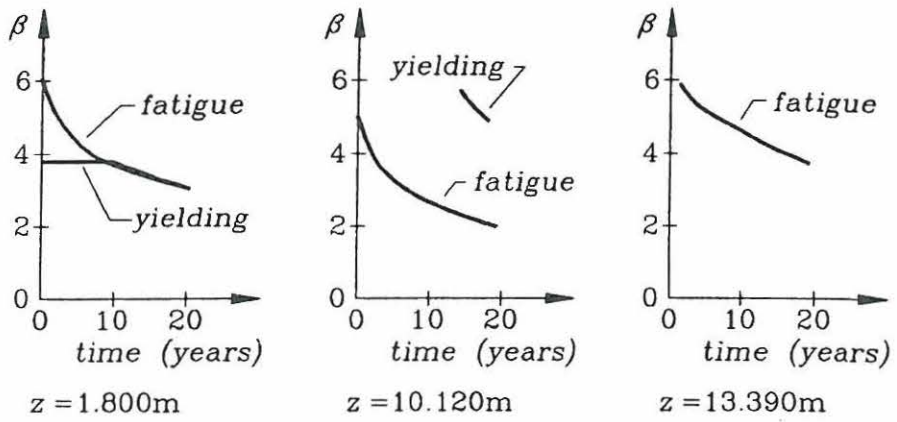

Figure 5.14 Reliability indices as a function of time.

The reliability index corresponding to fatigue failure β_F is decreasing from the bottom of the tanker to about 11 m above the bottom. This is caused by the longitudinal thicknesses getting smaller up the ship side. Above 11 m β_F increases because the stress range is decreased when a longitudinal is above the minimum water level (the troughs of the sea). The fact that the lowest β_F is found in a position a couple of

metres below the mean water level agrees with the observations that have been made in real life. The reliability index corresponding to yielding failure β_Y is generally increasing up the ship side because of the reduced water column. There are only minor exceptions when the longitudinal thickness is reduced.

In figure 5.15 the system reliability index β_S up the ship side is shown after 1 and 20 years. Except for the bottom longitudinals fatigue is the dominating failure mode. Before any corrosion or fatigue has developed the bottom longitudinal has the lowest β_S ($\beta_S = 3.9$) but after 20 years the longitudinal 10.120 m above the bottom has the lowest β_S. The β_S's for different longitudinals are quite alike. Based on the β_S after one year the longitudinals could be divided into three groups; longitudinals below $z = 3.0$ m with $\beta_S < 4.5$, longitudinals above $z = 3.0$ m and below $z = 13.0$ m with $4.5 < \beta_S < 6$ and finally longitudinals above $z = 13.0$ m with $\beta_S > 6$.

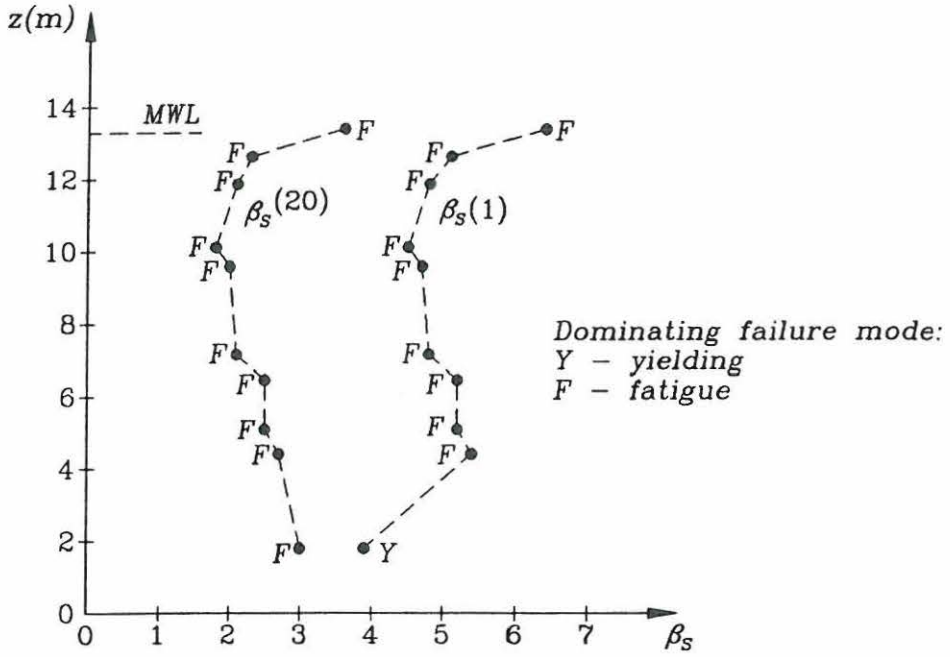

Figure 5.15 Reliability indices up the ship side after one year and after 20 years.

Of the two load contributions the water pressure on the ship side is dominating as the contribution from the hull bending moment is only about 1% of the contribution from the water pressure. This goes for the stresses calculated in the yielding failure function as well as for the damage functions calculated in the fatigue failure function.

5.8.3 Optimal Inspection Strategy

It is decided to base the inspection strategy on the yielding failure mode only. Therefore, the division of the longitudinals is made for $z = 4.0$ m and $z = 8.0$ m and in each group of longitudinals an optimal inspection strategy is calculated using the longitudinal with the lowest β_Y at $t = 1$ year, i.e. the longitudinals for $z = 1.800$ m, $z = 5.100$ m and $z = 8.070$ m.

Lifetime, T	20 years
Model uncertainty variable, Z_3 (log-normal)	$\mu = 1.0$ $\sigma = 0.1$
Critical longitudinal thickness, $t_{l,cr}$	$t_l - 2$ mm
Inspection cost per inspection, C_I	1
Repair cost per repair, C_R	10
Failure cost, C_F	100
Real interest rate, r	0.04
Minimum reliability index, $\beta^{\min}$	3
Minimum inspection interval, $t^{\min}$	1 year
Maximum inspection interval, $t^{\max}$	19 years

Table 5.6 Parameters used in optimizations.

The parameters shown in table 5.6 are used in addition to those already described unless something else is indicated. According to the Department of Ocean Engineering, Technical University of Denmark, the lifetime of a tanker is typically 20 years. The remaining parameters in table 5.6 are chosen by judgement. The program PRODIM2 is used and the optimization method VMCWD is chosen (see chapter 6). Each time a repair has taken place the initial time is set equal to the repair time and new corrosion parameters are generated for the following safety and event margins.

Before turning the attention to the calculation of an optimal inspection strategy the reliability index and the objective function are examined for the bottom longitudinal ($z = 1.800$ m).

Approximate Calculations of Probabilities

In the program PRODIM2 different options for approximate calculations of failure and repair probabilities are included (see appendix 3) and here an attempt is made to assess these approximations.

The input parameter INCBRAN indicates whether contributions from all parallel systems are included in the probability calculations, in other words, whether all branches in figure 4.6 are used (INCBRAN = 0) or only branches with no repair (INCBRAN = 1) or branches with maximum one repair (INCBRAN = 2). Considering the expressions (5.33) - (5.38), branches with no repair correspond to parallel systems where all indices of the last failure margin are equal to zero and branches with maximum one repair correspond to parallel systems where maximum one index is equal to one. Obviously, these approximations can reduce the calculation time considerably but examinations have shown that they reduce the repair probability and thereby the repair cost by up to 50 % for INCBRAN = 1 and 20 % for INCBRAN = 2 so INCBRAN = 1 or 2 should only be used if the repair cost contributes insignificantly to the total costs. The failure probability is only influenced slightly by INCBRAN.

The input parameter INCELEM indicates whether non-failure elements ($M_F > 0$, see the expressions (5.33) - (5.38)) are included or not. This approximation influences both failure and repair probabilitites but only by about 0 - 10 %.

The input parameter INACTV indicates whether inactive components of the parallel systems are included or not. In figure 5.16 these two methods are compared in case of three inspections and constant inspection intervals and furthermore, the reliability index without any inspections is shown. It shows that not including the inactive components has two effects which are both due to the fact that the probability contents of some parallel systems will be too big if inactive components are not included. The first effect is that $\beta_Y(20 \text{ years})$ gets smaller the more inspections made introducing an inconsistency which will cause trouble in the optimization procedure. This would probably not happen if $\beta_Y(t)$ was steeper than in the case considered here, because then the relative effect of the approximations would be smaller. The second effect is that those vertical jumps, which are always present at each inspection, are increased considerably. In the case where inactive components are included, the vertical jumps are so small that they are not recognizable in figure 5.16. The jump at 9 years corresponds to the first inspection at 5 years but the jump is postponed until corrosion starts. In some papers (see e.g. Sørensen and Faber, 1991, or Sørensen et al., 1991) similar jumps in the reliability index are shown and explained as representing the probability that failure occurs in connection with a repair, but considering figure 5.16 the more likely explanation is that the jumps for the most part are errors introduced by not including inactive components in the probability calculations.

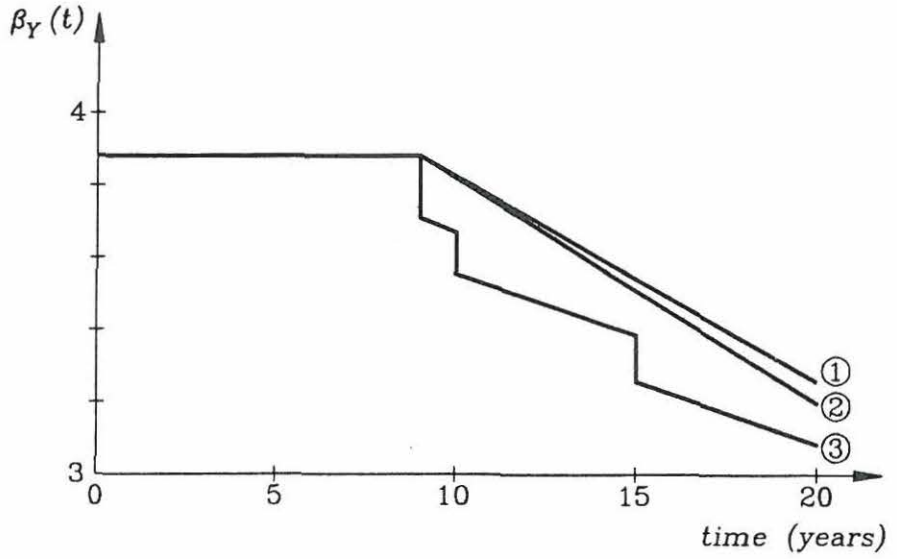

① 3 *insp., inactive comp. included*

② *no inspections*

③ 3 *insp., inactive comp. not included*

Figure 5.16 Effect of inactive components on $\beta_Y(t)$ for $z = 1.800$ m.

In figure 5.17 another example of the effect of inactive components is given showing the expected total costs for $n = 2$ and $T_2 = 15$ years as a function of T_1. This figure indicates that not including the inactive components will introduce bends and change the optimum of the objective function which experience also shows.

It is concluded that one must be very careful not to include inactive components.

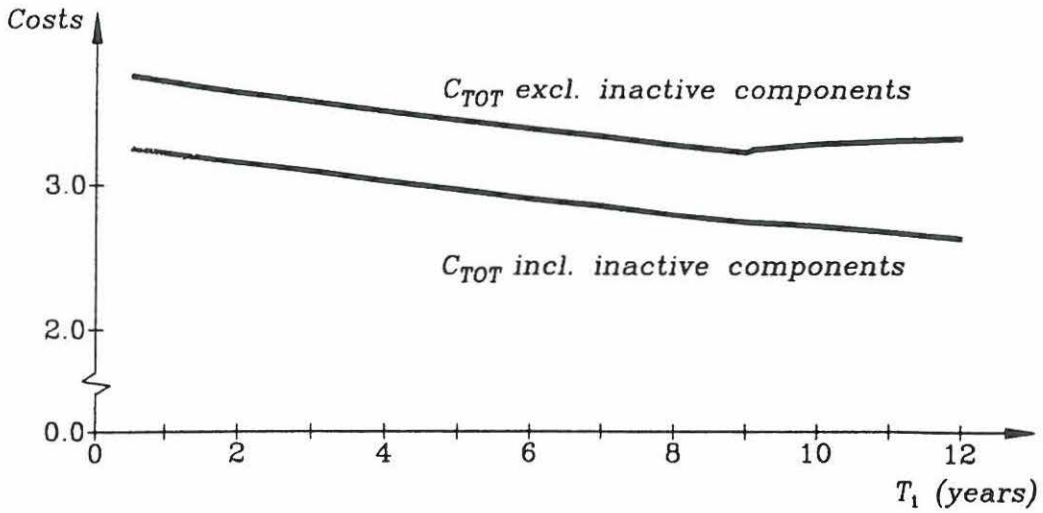

Figure 5.17 Effect of inactive components on C_{TOT} for $z = 1.800$ m, $n = 2$ and $T_2 = 15$ years.

Constant Inspection Intervals

In figure 5.18 the expected costs and the reliability index at the end of the lifetime $\beta_Y(20 \text{ years})$ for the bottom longitudinal are shown as a function of constant inspection interval ΔT. The expected costs are (see (5.39))

Total costs: $$C_{TOT} = C_{IN} + C_{RE} + C_{FA} \tag{5.45}$$

Inspection cost: $$C_{IN} = \sum_{i=1}^{n} C_I (1 - P_F(T_i)) \frac{1}{(1+r)^{T_i}} \tag{5.46}$$

Repair cost: $$C_{RE} = \sum_{i=1}^{n} C_R E[R_i] \frac{1}{(1+r)^{T_i}} \tag{5.47}$$

Failure cost: $$C_{FA} = \sum_{i=1}^{n+1} C_F (P_F(T_i) - P_F(T_{i-1})) \frac{1}{(1+r)^{T_i}} \tag{5.48}$$

As expected when comparing to figure 1.1, the inspection cost decreases with ΔT and the failure cost increases with ΔT (the failure cost is so small, however, that it does not show in figure 5.18). Due to the very small failure cost compared to inspection and repair cost the total costs are decreasing with ΔT, i.e. the minimum of the total costs is found for the maximum inspection interval and not for a medium interval as in figure 1.1. The reliability index $\beta_Y(20 \text{ years})$ decreases with ΔT which corresponds to the increasing failure rate in figure 1.1 but the inspection interval does not influence $\beta_Y(20 \text{ years})$ much as $\beta_Y(20 \text{ years})$ varies between 3.2 and 3.3. This is because of the relatively flat β_Y-function shown in figure 5.16. Regarding the three

contributions to the total costs, the inspection cost depends very little on the failure probability since $1-P_F(T_i) \simeq 1$ while the repair cost is highly dependent on the repair probability and the failure cost is highly dependent on the failure probability. This means that changing a parameter in the probability calculations will only influence the repair and failure costs. The conclusion that the optimal inspection strategy is not to inspect during the lifetime, even with the constraint that $\beta^{\min} = 3$, indicates that some of the parameters are not realistic which is examined in the following.

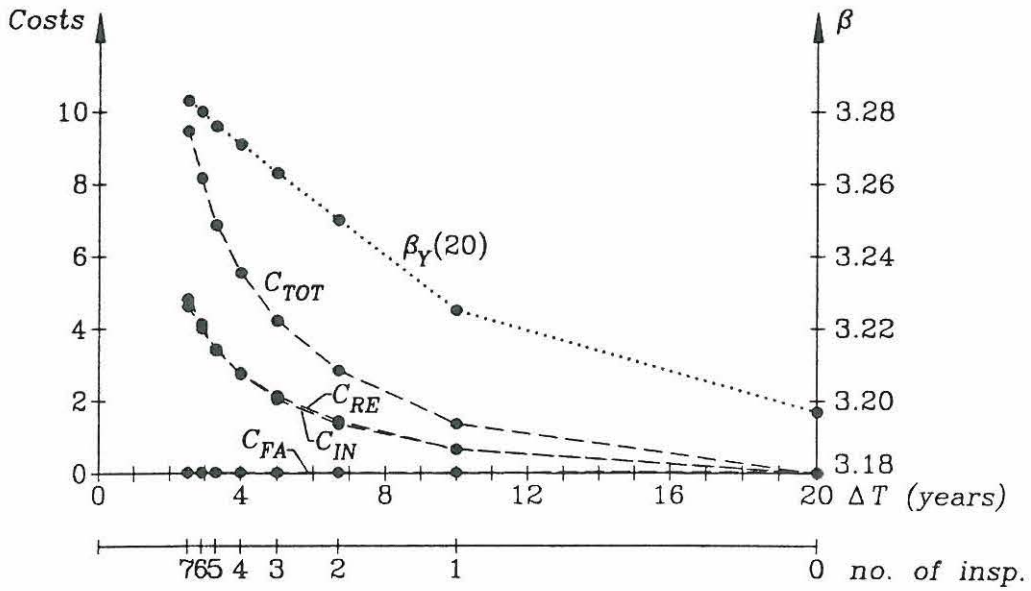

Figure 5.18 Costs and reliability index as functions of constant inspection interval for $z = 1.800$ m.

Two cases are considered where the contribution from the failure cost is increased, either by increasing C_F or by increasing the failure probability. In figure 5.19 C_F is equal to 500,000 which is probably unrealistic but the calculations are made to find out how much it takes to give the total costs a "bath tub" look. As expected the failure cost is totally dominating but as the increase in failure cost as a function of ΔT is smaller than the decrease in the inspection and repair costs for small inspection intervals, the total costs are minimal for $\Delta T = 4$ years.

In figure 5.20 the failure probability is increased by increasing the corrosion parameters. A and B are based on Løseth et al., 1992, as explained in section 5.2 and they are probably more realistic than the corrosion parameters based on Albrecht & Naeemi, 1984. Therefore, these corrosion parameters will be used in the optimizations later on in this chapter. For constant inspection intervals the minimum total costs are found for an interval of 5 years but the constraint that $\beta_Y(20 \text{ years})$ should be greater than 3 is not fulfilled even if inspections are performed each year, i.e. 19 inspections.

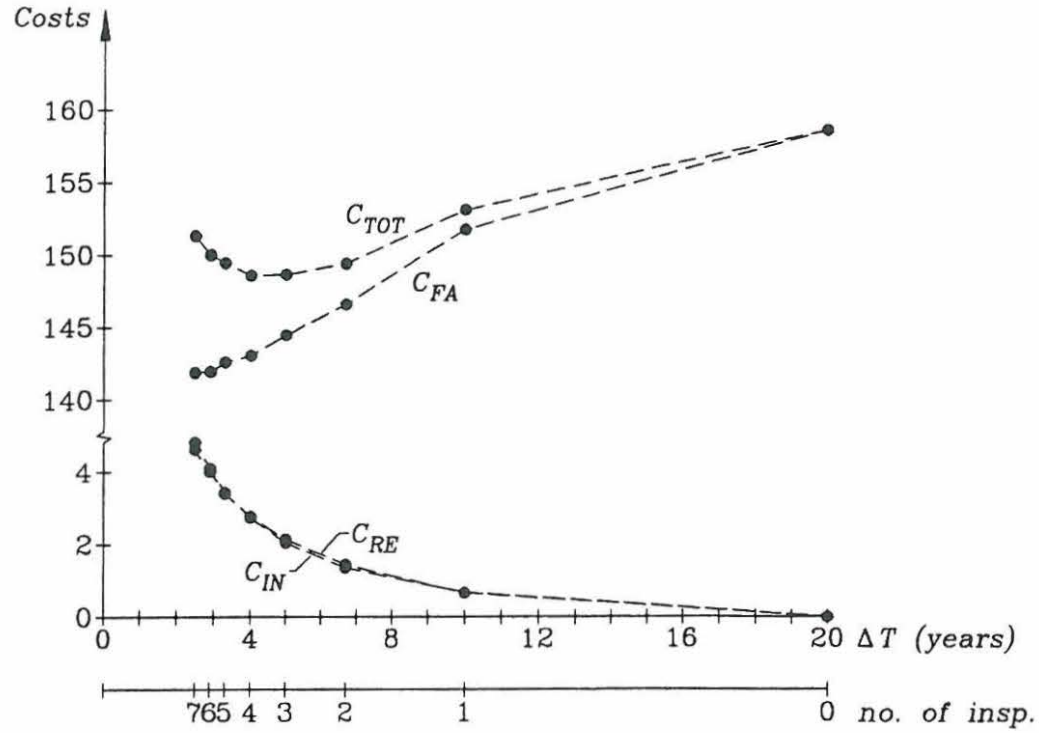

Figure 5.19 Costs as functions of constant inspection interval for $z = 1.800$ m and $C_F = 500,000$.

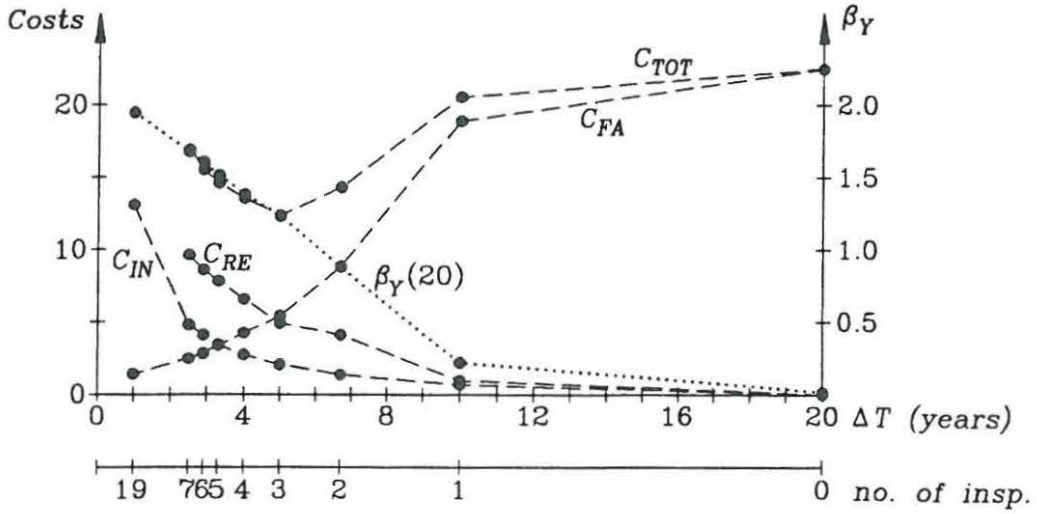

Figure 5.20 Costs and β_Y as functions of constant inspection interval for $z = 1.800$ m, A: N(200 μm per year, 40 μm per year) and B: N(1.1, 0.1).

Contour Lines

Part of the contour lines for the objective function C_{TOT} and β_Y(20 years) are shown in figures 5.21 - 5.24 in the case of two inspections. The complete sample space for T_1 and T_2 forms a triangle with corners in (T_1, T_2) = (0 years, 0 years), (0 years, 20 years) and (20 years, 20 years). The purpose is to examine if there are any bends or discontinuities in C_{TOT} and β_Y(20 years) and, if so, explain them. The effect of the coating is illustrated by showing the contour lines with and without coating. Considering figure 5.22 it shows that if no coating is assumed the objective function has two minima so the starting point for the optimization is essential. The ridge corresponds to equal inspection intervals, i.e. $T_1 = T_2 - T_1$, and the ridge can be recognized in figure 5.21 as the wedge at $T_1 \geq 9$ years and $T_2 - T_1 \geq 9$ years, i.e. where both inspection intervals are longer than the duration of the coating. Furthermore, the objective function shows a discontinuity at the lines $T_1 = 9$ years and and $T_2 - T_1 = 9$ years as indicated in figure 5.21. The contour lines will be explained in more detail later on in connection with figure 5.25. In figures 5.21 and 5.22 the minimum of C_{TOT} is found for $T_1 = T_2 = 20$ years which corresponds to figure 5.18 showing that the optimal strategy is no inspections.

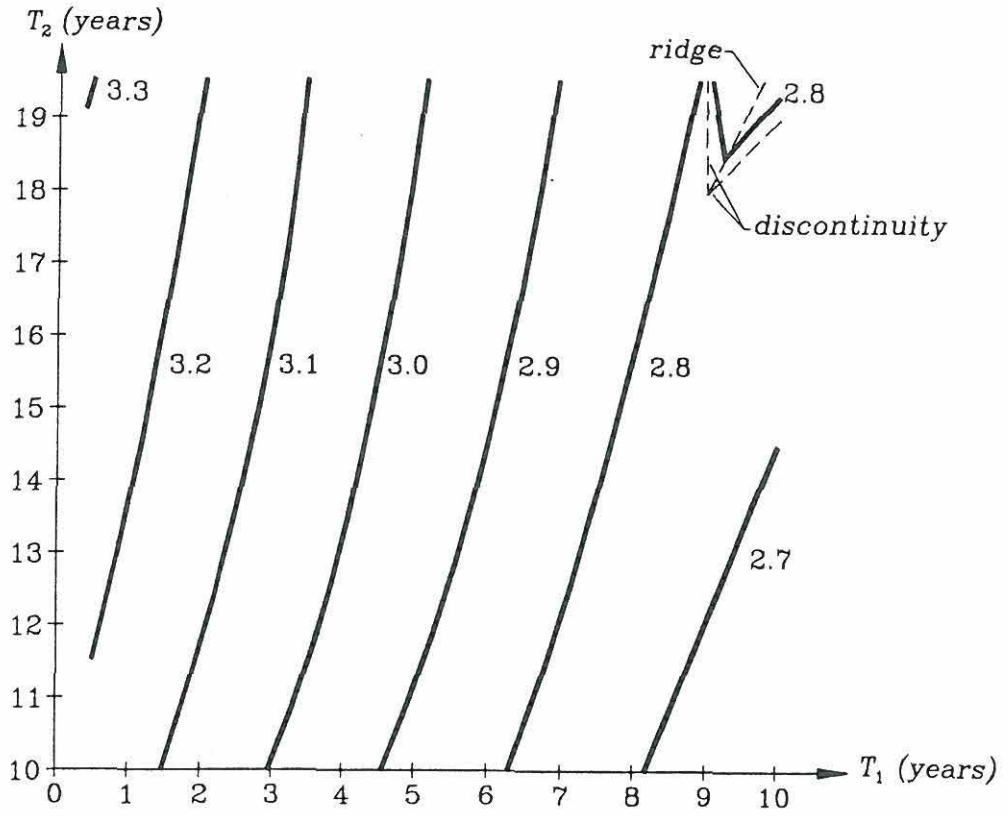

Figure 5.21 Contour lines for C_{TOT} for $z = 1.800$ m, $n = 2$ and T_c: N(9 years, 0.9 years).

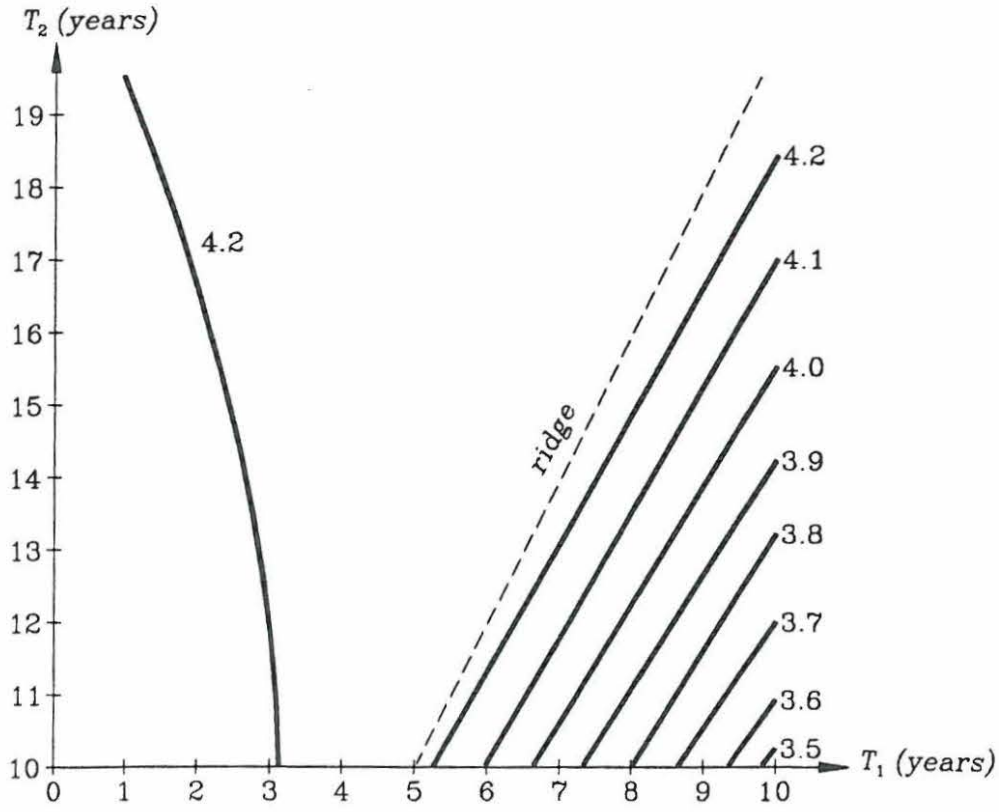

Figure 5.22 Contour lines for C_{TOT} for $z = 1.800$ m, $n = 2$ and $T_c = 0$ years.

Comparing figures 5.23 and 5.24 it shows that if coating is assumed $\beta_Y(20 \text{ years})$ becomes quite flat and almost independent of T_1 and T_2. In both cases the safest area is for large T_1 and for T_2 equal to about 15 - 17 years. Within the area in figure 5.23 where both inspection intervals are smaller than the duration of coating, i.e. $T_1 < 9$ years and $T_2 - T_1 < 9$ years, $\beta_Y(20 \text{ years})$ is independent of T_1 so the contour lines are parallel to the T_1-axis.

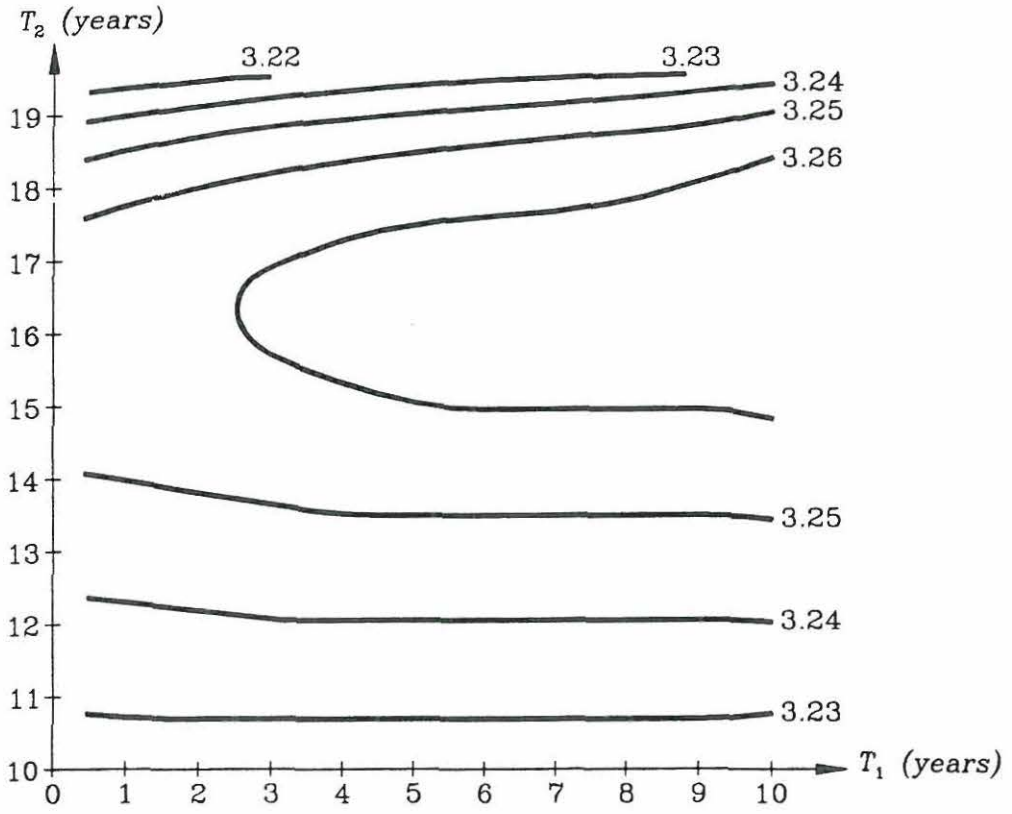

Figure 5.23 Contour lines for $\beta_Y(20 \text{ years})$ for $z = 1.800$ m, $n = 2$ and T_c: N(9 years, 0.9 years).

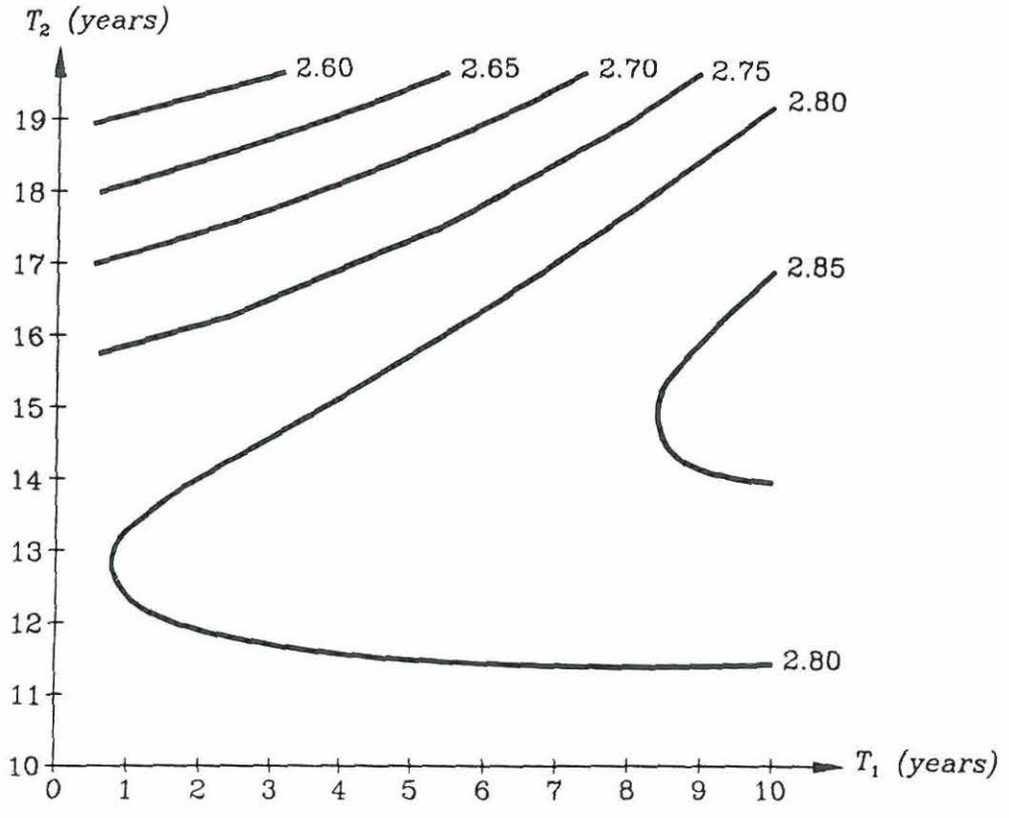

Figure 5.24 Contour lines for $\beta_Y(20 \text{ years})$ for $z = 1.800$ m, $n = 2$ and $T_c = 0$ years.

To explain the wedge in figure 5.21 the contributions to C_{TOT} are shown in figure 5.25 for $T_2 = 19.5$ years. The failure cost is so small that it does not influence the total costs while the inspection and repair costs are of the same size. The inspection cost decreases with time because of the real rate of interest, however, it is not influenced by the failure probability since $1 - P_F(T_i) \simeq 1$. The repair cost is influenced by both the real rate of interest, which contributes to the decrease in the repair cost, and the repair probability, which causes the characteristic bends and the wedge in figure 5.21.

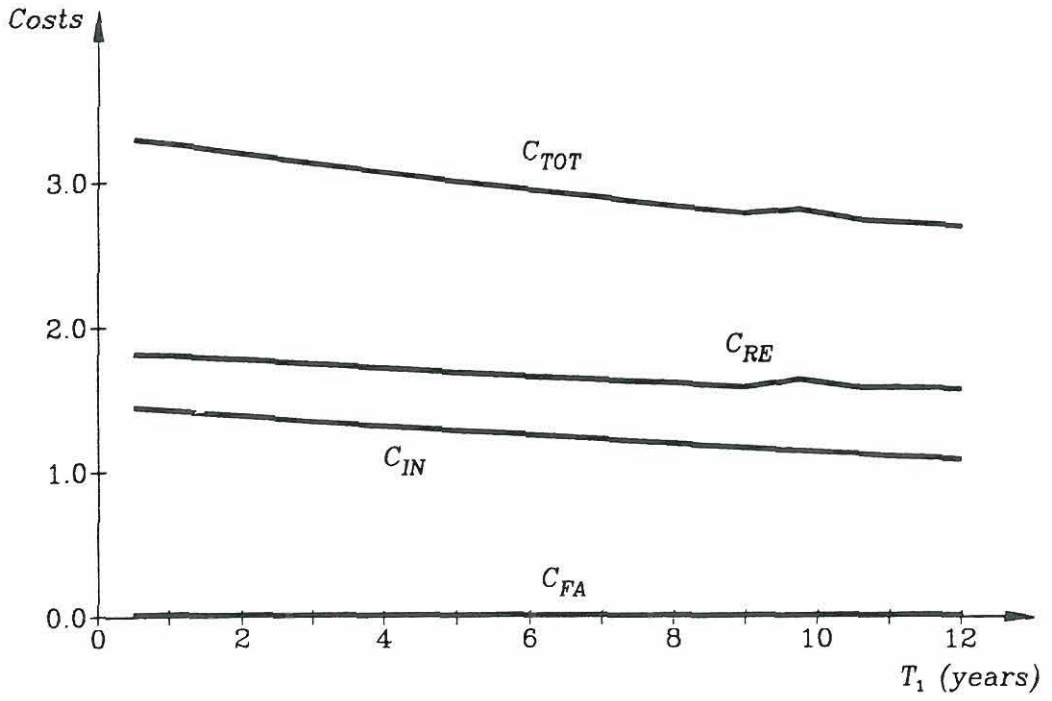

Figure 5.25 Costs as functions of T_1 for $z = 1.800$ m, $n = 2$, T_c: N(9 years, 0.9 years) and $T_2 = 19.5$ years.

The repair probabilities for the first and second inspection are calculated using the three following parallel systems (see also (5.36) and (5.37)).

$$E[R_1] = P(M_F(T_1) > 0 \bigcap H(T_1) \leq 0) \tag{5.49}$$

$$E[R_2^0] = P(M_F(T_1) > 0 \bigcap H(T_1) > 0 \bigcap M_F(T_2) > 0 \bigcap H(T_2) \leq 0) \tag{5.50}$$

$$E[R_2^1] = P(M_F(T_1) > 0 \bigcap H(T_1) \leq 0 \bigcap M_F^1(T_2 - T_1) > 0 \bigcap H^1(T_2 - T_1) \leq 0) \tag{5.51}$$

In figure 5.26 these repair probabilities are shown as a function of T_1. As expected, the probabilities are constant until the corrosion starts at $T_1 = 9$ years. During the calculations it was found that for $E[R_1]$ and $E[R_2^1]$ only the active repair element influences the result while for $E[R_2^0]$ both the active repair element and the inactive no-repair element influence the result. For $E[R_2^1]$ the repair element with the smallest time variable is active, i.e. for $T_1 < T_2 - T_1 \Rightarrow T_1 < 9.75$ years $H(T_1) \leq 0$ is active and for $T_1 > T_2 - T_1 \Rightarrow T_1 > 9.75$ years $H(T_2 - T_1) \leq 0$ is active. This means that the parallel systems can be approximated by the following systems.

$$E[R_1] \simeq P(H(T_1) \leq 0) \tag{5.52}$$

$$E[R_2^0] \simeq P(H(T_1) > 0 \bigcap H(T_2) \leq 0) \tag{5.53}$$

$$E[R_2^1] \simeq \begin{cases} P(H(T_1) \leq 0), & T_1 < T_2/2 \\ P(H(T_2 - T_1) \leq 0), & T_1 > T_2/2 \end{cases} \tag{5.54}$$

Considering these systems and knowing that $P(H(t) \leq 0)$ is increasing as a function of t if t is greater than the duration of the coating it is obvious why the curves in figure 5.26 look the way they do. Turning back to figure 5.25 the bends in the repair probability are caused by bends in $E[R_1]$, $E[R_2^0]$ and $E[R_2^1]$ for $T_1 = 9$ years and bends in $E[R_2^1]$ for $T_1 = 9.75$ years and $T_1 = 10.5$ years, and the wedge in figure 5.21 is there because corrosion has started in the elements in (5.54). Furthermore, there is a small bend in the contour lines in figure 5.21 for $T_1 = 9$ years and $T_2 = 9$ years according to the expressions (5.52) - (5.54).

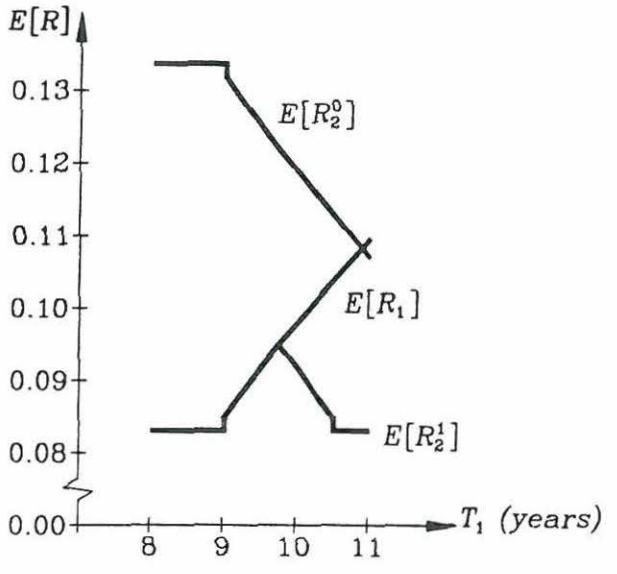

Figure 5.26 Repair probabilities (supplementing figure 5.25).

If more than two inspections are considered it is expected that there will be several bends and small discontinuities that might cause problems in the optimization procedure.

It should be stated that the effect of the real rate of interest is that the inspections are performed as late as possible which to some degree is counteracted by the repair probabilities (and failure probabilities if they are significant enough).

Optimization

Using the parameters in tables 5.5 and 5.6 it turned out in figure 5.18 that the optimal strategy is not to inspect the longitudinals due to the very small failure cost. To make the calculations more realistic the corrosion parameters are increased to the values used in figure 5.20. Unfortunately this means for some longitudinals that the reliability index after 20 years is smaller than $\beta^{\min} = 3$ even if inspections take place every year during the lifetime. Nevertheless, the optimization calculations are

made using these parameters, and the results are shown in tables 5.7 - 5.9 for the three longitudinals considered. Since the number of inspections is part of the input to PRODIM2, the procedure is to calculate optimal inspection strategies for different values of n and by comparison find the optimal strategy.

In the tables results are shown both for constant inspection intervals and for optimal inspection intervals to make it possible to see how much the costs are reduced and how much the reliability is improved by optimizing.

The calculations for $n = 19$ are approximated as indicated in table 5.7. This has been done to save calculation time since 19 inspections would create $2^{19} + \sum_{i=1}^{19} 2 \cdot 2^{i-1} \simeq 1.6 \cdot 10^6$ parallel systems to be calculated and that would take more than 1000 CPU-hours. Using INCBRAN = 1 only $1 + 19 \cdot 2 = 39$ parallel systems are created but as explained earlier this means that only the failure probabilities can be trusted, not the repair probabilities (and thereby not the repair cost and total costs). In those cases where the constraint that $\beta_Y(20 \text{ years}) \geq \beta^{\min}$ cannot be fulfilled the solution with the largest $\beta_Y(20 \text{ years})$ is shown.

With constant inspection intervals:						
n	0	1	2	3	4	$19^{(1)}$
C_{TOT}	22.5	20.5	14.3	12.3	13.5	(22.4)
C_{IN}	0.0	0.7	1.4	2.0	2.7	13.1
C_{RE}	0.0	1.0	4.1	4.9	6.6	(7.9)
C_{FA}	22.5	18.9	8.8	5.4	4.2	1.4
β_Y(20 y.)	0.02	0.2	0.9	1.2	1.4	1.9
With optimal inspection intervals:						
n	$1^{(2)}$	$2^{(2)}$	$3^{(2)}$		$10^{(3)}$	
C_{TOT}	9.3	8.9	9.7		**18.8**	
C_{IN}	0.5	1.1	1.6		**5.6**	
C_{RE}	2.8	4.6	5.6		**11.8**	
C_{FA}	6.0	3.3	2.4		**1.4**	
β_Y(20 y.)	1.2	1.5	1.7		**1.9**	
$\overline{T}$ (years)	15.1	13.9, 16.5	13.5, 15.4, 17.4		$\mathbf{T_1 = 10.0, \Delta T = 1.0}$	

[1] Only branches without repair incl. in the reliability calculations (INCBRAN=1).
[2] The "optimal" point is found as the point with the largest $\beta_Y(20)$ years.
[3] Not optimized ($\overline{T}$ is part of the input to PRODIM2).

Table 5.7 *Optimization results for $z = 1.800$ m,*
A: N(200 μm per year, 40 μm per year) and B: N(1.1, 0.1).

With constant inspection intervals:						
n	0	1	2	3	4	6
C_{TOT}	15.6	14.9	9.6	7.7	9.3	11.9
C_{IN}	0.0	0.7	1.4	2.1	2.7	4.1
C_{RE}	0.0	0.7	3.7	4.2	5.7	7.5
C_{FA}	15.6	13.5	4.5	1.4	0.8	0.3
β_Y(20 y.)	0.4	0.5	1.3	1.9	2.1	2.5
With optimal inspection intervals:						
n	$1^{(1)}$	$2^{(1)}$	$3^{(1)}$		6	
C_{TOT}	4.8	6.0	7.4		**11.3**	
C_{IN}	0.5	1.1	1.6		**3.3**	
C_{RE}	2.7	4.5	5.6		**8.0**	
C_{FA}	1.5	0.4	0.2		**0.1**	
β_Y(20 y.)	1.9	2.4	2.7		**3.0**	
$\overline{T}$ (years)	15.4	14.1, 16.7	13.4, 15.5, 17.5		**12.0,14.0,15.2, 16.2,17.3,18.5**	

[1] The "optimal" point is found as the point with the largest β_Y(20) years.

Table 5.8 Optimization results for $z = 5.100$ m,
A: N(200 μm per year, 40 μm per year) and B: N(1.1, 0.1).

With constant inspection intervals:					
n	0	1	2	3	4
C_{TOT}	7.6	7.8	6.5	6.5	8.6
C_{IN}	0.0	0.7	1.4	2.1	2.7
C_{RE}	0.0	0.7	3.7	4.2	5.7
C_{FA}	7.6	6.4	1.5	0.2	0.1
β_Y(20 y.)	1.0	1.1	1.9	2.6	3.0
With optimal inspection intervals:					
n	$1^{(1)}$	2	3		
C_{TOT}	3.5	**4.8**	5.7		
C_{IN}	0.5	**1.1**	1.6		
C_{RE}	2.7	**3.6**	4.1		
C_{FA}	0.2	**0.1**	0.1		
β_Y(20 y.)	2.7	**3.0**	3.0		
$\overline{T}$ (years)	15.4	**15.0, 16.3**	15.2, 16.2, 17.2		

[1] The "optimal" point is found as the point with the largest β_Y(20) years.

Table 5.9 Optimization results for $z = 8.070$ m,
A: N(200 μm per year, 40 μm per year) and B: N(1.1, 0.1).

Not surprisingly, the calculations show that inspections during the first 9 years, where corrosion is prevented by coating, only have a minor effect on the reliability. In other words, the reliability achieved by 19 inspections can also be achieved by only 10 inspections performed at one year intervals from 10 to 19 years and then the costs are considerably lower.

For $n = 1$ the optimization reduces the total costs by 50-60% and increases the reliability index by 150-500% and for $n = 3$ the total costs are reduced by 10-20% and the reliability index is increased by 15-40% so the more inspections made the less is gained by optimizing assuming that the number of inspections is known.

Without constraints on the reliability index the optimal inspection strategy for the bottom longitudinal ($z = 1.800$ m) is two inspections, i.e. after 13.9 and 16.5 years, and for the longitudinals at $z = 5.100$ m and $z = 8.070$ m it is one inspection after 15.4 years (see table 5.7 - 5.9).

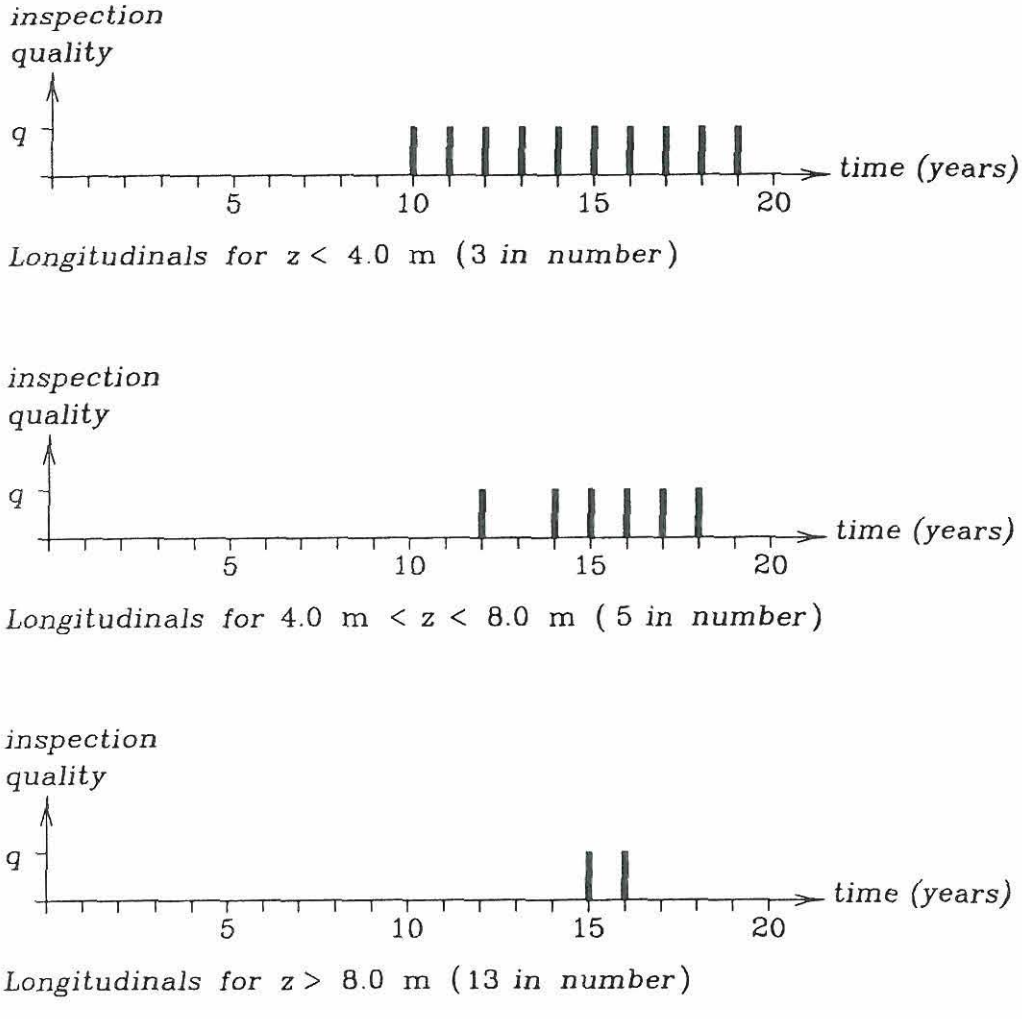

Figure 5.27 Inspection strategy.

For $\beta^{\min} = 3$ the bottom longitudinal cannot, as mentioned before, fulfil the safety requirements but the maximum reliability is achieved by carrying out inspections each year after the first 9 years. The longitudinal at $z = 3.320$ m can achieve a minimum reliability index of 2.9 by inspecting every year after the first 9 years and this may be acceptable considering the reliability of reliability calculations. For the longitudinal at $z = 5.100$ m the optimal strategy is 6 inspections, i.e. after 12.0, 14.0, 15.2, 16.2, 17.3 and 18.5 years and for the longitudinal at $z = 8.070$ m the optimal strategy is two inspections at 15.0 and 16.3 years. The inspection strategy is illustrated for the three groups of longitudinals in figure 5.27 rounding off the inspection times to whole years.

It should be stated that for most longitudinals above 4.0 m fatigue is the dominating failure mode so if fatigue was included these longitudinals would probably need more inspections.

A rough estimate of the savings by using different inspection strategies for different longitudinals can be calculated by summing up the expected costs for all 21 longitudinals. The total inspection cost for the three groups of longitudinals is (see tables 5.7 - 5.9) $3 \cdot 5.6 + 5 \cdot 3.3 + 13 \cdot 1.1 \simeq 48$ using different strategies and $21 \cdot 5.6 \simeq 118$ using the same strategy (i.e. the one calculated for $z = 1.800$ m) which means that the inspection cost is reduced by 59% by using different strategies. In this estimate though, the effect of inspecting several longitudinals at a time, which will reduce the inspection cost per longitudinal, is not included. The total repair cost is probably reduced by 30-50% by using different strategies but it cannot be calculated without making calculations for each of the 21 longitudinals. The failure cost of the upper longitudinals is increased by using different strategies but when different strategies are used the failure cost is only 1-2% of the total costs for the longitudinals above 4.0 m (see tables 5.8, 5.9), so this effect is insignificant. Considering all longitudinals as a whole, calculations for each longitudinal should be made on the assumption that all other longitudinals have not failed since it is assumed in the model that if a longitudinal has failed it cannot be repaired. This will probably not have much influence on the results since the probability of non-failure is close to one, as mentioned before . Conclusively, assuming that the parameters and the failure modelling used in the calculations are realistic, the total costs are estimated to be reduced by 20-40% by using different inspection strategies for the longitudinals instead of inspecting all longitudinals according to the needs of the poorest.

Since the very low reliability of the bottom longitudinal does not seem realistic the most conservative assumptions affecting the reliability are reviewed and revalued.

- The assumption that the longitudinals are fixed at the bulkheads and the web frames must be a fairly good approximation since the longitudinals are continuous and partly fixed at the bulkheads and the web frames.
- The L-shaped cross-section of the longitudinals is approximated to a rectangular cross-section which may have increased the stress contribution by more than

100 %.

- Calculating only for the full cargo condition is not realistic since a tanker will be in the ballast condition for up to 50% of its lifetime and in the ballast condition there will be less water pressure on the side longitudinals. For the lowest longitudinals, however, the water pressure will be about the same in the two conditions. The resulting depth of the water column above the lowest longitudinal is about 11 m in both cases as the ballast tank is full in the ballast condition.
- Assuming no correlation between the two load contributions to yielding failure does not influence the results since the stress contribution corresponding to the hull bending moment is less than 1% of the stress contribution corresponding to water pressure on the ship side. Apart from this the correlation may be positive for some longitudinals up the ship side so the assumption is in some cases non-conservative.
- Due to the previous item the modelling of the corrosion is only important with regard to the load contribution from the water pressure on the ship side, i.e. the modelling of each longitudinal cross-section, and here it is probably too conservative to assume corrosion on the underside of the longitudinals. However, the size of the corrosion parameters and the duration of the coating seem realistic according to Løseth et al., 1992.
- Another conservative assumption is that the coating is not maintained unless a repair is needed which will hopefully not be the case in real life.
- It is not known whether the repair criterion, which is 2 mm corrosion of the longitudinals, is realistic or not but in Condition Evaluation.., 1991, it is mentioned that the Classification Societies generally accept a 10% reduction of the hull section modulus in the wasted condition provided this does not involve an unacceptable risk of buckling. A 10% reduction of the moment of inertia corresponds to a corrosion penetration of 1 mm (see (5.43)), i.e. 2 mm corrosion of the longitudinals which are assumed to corrode on both sides.

These assumptions can easily have caused an underestimation of the reliability of the longitudinals, especially the assumptions about rectangular cross-sections of the longitudinals and corrosion developing on the underside of the longitudinals. On the other hand some non-conservative assumptions have been made in connection with the selection of load contributions.

- The shear stress due to the hull shear force and due to the water pressure on the ship side is neglected. But, with the approximation of rectangular cross-sections of the longitudinals, the shear stress is zero at the tip of the cross-section where the axial stress and the Von Mises' stress is largest so this assumption hardly influences the calculations for yielding failure. It is not known to which degree a shear stress will increase the fatigue crack growth.
- The hull bending moment around the vertical axis is not included as it is not calculated by the ISH-DESIGN programmes described in section 5.8.1. It may

be of some importance though if it is considerably bigger than the hull bending moment around the horizontal axis which for the lowest longitudinals gives axial stresses of only 1 - 2 N/mm^2. Furthermore, the vertical bending stiffness is about 2.6 times bigger than the horizontal bending stiffness.

- As mentioned in section 5.3, an important load contribution is the secondary stresses induced by the relative transverse deflection between adjacent bulkheads and web frames.

Especially, the last assumption has influenced the results and the calculations could be refined with more knowledge about the problem.

5.9 Conclusion

Several assumptions are made in the calculations which means that it is difficult to assess the reliability of the structure. The most conservative assumptions are that the cross-section of the longitudinals is assumed to be rectangular and that general corrosion is assumed to develop on all inner surfaces of the tanker. The most non-conservative assumption is that the relative deflection between adjacent bulkheads and web frames is neglected. The reliability calculations are made using corrosion parameters that later on were found to be too low so conclusions are only made for the mutual differences between the reliability indices. The yielding failure mode is not considered as a first-passage problem which would be more realistic than the model used.

The reliability calculations show that of the two failure modes considered fatigue is the dominating failure mode for all longitudinals at the ship side except for the three lowest longitudinals, where yielding is dominating. The system reliability index at the end of the lifetime without inspections only show minor variations up the ship side, which indicates that the design of the longitudinals is rational. The lowest fatigue reliability index is found a couple of metres below the load waterline which agrees with observations of fatigue failure in tankers. However, these observations are made for oil tanks at the ship side and they show that fatigue cracks propagate from the inside of the longitudinals at connections to bulkheads since the pressure of the oil inside the tank is higher than the water pressure outside the ship. The calculations made in this chapter show that for ballast tanks at the ship side fatigue cracks are expected to propagate from the outside of the longitudinals at connections to bulkheads since the ballast tanks are empty under the full cargo condition. As expected, the lowest yielding reliability index is found for the bottom longitudinal where the water pressure is largest.

In the optimization calculations only yielding failure is considered. When calculating an optimal inspection strategy several options are available for approximate calculations of failure and repair probabilities in the program PRODIM2 but examinations show that one should be very careful by using these options as they may give misleading results.

Considering the three contributions to the expected total costs as a function of the constant inspection interval ΔT, the inspection cost and repair cost decrease with ΔT and the failure cost increases with ΔT, so the more dominating the failure cost, the greater the optimal number of inspections (not considering constraints on the reliability index). The contour lines of the expected total costs for two inspections indicate that for a larger number of inspections several bends and small discontinuities may occur in the total costs, however, this has caused no problems in the optimizations made. An optimal inspection strategy is calculated for three longitudinals at the ship side representing three groups of longitudinals. In these calculations larger and more realistic corrosion parameters than in the remaining calculations are used. Based on the optimizations an inspection strategy is suggested where 3 longitudinals are inspected 10 times, 5 longitudinals are inspected 6 times and 13 longitudinals are inspected twice during the lifetime of the tanker and it is rendered probable that the total costs can be reduced considerably by using different inspection strategies for different longitudinals.

Considering conventional inspection strategies the ship hull will typically be inspected visually each year and carefully every 4 years. The type of inspection referred to in this chapter is considered to be a "careful" inspection since the thickness of the longitudinals is measured. During the last period of the lifetime where coating is assumed not to be effective, i.e. after 9 years, a traditional inspection strategy would result in 2 - 3 careful inspections which for the 8 lowest longitudinals is a lot fewer than calculated here but again the reliability may be too approximate and thereby, the optimal number of inspections may be overestimated.

5.10 References

Albrecht, P.; A.H. Naeemi (1984), *Performance of Weathering Steel in Bridges*, Report 272, NCHRP, Transportation Research Board, Washington.

Chandler, Kenneth A. (1985), *Marine and Offshore Corrosion*, Butterworth & Co. Ltd., U.K.

Condition Evaluation and Maintenance of Tanker Structures (1991), Addendum to *Guidance Manual for the Inspection and Condition Assessment of Tanker Structures*, 1986, Tanker Structure Co-operative Forum.

Cracking of HTS Longitudinals of VLCC (1991), Danish Technical Committee-I/WP-4-3.

Det Norske Veritas (1992), *Guidelines for Corrosion Protection of Ships*, by DSO-230, Paper Series No.: 92-P001, Høvik, Norway.

Ferguson, J.M; A.G. Gavin (1991), *Aspects of Oil Tanker Structural Inspection, Maintenance and Monitoring*, Lloyd's Register of Shipping, London.

Guidance Manual for the Inspection and Condition Assessment of Tanker Structures (1986), Int. Chamber of Shipping, London.

Hellan, Kåre (1985), *Introduction to Fracture Mechanics*, McGraw-Hill International Editions.

Huss, Mikael (1990), *Combined Wave Induced Stresses in a OBO Carrier, Application of a Rationally Based Direct Calculation Method, Part 2*, Report TRITA-SKP 1065, Royal Institute of Technology, Department of Naval Architecture S-100 44 Stockholm, Sweden.

Jansen, Piet (1978), *Indenbordskorrosion i stålfiskefartøjer*, Korrosionscentralen, Skibsforsikringsforeningen i Frederikshavn.

Lin, Y.K. (1967), *Probabilistic Theory of Structural Dynamics*, Robert E. Krieger Publishing Company, Florida, reprint 1986.

Lloyd's Register of Shipping (1984), *Rules and Regulations for the Classification of Ships*, Part 1, Chapter 2 and 3, London.

Løseth, Robert; Geir Sekkesæter; Sverre Valsgård (1992), *Economics of High-Tensile Steel in Ship Hulls*, PRADS '92, Newcastle.

Madsen, Henrik O. (1989), *Stochastic Modelling of Fatigue Crack Growth*, ISPRA Course, Structural Reliability, Lisboa.

Madsen, H.O.; S. Krenk; N.C. Lind (1986), *Methods of Structural Safety*, Prentice-Hall.

Pedersen, P. Terndrup; J. Juncher Jensen (1983), *Styrkeberegning af maritime konstruktioner, Del 1, Belastninger og global analyse*, Den private Ingeniørfond.

PROBAN-2, Example Manual (1989), A.S. Veritas Research Report No. 89-2025, Høvik, Norway.

PRODIM, Theoretical Manual (1988), A.S. Veritas Research Report No. 88-2029, Høvik, Norway.

Recommended Practice for the Protection and Painting of Ships (1972), British Ship Research Association, U.K.

Seawater Corrosion Handbook (1979), edited by M. Schumacher, Noyes Data Corporation, U.S.A.

SSC-318 (1983), *Fatigue Characterization of Fabricated Ship Details for Design*, Ship Structure Committee, U.S. Coast Guard, Washington D.C.

Sørensen, J.D.; M.H. Faber (1991), *Optimal Inspection and Repair Strategies for Structural Systems*, Proc. IFIP WG 7.5, Conference on Reliability and Optimization of Structural Systems (eds. R. Rackwitz and P. Thoft-Christensen), Springer-Verlag, Lecture Notes in Engineering, Vol. 76, pp. 383-394.

Sørensen, J.D.; M.H. Faber; R. Rackwitz; P. Thoft-Christensen (1991), *Modelling in Optimal Inspection and Repair*, Proceedings of OMAE 1991, Stavanger, Norway, ASME, Vol. II, pp. 281-288.

Sørensen, J.D.; P. Thoft-Christensen (1988), *Inspection Strategies for Concrete Bridges*, Proc. IFIP WG 7.5, Conference on Reliability and Optimization of Structural Systems (edt. P. Thoft-Christensen), Springer-Verlag, Lecture Notes in Engineering, Vol. 48, pp. 325-335.

Taggert, R. et al. (1980), *Ship Design and Construction*, SNAME.

CHAPTER 6
RELIABILITY AND OPTIMIZATION PROGRAMS

In this chapter the programs used for reliability calculations and optimization are described and the changes made in them are explained.

6.1 PROBAN-2

PROBAN-2 (PROBabilistic ANalysis program) is a commercial program made by A.S. Veritas Research and the program is described in the manuals listed in section 6.4. PROBAN-2 has been used for the reliability calculations in chapters 4 and 5 - calculating failure probabilities for single elements as well as series systems. The intention was to use it in the optimization program PRODIM2 too for calculation of failure probabilities and sensitivity factors for parallel systems but as explained later this did not succeed.

A number of limit state functions were programmed. In chapter 4 the three failure modes are bending, shear and bearing in a corroding steel girder and in chapter 5 two failure modes are considered namely yielding and fatigue in a corroding longitudinal in a tanker. Furthermore, a repair criterion for a longitudinal was defined and the corresponding limit state function programmed.

PROBAN-2 uses the NLPQL algorithm for optimization (see e.g. Schittkowski, 1986) which is a sequential quadratic programming technique. In chapters 4 and 5 the First Order Reliability Method (FORM) was used for probability calculations.

At first PROBAN-2 was also used for calculation of probabilities and sensitivity factors in PRODIM2 but some probability calculations did not succeed due to properties of the optimization algorithm. For instance, occasionally a stochastic parameter takes on an unrealistic value leading to numerical problems and then the program stops. The problem arises if the limit state function is too flat. Another example is that the probability for some parallel systems is calculated but is clearly wrong being outside the simple bounds for positively correlated elements. Consider for instance the parallel system with two elements in table 6.1, where M is the failure margin for yielding and H is the failure margin for repair used in chapter 5. FORM has been used for the reliability calculations but using SORM in PROBAN-2 gives about the same results.

	PROBAN-2	PARLSENSI
$P_R = P(H(T_1) \leq 0)$	$9.791 \cdot 10^{-2}$	$9.791 \cdot 10^{-2}$
$P_F = P(M(T_2) \leq 0)$	$6.929 \cdot 10^{-4}$	$6.948 \cdot 10^{-4}$
$P(H(T_1) \leq 0 \bigcap M(T_2) \leq 0)$	$2.004 \cdot 10^{-6}$	$8.084 \cdot 10^{-5}$
Simple lower bound:		
$P_R \cdot P_F$	$6.784 \cdot 10^{-5}$	$6.803 \cdot 10^{-5}$
Simple upper bound:		
$\min(P_R, P_F)$	$6.929 \cdot 10^{-4}$	$6.948 \cdot 10^{-4}$

$T_1 = 10$ years, $T_2 = 20$ years, $\rho_{RF} = 0.041$

Table 6.1 Comparison between PROBAN-2 and PARLSENSI.

It shows that the probability of the parallel system calculated by PROBAN-2 is smaller than the simple lower bound. Since these problems create great difficulties for the optimization in PRODIM2 it was chosen to use another program PARLSENSI for calculation of probabilities and sensitivity factors.

6.2 PARLSENSI

PARLSENSI is made by Ib Enevoldsen and John Dalsgård Sørensen, University of Aalborg and a description is available in Enevoldsen, 1991, see also Enevoldsen and Sørensen, 1992 and 1993. It is used in the optimization program PRODIM2 for calculation of probabilities and sensitivity factors for elements or parallel systems. PARLSENSI uses an optimality criterion based optimization technique (the algorithm JOINT3, see Enevoldsen, 1991, is used) and FORM is used for reliability calculations. Sensitivity factors are calculated semi-analytically.

A number of changes has been made in PARLSENSI. The most important ones are listed below:

Limit State Functions
Six limit state functions are programmed; yielding, no-yielding, fatigue, no-fatigue, repair and no-repair (described in chapter 5).

Editorial and Other Minor Corrections

- Information which sensitivity factors to calculate are given in the input file instead of being included in the program.
- Computing time is saved by treating deterministic variables as constants instead of treating them as variables.
- Computing time is saved when calculating the Hessian matrix benefitting from symmetry properties.
- In JOINT3 a limit on the number of sub-iterations is introduced.
- An inconsistency in some optimality parameters in JOINT3 is corrected (leading to the possibility that inactive components, which are not included in the calcu-

lations, could be bigger than allowed in the convergence criterion for the failure functions and therefore the calculation would show no convergence).

- A few errors are corrected.

Including Inactive Components
The original version of PARLSENSI does not include inactive components of parallel systems in the calculations. In the revised version an option is included for linearization of inactive components because the inactive components sometimes influence the probability and sensitivity factors considerably. After having calculated the joint design point for the active components, a joint design point is determined for each of the inactive components keeping the actual component active by putting an equality constraint on the limit state function. Exceptions are made for "permanently" inactive components as described below.

Highly Correlated Components
To avoid numerical problems the following is included. If two components have a coefficient of correlation close to 1, the component with the lowest failure function value in the mean value point is removed permanently from the active set, see figure 6.1. I.e. even if inactive components are included in the calculations this component will not be included.

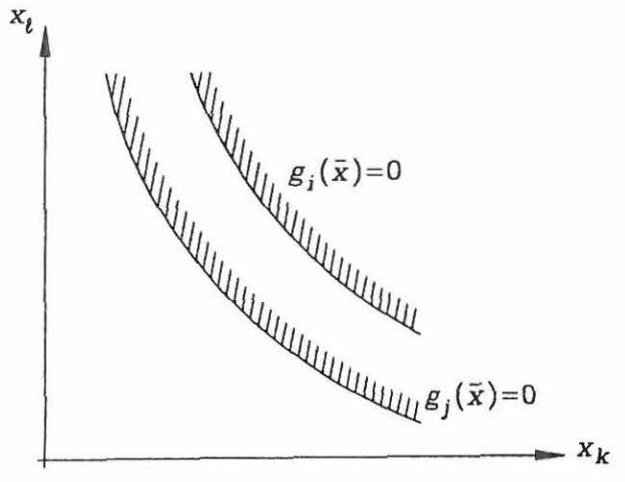

If $\rho_{ij} \geq 0.94$ component no. j $(g_j(E[\mathbf{X}]) \leq g_i(E[\mathbf{X}]))$ is removed permanently from the active set.

Figure 6.1 Highly correlated components.

Disjoint Components
If two components in the parallel system are disjoint the probability is set equal to zero. This is done by comparing all components using the same failure function (yielding failure or repair) with an opposite sign, i.e. failure and non-failure. If the coefficient of correlation is close to -1 and minus the non-failure function value is smaller than the failure function value in the mean value point, then P_F and the sensitivity factors are set equal to zero, see figure 6.2.

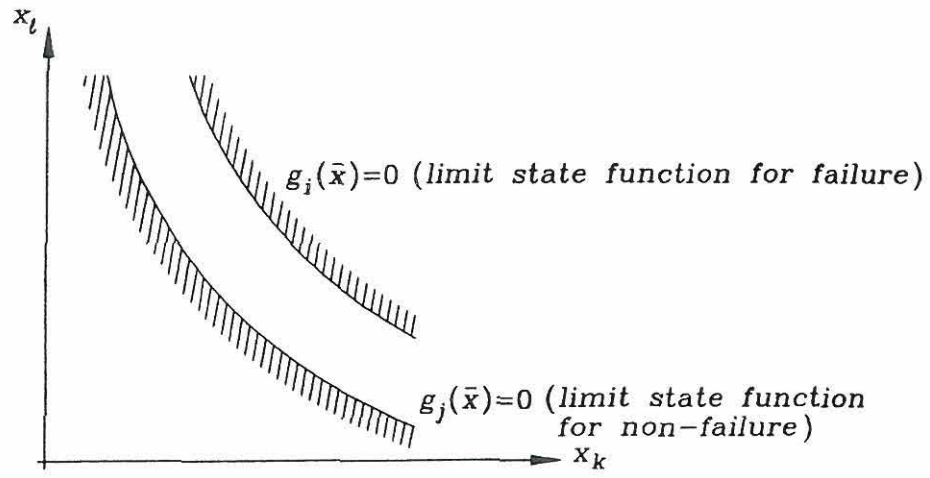

If $\rho_{ij} \leq -0.94$ and $-g_j(E[\mathbf{X}]) \leq g_i(E[\mathbf{X}])$ then, $P_F = 0$.

Figure 6.2 *Disjoint components.*

A disadvantage of the program is still that it cannot calculate the probability if all failure functions are negative in the mean value point, i.e. the system reliability index is negative, but this could easily be incorporated if wanted.

6.3 PRODIM2

The first version of PRODIM (PRobability-based Optimization of Design, Inspection and Maintenance program) was developed in a cooperation between A.S. Veritas Research, Danish Engineering Academy and Computational Safety and Reliability, Aalborg, Denmark. PRODIM calculates optimal design parameters and inspection plans considering damage caused by fatigue crack growth in steel. The total expected cost of design, inspection, repair and failure is minimized with a constraint on the failure probability. It is possible to choose between two optimization methods which are both sequential quadratic programming techniques (NLPQL, see e.g. Schittkowski, 1986, and VMCWD, see e.g. Powell, 1982). The program is described in PRODIM, 1988, and the first version of PROBAN is used for calculation of probabilities and sensitivity factors.

In short the following changes have been made:

- To begin with PROBAN-2 was called instead of PROBAN-1. Due to major changes in the input file for PROBAN this caused a complete change of some of the subroutines (SMARGM and SMARGP) in PRODIM.
- PARLSENSI is called instead of PROBAN-2 and changes corresponding to the input file to PARLSENSI have been made.
- Only inspection times are considered as optimization variables. In the first version of PRODIM also design parameters and inspection qualities are included. This

was done to simplify the problem and due to lack of time these variables were not included again.

- Only one repair strategy is included compared to four strategies in the first version. The possible decisions after an inspection are repair or no repair. Repair means that the structure is brought back to the initial state, i.e. each time a repair has taken place the initial time is set equal to the repair time and new corrosion parameters are generated for the following safety and event margins.
- New limit state functions for failure and repair are introduced, i.e. yielding and repair in a longitudinal. This influences the input file to PRODIM2 and the input created for PROBAN-2 or PARLSENSI.
- The parameter IFAIL is included in the input file to PRODIM2. This allows an option for checking gradients if the optimization method VMCWD is used.
- A couple of minor errors are corrected.

6.3.1 Description of PRODIM2

In figures 6.3 and 6.4 the organization of PRODIM2 is shown. The figures are taken from PRODIM, User's Manual, 1988 and modified.

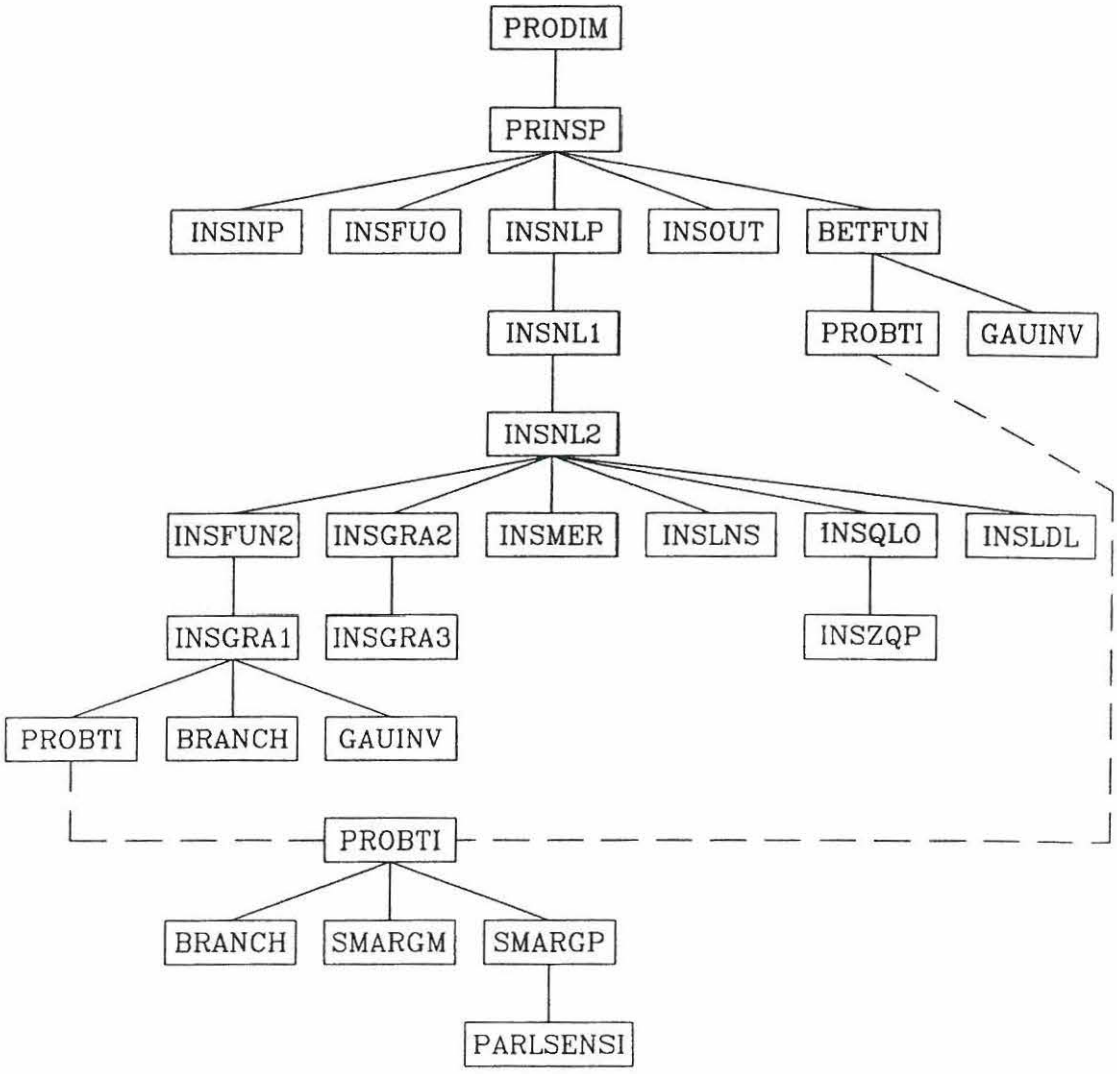

Figure 6.3 Organization of PRODIM2 with call of NLPQL.

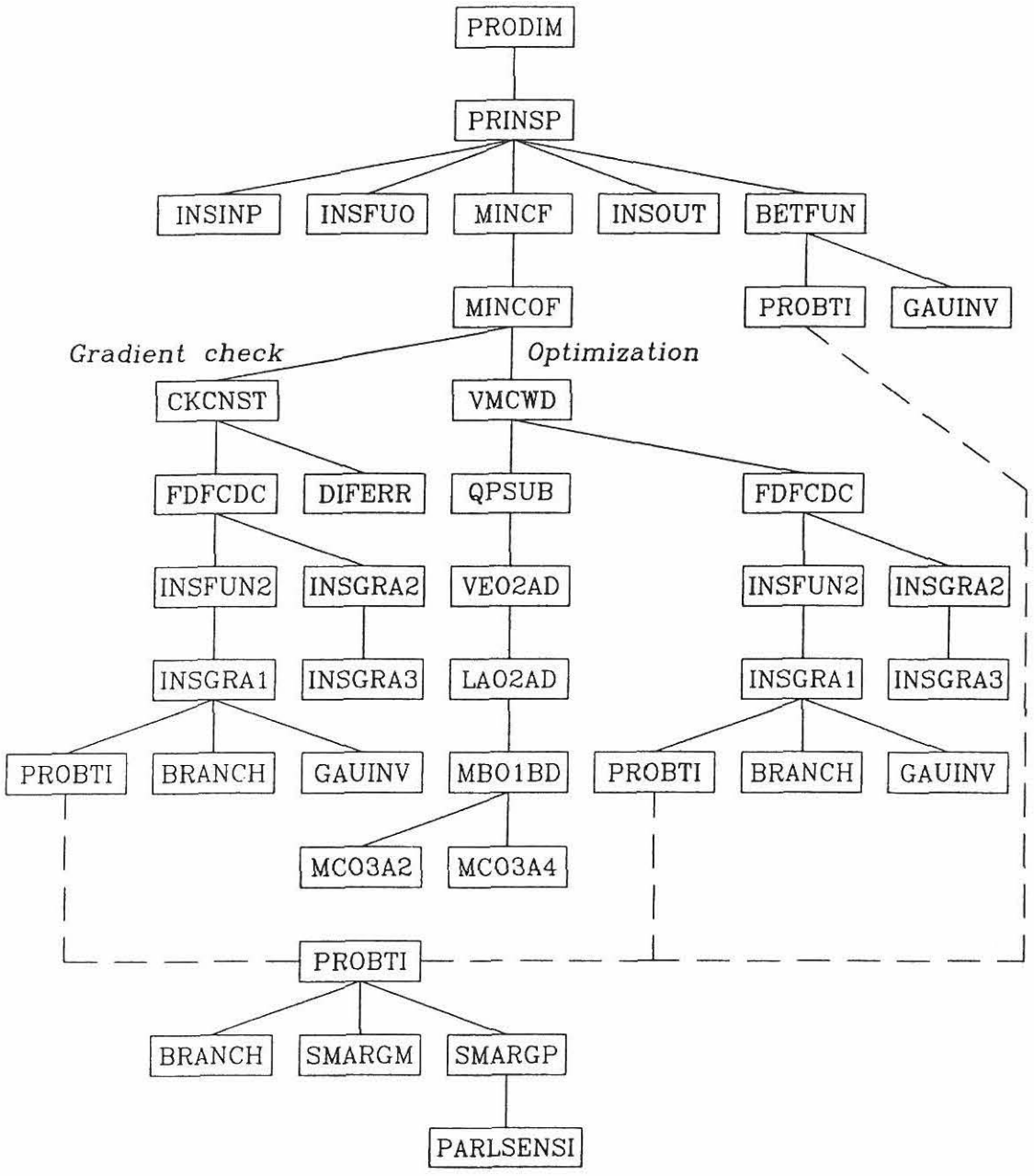

Figure 6.4 Organization of PRODIM2 with call of VMCWD.

The subroutines are described in short in the following.

PRODIM2	Main program.
PRINSP	Main subroutine. Initialization of main working arrays.
INSINP	Data input.
INSFU0	Initialization of optimization variables.
INSOUT	Print of result of optimization.

BETFUN	Print of reliability index β as a function of time.
INSFUN2	Calculation of objective function and constraints. Called from optimization algorithm.
INSGRA1	Main subroutine for calculation of objective function and constraints. Also the gradients of the objective function and the constraints are calculated and stored.
PROBTI	Estimation of increase in probability of failure $\Delta P_F(T_{i-1}, T_i)$ from T_{i-1} to T_i. Estimation of expected number of repairs $E[R_i]$ at the time T_i.
BRANCH	Determination of inspection events in a given branch.
GAUINV	Inverse standard normal distribution function.
INSGRA2	Calculation of gradients of objective function and constraints. Called from an optimization algorithm.
INSGRA3	Gradients calculated by INSGRA1 are read.
SMARGM	Generation of input to PARLSENSI for variables.
SMARGP	Generation of system description (input to PARLSENSI, call of PARLSENSI and identification of β and gradients of the system from output of PARLSENSI.
PARLSENSI	The probabilistic analysis program.

NLPQL subroutines:

INSNLP, INSNL1, INSNL2, INSMER, INSLNS, INSQL0, INSZQP, INSLDL

VMCWD subroutines:

MINCF, MINCOF, CKCNST, FDFCDC, DIFERR, VMCWD, QPSUB, VE02AD, LA02AD, MB01BD, MC03A2, MC03A4

The input to PRODIM2 is described in appendix 3.

6.4 References

Enevoldsen, Ib (1991), *Reliability-Based Structural Optimization*, Ph.D.-Thesis, Structural Reliability Theory, Paper no. 87, The University of Aalborg, Denmark.

Enevoldsen, I.; J.D. Sørensen (1992), *Optimization Algorithms for Calculation of the Joint Design-Point in Parallel Systems*, Structural Optimization, Vol. 4, pp. 121-127.

Enevoldsen, I.; J.D. Sørensen (1993), *Reliability-Based Optimization of Series Systems of Parallel Systems*, Journal of Structural Engineering, Vol. 119, No. 4, ASCE, U.S.A.

Powell, M.J.D. (1982), *VMCWD: A Fortran Subroutine for Constrained Optimization*, Report DAMTP 1982/NA4, Cambridge University, England.

PROBAN-2, Theory Manual (1989), A.S. Veritas Research Report No. 89-2023, Høvik, Norway.

PROBAN-2, User's Manual (1989), A.S. Veritas Research Report No. 89-2024, Høvik, Norway.

PROBAN-2, Example Manual (1989), A.S. Veritas Research Report No. 89-2025, Høvik, Norway.

PROBAN-2, Distribution Manual (1989), A.S. Veritas Research Report No. 89-2026, Høvik, Norway.

PROBAN-2, Command Reference (1989), A.S. Veritas Research Report No. 89-2027, Høvik, Norway.

PRODIM, Theoretical Manual (1988), A.S. Veritas Research Report No. 88-2029, Høvik, Norway.

PRODIM, User's Manual (1988), A.S. Veritas Research Report No. 88-2030, Høvik, Norway.

PRODIM, Examples Manual (1988), A.S. Veritas Research Report No. 88-2036, Høvik, Norway.

Schittkowski, K. (1986), *NLPQL: A Fortran Subroutine Solving Constrained Nonlinear Programming Problems*, Annals of Operations Research, 5, pp. 485-500.

CHAPTER 7
CONCLUSION

Conventional strategies for inspection and maintenance are based on experience as described in chapter 2. They are normally performed with constant time intervals between inspections and in many cases a structure is subject to different types of inspection characterized by varying thoroughness and different inspection intervals.

The wish to make inspections cheap and the structure reliable has lead to the development of optimal reliability-based strategies which normally means optimal with regard to the expected cost but in a few of the models described the availability of the structural system is optimized. Three categories of models are described in chapter 3. In the first category the failure mode is not specified and the system can be in only two states - the failure state or the non-failure state, in the second category a Markov model is used to describe the state of the system and in the third category the development of fatigue cracks or corrosion is described by continuous deterioration laws, e.g. the Paris and Erdogan equation. In the third category the most realistic models are included and for these models, which are developed first of all at A.S. Veritas Research, the Danish Engineering Academy (until recently) and the University of Aalborg, the practical use seems to be within reach.

In this thesis inspection strategies have been considered for two different structures - a steel girder bridge (chapter 4) and a tanker (chapter 5). The models developed are based on model 3.1 described in chapter 3. The most important difference from model 3.1 is that the models presented here do not consider the structure as one system with a number of failure modes. Instead advantage has been taken of the fact that if the structure consists of several structural components that are almost alike but with different dimensions and/or loadings then the cost might be reduced by inspecting these components at different intervals. Consequently the components are divided into groups and for each group an inspection strategy is determined. It is assumed that the most rational would be to restrict the inspections of components with rare inspections to take place when the remaining components are inspected.

For the steel girder bridge the above-mentioned structural components correspond to the girders. For each girder three failure modes are included and these failure modes - bending, shear and bearing failure - are modelled in a series system. The capacity of the steel girders are assumed to decrease with time due to corrosion. Based on the failure probability as a function of time for each girder an inspection strategy is proposed and it turned out that the same inspection interval should be applied

to all girders for the highway bridge under consideration as the reliability indices of individual girders decrease to the minimum reliability index after the same period of time. The calculations could be improved by including fatigue failure, by assuming that the steel girders are protected against corrosion for a period of time and by updating the reliability indices after each of the scheduled inspections.

For the tanker the above-mentioned components are the longitudinals at the ship side. The cross-section of the tanker is exposed to corrosion and reliability calculations are made for each longitudinal based on a series system with two failure modes - yielding and fatigue failure. Based on the yielding failure mode optimal inspection strategies are determined for three longitudinals representing three groups of longitudinals with different reliability levels. The calculations show that the expected total costs can be reduced and the safety of the structure improved for a given number of inspections using optimal inspection intervals instead of constant inspection intervals and furthermore, the expected costs can be reduced by using different strategies for the longitudinals instead of using the same strategy for all longitudinals. The calculations also show that if the expected failure cost contribute considerably to the expected total costs then the optimal strategy is not to wait as long as possible, with due regard to safety requirements, before inspecting, so a reliability-based inspection strategy will not necessarily be optimal. The calculations could be improved by including fatigue failure and by modifying some of the conservative and non-conservative assumptions described in chapter 5.

In chapter 6 the programs used for reliability calculations and optimizations are described. Due to problems with the commercial program PROBAN-2 it was decided to use the program PARLSENSI for reliability calculations in the inspection optimization program PRODIM2. The most important change made in PARLSENSI is that inactive components can now be included in the calculation of probabilities and sensitivity factors which was not possible in the original version. To improve the program further, corrections should be made so that parallel systems with a negative system reliability index could be calculated. In PRODIM2 (and in the original version of PRODIM) options are included for approximated calculations of probabilities of parallel systems. For instance, it is possible to exclude inactive components, but during the calculations concerning the tanker in chapter 5 it was realized that this approximation may give misleading results, for example that the reliability index gets smaller the more inspections made. So it is concluded that this option should be treated with care.

Finally, some suggestions for improvement of the inspection optimization program PRODIM2 are listed.

- A complicated system of series and parallel elements should be available to be able to describe a realistic structure. Some work is being done in that area, see e.g. model 3.1 in chapter 3.
- The user of the program should be able to define the failure modes and repair events.

- More optimization variables should be included. In some models in chapter 3 the inspection qualities and a design parameter are optimization variables in addition to the inspection times (these variables are included in the original version of PRODIM). The inspection quality could be separated into two contributions namely the reliability and accuracy of the inspection method and the skills of the inspector which are both connected to the cost of an inspection. Eventually, repair qualities could be introduced as optimization variables describing the degree to which the structural component is brought back to the initial state.

Research could also be made to improve the description of the deterioration processes (fatigue and corrosion), the inspection qualities, the effect of repair and the total expected cost of a structure during its lifetime.

Since reliability and optimization calculations are expensive and time-consuming, the benefit from using optimal reliability-based inspection strategies probably have to be considerable before the authorities responsible for inspection of structures are motivated to use them. Furthermore, it is normally necessary that the user of a reliability or optimization program is well educated to be able to use the program correctly. Not least, for some inspection planners it will require a change of attitude and more flexibility to accept varying instead of constant inspection intervals. In the future optimal inspection strategies may be used for large structures or if a large number of similar structures is present so that the investments required can be counterbalanced by the savings.

APPENDIX 1
NON-DESTRUCTIVE INSPECTION AND REPAIR OF STEEL STRUCTURES

A1.1 Introduction

A number of different methods for inspection of steel structures for cracks or corrosion exists. These methods can be divided roughly into two categories:

- Visual inspection, supplemented by video recordings and photos.
- Non Destructive Examination (NDE)/Non Destructive Testing (NDT).

The abbreviations in NDE ståbi, 1987, have been used. NDT covers methods used for production control (pre-service inspection) and NDE covers methods used for in-service inspection. The NDE-methods consist of four main types of technique:

- Electromagnetic methods.
- Ultrasonic methods.
- Acoustic emission.
- Radiographic methods.

The electromagnetic and ultrasonic methods, of which there are a great variety, are the most widespread, for instance some of them are referred to in rules from Det Norske Veritas and Lloyd's. The radiographic methods are also well known but not so widely used. Many of the methods can be used for both crack detection and thickness measurement, i.e. corrosion detection, and some of the methods may have other features but they are not referred to here. A NDE-technique for detection of cracks or corrosion which is investigated by a growing number of researchers is modal analysis using strain-gages, accelerometers and/or displacement transducers for monitoring the structure, see Proceedings of OMAE, 1992. The technique is not described further here since it is not very widespread.

A detailed description of most of the methods is given in Underwater Inspection..., 1989, and NDE ståbi, 1987. In Sommer and Thoft-Christensen, 1990, a summary similar to this appendix is available.

A1.2 Visual Inspection

Visual inspection will indicate gross defects and areas that need a closer examination and according to Miki et al., 1990, visual inspection is so far the most reliable method if the testing is performed by a skilled technician. Below water the result

of a visual inspection is not very reliable, for the reason among others that the divers normally have fewer formal qualifications than an above water inspector. A visual inspection can be performed directly by an engineer inspector, a diver or by a manned submersible or it can be performed indirectly by remotely operated vehicles (ROV)/remotely controlled vehicles (RCV) (see Offshore vedligeholdelse, 1984, or Det Norske Veritas, 1980). Normally the inspection results are reported as photographs or video recordings. Surface breaking cracks can also be detected by dye penetrant.

According to Det Norske Veritas, 1981, all welds are to be visually inspected, whereas they are tested non-destructively to an extent varying from 5 to 100%.

A1.3 Electromagnetic Methods

These methods are based on a magnetic and/or electric field in the material. The disturbances caused by surface breaking irregularities are measured.

Magnetic Particle Inspection (MPI)
MPI is the most frequently used NDE-method and there are several different magnetization methods. In Offshore Technology, 1984, the following methods are mentioned:

- Prods, which impress a current that induces the magnetic field.
- Coils and conductors, the current again produces the magnetic field.
- Permanent magnets (produce a weak magnetic field).
- Yokes.

If the magnetic field is produced by a current both alternating current, pulsing direct current and direct current can be used. The strength of the magnetic field must neither be too high - then non-existent defects will be found - nor too low - then defects will not be detected. The magnetic flux lines are disturbed by discontinuities such as surface breaking cracks and the flux will either pass around the tip or bridge the discontinuity at the surface - called flux leakage, see figure A1.1.

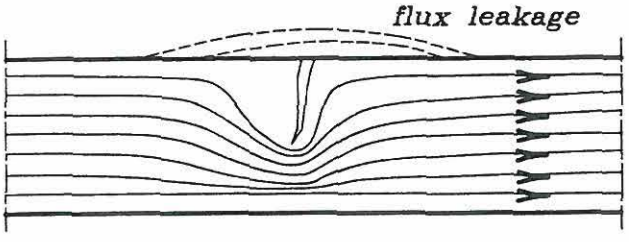

Figure A1.1 MPI-method.

The flux leakage is revealed by covering the surface with magnetic particles. If the

inspection is below water a magnetic ink is used, which consists of magnetic particles in a liquid carrier. Usually, the liquid carrier is a fluorescent water base, i.e. the surface can be examined under ultraviolet light in dark areas.

To detect all defects it is necessary to magnetize the steel in two mutually perpendicular directions as defects parallel to the flux lines are not discovered. The surface of the material must be cleaned to the bare metal according to Det Norske Veritas, 1981, and it is recommended to grind the surface to make it very smooth.

MPI is usually used to detect surface breaking cracks, but it can also size the crack length. According to Offshore Technology, 1984, the smallest detectable crack length is 5 mm +/− 1 mm. According to NDE ståbi, 1987, it is 2 - 3 mm under optimum conditions. In Miki et al., 1990, a number of tests is described showing that the smallest detectable crack length is 2 - 5 mm and the smallest detectable crack depth is 0.5 mm. In Lassen, 1991, the probability of detection is plotted as a function of crack depth for MPI showing that the probability is 0% for a crack depth of 1 mm and 80 % for a crack depth of 3 mm. According to Miki et al., 1990, the crack length is often overestimated with up to 5 mm. The probability of detection is reduced, when the cracks are tight and the faces are getting into contact.

There are several ways to record the MPI results. The best way is to photograph the magnetic particles using ultraviolet flash gun, another way is to take an imprint of the particles using a magnetic tape and a third way is to use a plastic envelope with epoxy, hardener and ink, which is mixed on the work site and applied over the weld (Mills, 1984).

Most of the time used for inspection is cleaning time. If the inspection takes place under water a ROV can clean the member faster than a diver and that makes the cleaning about 50% cheaper than if it is performed by a diver. MPI is as cheap or even cheaper than other NDE-methods.

Eddy Current (EC) Technique
This technique is not so widely used but it is expected to be more frequently used for underwater inspection in the future.

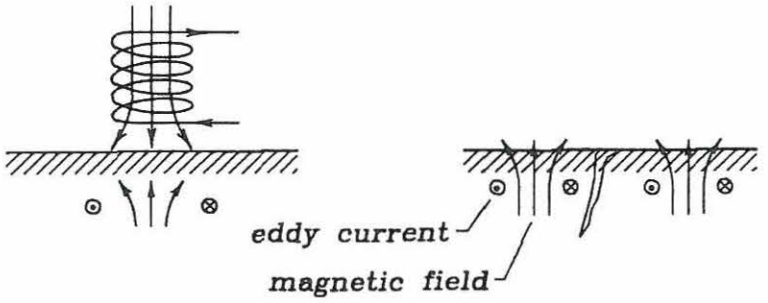

Figure A1.2 Eddy Current technique.

A coil with an alternating current produces a magnetic field so if the coil is held close to the material to be examined the magnetic field will induce currents, called eddy currents, in the metal. The eddy currents will produce a magnetic field in the metal with the same frequency as in the coil but with opposite directions.

A defect in the metal close to the surface will cause a characteristic phase shift between the exciting and the induced field, as the induced current will pass either around or under the crack. The changes in the induced electromagnetic field can be amplified and displayed and thereby cracks can be detected but the crack signals might be confused with changes due to e.g. surface roughness or heat affected zones. By using an alternating current with high frequency, surface breaking cracks are detected, and with low frequency buried cracks and corrosion are detected.

There are no strong requirements for the cleaning of the surface, only that it should be so smooth that the probe lift-off is max $+/-$ 2 mm.

The EC technique can be used to detect surface breaking cracks or corrosion, but it can also size the crack length. According to Miki et al., 1990, the smallest detectable crack length is 5 - 6 mm and the smallest detectable crack depth is 1 mm. Cracks over 30 mm in length are overestimated with up to 20 mm so it is concluded that the EC technique is not suitable for estimation of the crack length. The probability of detection is between 25 and 40% depending on the equipment used according to Offshore Technology, 1984. Referring to NDE ståbi, 1987, the reliability of the method is the same as for MPI. Filled cracks do not affect the reliability of detection. Compressive loads giving tight cracks decrease the signals but not seriously.

The results can be stored by videotaping the positions corresponding to the measurements. The method requires less time for cleaning than MPI, but the total costs are about the same.

Alternative Current Potential Drop (ACPD)/
Alternative Current Field Measurement (ACFM)
It should be mentioned that in Underwater Inspection..., 1989, ACPD is an abbreviation for *Alternating Current Potential Drop* while the abbreviations given above are used in Offshore Technology, 1984.

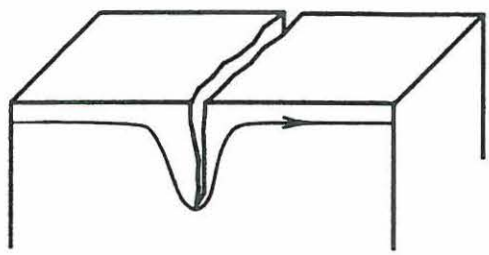

Figure A1.3 Alternative Current Potential Drop.

Using these methods an electric field is produced in the metal. There are several ways to do this. The frequency of the current is between 50 Hz and 1 MHz and depending on this frequency the current will penetrate from 0,1 mm to 2 mm into the metal (Offshore Technology, 1984). The potential difference between two probes placed on the metal is proportional to the distance of the probes and if there is a crack between the probes the distance will increase by twice the crack depth as the current passes under the crack.

If the crack is short compared to the depth (i.e. the depth > 20% of the length), the current might pass around the crack instead and another problem is that the crack depth is undersized if the angle between the surface and the crack is less than 60°.

The surface only needs to be cleaned to the bare metal below the probes. The method is used to size depth of surface breaking cracks provided that the depth is at least 2 mm and the accuracy of the sizing is about +/− 1 mm according to Mills, 1984. But if the cracks are tight the sizing of the depth might be affected.

The results are recorded manually. The time required and the costs are the same as for MPI.

A1.4 Ultrasonic Methods

Sound waves are defined as elastic oscillations in gases, liquids or solids. They consist of three groups (f is the frequency):

- Infrasound, $f < 10$ Hz.
- Sound, 10 Hz $< f <$ 20,000 Hz (perceptible for human beings between 15 Hz and 17,000 Hz).
- Ultrasound, $f >$ 20,000 Hz.

When testing by ultrasonic methods it is recommended by Det Norske Veritas, 1981, that the frequency range should be 2 - 6 MHz. The methods rely on evaluating the wave propagation in the material, which is composed of:

- Propagation of undisturbed wave.
- Diffraction, i.e. the wave propagates from the corner of a defect, e.g. a crack, with a cylindrical wave front.
- Refraction, i.e. the bending of the beam by passing through materials of varying optical density.
- Reflection by the back wall of the material or by discontinuities, e.g. a defect.

The velocity of the ultrasonics is a known property of the material. Referring to Underwater Inspection..., 1989, the energy can propagate in the steel in two ways at different speeds, i.e. as compression waves perpendicular to the steel surface (used for thickness measurement) or as shear waves at an oblique angle to the surface (used for defect characterization). Compression waves can also be used at an oblique angle

to the surface, but then they generate undesired shear waves according to Silk et al., 1987. By measuring the time lag between the transmission of the signal and the reception of the reflected or diffracted wave, a crack or other discontinuities are detected.

Methods Based on Reflected Waves

There is a great variety of techniques based on reflected waves and only a few is mentioned here. In most techniques the angle of the beam is varied, since otherwise some defects may be missed because of their orientation. One of the most commonly used methods is the pulse echo technique which is performed with straight beams or angle beams of 45°, 60°, 70° or 80° to the surface, see figure A1.4.

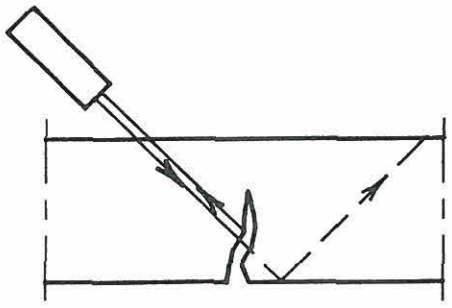

Figure A1.4 Pulse echo technique.

Another common method is the double probe technique using one probe for emission of the ultrasonic beam and another for receiving the echo. The angle of the beams is normally 45°. Both methods are mentioned in Det Norske Veritas, 1981. There are several variations of the double probe technique, see e.g. Silk et al., 1987.

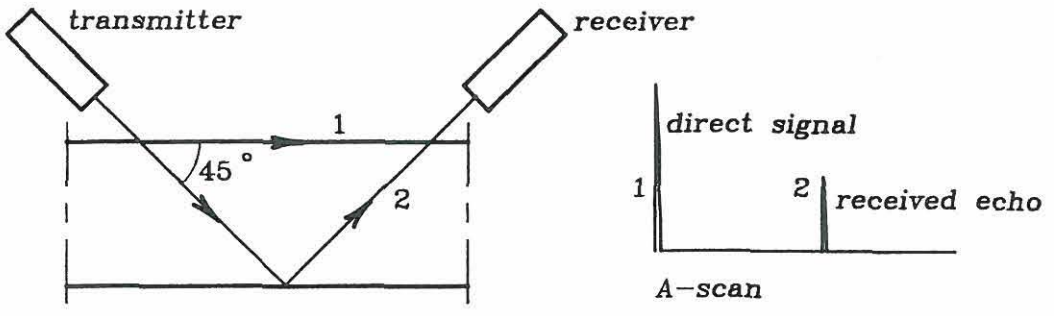

Figure A1.5 Double probe technique.

The signal received can be measured in several ways and in Silk et al., 1987, A-Scan, B-Scan and C-Scan are described. A-Scan is the trace produced on an oscil-

loscope after amplifying the signal received, i.e. the signal is depicted as a function of time/distance, see figure A1.5. In this case the transducer is not moved. B-Scan indicates a series of A-Scans, i.e. the transducer is moved in one dimension between each pulse thereby depicting various cracks in the specimen. The A-Scans are stacked so that the signals from one crack are placed beneath each other, i.e. the signals are depicted as a function of distance from the same point. C-Scan also indicates a series of A-Scans, but in this case the transducer is moved in two directions. It is also possible to use digital display, if the purpose of the test is merely to measure plate thickness.

In the projection image scanning (P-Scan) technique the defect position is visualized by projecting the defect on two planes, i.e. one parallel to the surface and one perpendicular to the surface and parallel to the weld. That produces a three-dimensional location of the defects.

It is required that the surface of the material is very smooth, i.e. marine growth, paints in bad condition and thick rust are to be removed before examination. The methods are used to detect corrosion or cracks - both buried and surface breaking cracks and it is also possible to size the crack depth or length. The reliability of crack detection is not too good. About 30% of the cracks are detected according to Offshore Technology, 1984. In Miki et al., 1990, the minimum detectable crack depth is found to be 1 mm. According to Jubb, 1984, it is said that 50% of ultrasonic operators only find 50% of the cracks. The accuracy of sizing the cracks is about +/− 5 mm for the depth and +/− 44 mm for the length with a deviation of 140 mm (Offshore Technology, 1984, Mills, 1984). In Miki et al., 1990, the accuracy of the sizing of the crack depth is +/− 1 mm if the crack is deeper than 2 - 5 mm and the sizing of the crack length is unreliable. The methods might have problems with detecting cracks that are filled with e.g. corrosion products or that are tight according to compressive loads.

The results are recorded by storing the received signals in a computer and the probe positions on a video.

At the inspection most of the time is used for cleaning and Mills, 1984, states that ultrasonic methods require more cleaning and surface preparation than MPI and the testing is more time consuming and therefore more expensive than MPI. However, automated methods are being developed which will make ultrasonic methods faster and cheaper.

Time-of-Flight-Diffraction (TOFD)

The method requires two probes, one for transmitting the signal and one for receiving it, and as the name indicates it relies on the diffracted waves measuring the time-of-flight from the signal is transmitted till it is received. Defects will change the path of the signal and thereby the time-of-flight so the method can be used to size and locate both hidden and surface-breaking cracks, see Underwater Inspection..., 1989.

Acoustic Pulsing

Acoustic Pulsing is a relatively new ultrasonic technique which can be used for mon-

itoring, which means a continuous surveillance of the structure. The technique is described in Bartle and Mudge, 1983. A network of widely spaced transducers (e.g. spaced 10 m) is placed on the surface of the structure. Defect growth will change the signal between at least one pair of transducers and hence cracks will be detected by comparing new results with earlier records. In this way suspect areas to be examined closely can be located. The advantages of the method are that underwater structures can be monitored without divers and the monitoring system does not have to run continuously which makes it cheaper than acoustic emission. Until now the method has only been used in laboratory studies.

A1.5 Acoustic Emission (AE)

The presentation here of AE is based on the book by Williams, 1980. When a material is subjected to stress levels causing atomic rearrangements due to deformation or cracking, these rearrangements produce elastic waves (discrete, acoustic wave packets) in the material. At the surface these waves can be detected by transducers. This goes for most structural materials, e.g. steel, aluminium and concrete. Acoustic emission is normally only generated when the loading exceeds previous loadings as it requires changes at the atomic level. By analysing the emissioned energy and the frequency spectrum the deformation can be characterized. The position of the acoustic emission source is detectable by using 3 or more transducers and measuring the arrival times of the signal.

A great advantage of the method is that the transducers do not have to be so near the area to be examined as for ultrasonic methods and this means that a complex structure can be examined or monitored using much fewer transducers. As a matter of fact AE is the best suited method for monitoring among the available NDE-methods. Monitoring has the advantage that cracks are detected before they get too big, i.e. the repair is cheaper.

A problem by this method is to distinguish the acoustic emission from background noise, but equipment has been developed to deal with that (Williams, 1980). Other problems are that in some metals crack growth does not produce acoustic emission, and sometimes acoustic emission is produced by other sources than crack growth (Mills, 1984). But the technique is still being developed.

The frequency response of the transducer can be both narrow and wide-banded. In Williams, 1980, it is stated that for industrial applications the frequency response should be in the range from 100 kHz to 1 MHz, but in most investigations a narrow frequency range has been used.

The method does not require any cleaning of the surface. The equipment for acoustic emission is quite expensive, but it is not clear how the costs and time required are to be compared with other NDE-methods.

Williams, 1980, states that strains greater than 0.05% can be measured.

According to Williams, 1980, the AE-method is becoming widespread for 24 hour

monitoring supplemented by visual, electromagnetic or ultrasonic examinations when the monitoring detects critical areas but referring to Underwater Inspection..., 1989, AE is suitable for temporary installation, monitoring known defects, since permanent monitoring of a structure is often too costly.

A1.6 Radiographic Methods

For radiography, x-rays and gamma rays can be used. The principle of the technique is shown in figure A1.6.

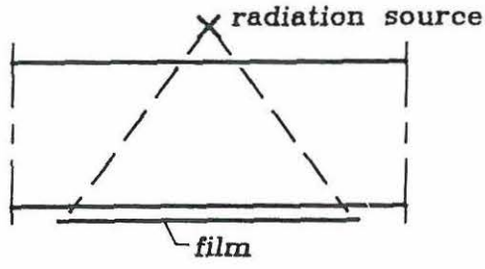

Figure A1.6 Radiography.

Cracks or other variations in the material will appear on the film/radiograph as cavities permit a bigger part of the rays to pass through the material and blacken the film. The film length may vary. The panorama technique makes it possible to radiograph the full length of a weld on one film by using several radiation sources. It is possible to determine the defect position by taking three radiographs from different directions and using numerical image processing techniques.

The methods are used to detect corrosion or cracks in critical areas but not to examine the whole structure. An inconvenience of the method is that both sides of the subject must be accessible.

The radiographic methods are not so widely used and when they are used it is normally above water. In Det Norske Veritas, 1981, radiographic testing is only required for between 0 and 20% of the welds at pre-service inspection.

Information of the cost, time consumption and reliability of the radiographic methods is not available but in NDE ståbi, 1987, the accuracy is stated to be +/− 5% or +/− 0.3 mm.

A1.7 Applicability of the Techniques

With the information available it is not possible to make any choice between inspection methods solely on the basis of the cost of the methods. The judgement must first of all be based on the properties of the methods.

Regarding crack detection the usable methods are MPI, the EC-method, ultrasonic methods based on reflected waves, AE and radiographic methods. MPI and the EC-method are only capable of detecting surface breaking cracks while ultrasonic methods based on reflected waves detect both surface breaking and buried cracks. MPI is the most reliable of the electromagnetic and ultrasonic methods, the technique detects about 80% of the cracks. AE is well suited for permanent surveillance, besides it only registers the deformation as it is propagating so it could not be used for periodic inspection.

Sizing of crack length can be performed by MPI (surface breaking cracks) and ultrasonic methods based on reflected waves (unreliable) and sizing of crack depth can be done by the ACPD-method (surface breaking cracks) and ultrasonic methods based on reflected waves.

Mills, 1984, states that fatigue cracks are usually surface breaking cracks, i.e. MPI is normally sufficient for in-service crack detection. In practical applications it is often only necessary to size the crack depth, but even then it is obvious that several methods must be used to detect and size all cracks.

The corrosion protection system (e.g. coating, cathodic protection), if there is one, has to be inspected of course but this is not described here. The corrosion penetration is normally measured by measuring the thickness of the steel and this can be done using the EC-method, ultrasonic methods based on reflected waves or radiographic methods.

Techniques are being developed for using ROVs for cleaning the surface and for NDE. This will make inspections faster and cheaper.

In Det Norske Veritas, 1981, it is required for pre-service inspection that MPI and/or ultrasonic testing of all welds is performed for special structural steel and for secondary structural steel 0 - 5% of the welds must be inspected. Radiography is used for a minor part of the welds. MPI and the ultrasonic methods are also the NDE-techniques most often referred to by Lloyd's.

This review indicates that the applicability as well as the reliability of the available methods is poor and in accordance with normal practice a combination of MPI and ultrasonic methods is concluded to give the best results.

A1.8 Repair Techniques

If corrosion or a crack is detected there are four possibilities with respect to repair:

1. The damage is so small that it can be accepted in the structure and crack propagation can be stopped by drilling arrestor holes in the toes of the crack.
2. If the damage is not too deep it may be removed by grinding. According to Det Norske Veritas, 1981, the area is to be examined by MPI or other NDE-techniques afterwards.
3. The damaged part of the structure is replaced.

4. The structure is reinforced by adjusting structural parts to it so the original strength of the structure is either restored or increased.

Repair techniques for offshore structures and steel ships are briefly explained in the following.

Offshore Structures

Repair performed by welding is extensively used and earlier it was the predominant repair technique (Tebbett and Lalani, 1986). Welding repair can be used to replace a damaged part or to install additional members supporting the damaged member. Replacement implies that the structure can manage without the damaged member or part of the member for some time. Additional members cause extra loads on the structure and one must make sure that the load capacity of the structure is sufficient.

Below water the welding can be performed as wet welding or dry welding. In Tebbett, 1987, however, it is stated that the quality of wet welding is constrained by the fact that the weld area is only protected locally against the seawater by the welding process. Dunn, 1984, who has some experience based on the Gulf of Mexico, says that the quenching effect of the surrounding water may cause more problems than the wet welding solves but work is being done to improve the quality. Wet welding is only used for secondary and tertiary structures.

Dry welding below water can be performed by surrounding the part of the structure to be repaired by a sort of box or chamber (Offshore vedligeholdelse, 1984). The air pressure in the chamber can be hyperbaric or atmospheric depending on the design of the chamber. All the dry welding methods are more expensive than the wet welding method because of the chambers to be constructed.

Clamped repairs are developed as an alternative to welded repairs. If a member of a structure is damaged it may indicate that it is required to strengthen the member. In that case a clamped repair is more appropriate than a welded repair according to Tebbett and Lalani, 1986.

Clamps are cylindrical pieces which are bolted together around the damaged member or joint. Mechanical clamps are fabricated to fit exactly to the existing member, and the bolts are prestressed. The forces will be transferred as friction between the steel surfaces but normally the clamps are made with some tolerance, which is less expensive. If the cavity between the steel surfaces is sealed and grouted with cement, then the forces are transferred as a bond between steel and grout (Tebbett and Lalani, 1986) and the clamps are called grouted clamps. The shear capacity can be increased by prestressing the bolts thereby giving a friction contribution and it can also be increased by welding mechanical shear connectors (usually weld beads) on the steel surfaces in contact with the grout. Clamps can be used to install additional members, replace damaged members, re-establish damaged members or reinforce existing (damaged) members. Figure A1.7 shows some examples of clamp cross-sections.

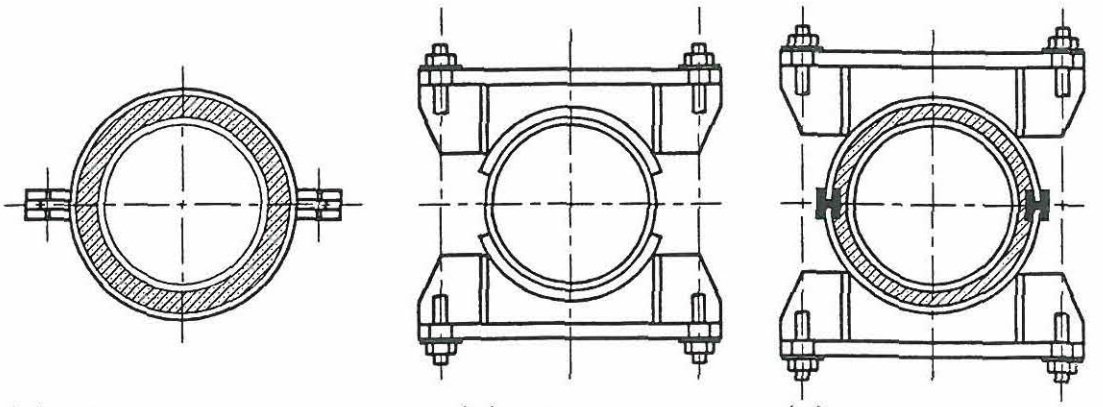

Figure A1.7 Clamp cross-sections (Tebbett and Lalani, 1986).

Welded and clamped repairs have different advantages and disadvantages compared to each other. According to Tebbett and Lalani, 1986, grouted clamped repairs have the following advantages:
- The clamps need not be fabricated to a close fit with the original construction.
- Geometrical damage is easily accommodated.
- The strength of the damaged part can be readily reinstated.
- The original strength of the damaged part can be increased.
- Reduction of underwater work.
- There is no need for specially constructed habitats or cofferdams.

The advantages of welded repairs are:
- By replacement the weight of the structure is unchanged.
- The strength of the repair is more predictable than for clamped repair.

In some cases the property of unchanged weight is essential and a welded repair is chosen even though it is more expensive than a clamped repair. According to Tebbett, 1987, welding is preferred in the case of replacement of the original structure and clamping is preferred when strengthening is required, in case of time trouble or if the physical conditions are difficult (e.g. deep water).

Steel Ships

According to Condition Evaluation..,1991, repair of tanker structures is normally performed as a combination of replacements, reinforcement and improved corrosion protection. The repair strategy should be chosen so the requirements of the owner and the classification societies are fulfilled at the same time as the cost is kept at a minimum. Reinforcement of the structure is often cheaper than renewals but if replacement is chosen it is recommended that complete panels and not only individual members such as stiffeners should be replaced. This may be the most reliable and

cost effective method.

A1.9 References

Bartle, P.M.; P.J. Mudge (1983), *Acoustic Pulsing - A Technique for Remote Defect Monitoring*, The Welding Institute Research Bulletin, London, Sept. 1983.

Condition Evaluation and Maintenance of Tanker Structures (1991), Addendum to *Guidance Manual for the Inspection and Condition Assessment of Tanker Structures*, 1986, Tanker Structure Co-operative Forum.

Det Norske Veritas (1981), *Rules for the Design, Construction and Inspection of Offshore Structures*, Høvik, Norway.

Det Norske Veritas (1980), *Rules for the Design, Construction and Inspection of Offshore Structures, Appendix I, In Service Inspection,* Høvik, Norway.

Dunn, F.P. (1984), *Offshore Platform Inspection*, Proc. Int. Symp. Nov. 1983, Washington, *The Role of Design, Inspection and Redundancy in Marine Structural Reliability*, (Faulkner et al. (eds.)), pp. 199-219.

Jubb, J.E.M. (1984), *Strategies for Assessing Design and Inspection Requirements for Redundant Structures*, Proc. Int. Symp. Nov. 1983, Washington, *The Role of Design, Inspection and Redundancy in Marine Structural Reliability*, (Faulkner et al. (eds.)), pp. 118-137.

Lassen, Tom (1991), *Markov Modelling of the Fatigue Damage in Welded Structures Under In-Service Inspection*, International Journal of Fatigue, Vol. 13, No. 5, pp. 417-422.

Miki, C.; M. Fukazawa; M. Katoh; H. Ohune (1990), *Feasibility Study on Non-Destructive Methods for Fatigue Crack Detection in Steel Bridge Members*, British Journal of Non-Destructive Testing, Vol. 32, No. 6, pp. 293-302.

Mills, R.G. (1984), *Underwater Methods of Assessing and Monitoring the Size of Defects in Steel Weldments*, Underwater Engineering - 6th symposium, IRM/AODC Conference, U.K.

NDE ståbi (1987), *Metoder til ikke-destruktiv tilstandskontrol*, Teknisk Forlag A/S, Danmark.

Offshore Technology Report 84 203 (1984), *The Effectiveness of Underwater Non-destructive Testing - Summary Report of a Programme of Tests*, Techword Services for the Department of Energy, London.

Offshore vedligeholdelse (1984), Petroconsult ApS, Formidlingsrådet, Danmark.

Proceedings of OMAE (1992), Vol. I-B, Calgary, Canada, ASME.

Silk, M.G.; A.M. Stoneham; J.A.G. Temple (1987), *The Reliability of Non-destructive Inspection*, Adam Hilger, Bristol, England.

Sommer, A.M.; P.Thoft-Christensen (1990), *Inspection and Maintenance of Marine Steel Structures - State-of-the-Art*, Structural Reliability Theory, Paper no. 74, The University of Aalborg, Denmark.

Tebbett, I.E. (1987), *The Last Five Years Experience in Steel Platform Repairs*, Annual Offshore Technology Conference, Texas, OTC 5385.

Tebbett, I.E.; M. Lalani (1986), *Recent Development in the Reassessment, Maintenance, and Repair of Steel Offshore Structures*, Annual Offshore Technology Conference, Texas, OTC 5113.

Underwater Inspection of Steel Offshore Installations: Implementation of a New Approach (1989), MTD Ltd. Publication 89/104, London.

Williams, R.V. (1980), *Acoustic Emission*, Adam Hilger Ltd. Bristol, England.

APPENDIX 2
THEORY OF STRUCTURAL RELIABILITY

A2.1 Introduction

In this appendix some basic concepts in structural reliability theory are defined. Reliability theory is explained in more detail in e.g. Madsen et al., 1986, Thoft-Christensen and Baker, 1982, and Thoft-Christensen and Murotsu, 1986, and this appendix is based on these references.

All the different states of a structural system constitute a sample space for the state of that structure, i.e. the sample space is defined by the parameters used to describe the structure completely. A subset of this sample space is called an *event.* All the safe states of the structure constitute the *safe event, safe set* or *safe region* and all the failure states constitute the *failure event, failure set* or *failure region.* A structural system can break down, i.e. get into a failure state, in different ways called *failure modes* and for each failure mode a *failure function* or *limit state function* $g(\mathbf{x})$ is defined determining whether the structure has failed or not. g is a function of deterministic and random variables $\mathbf{x}$ (e.g. dimensions, strength, loads, deterioration parameters, time). A random variable called the *safety margin* M is defined for each failure mode as $M = g(\mathbf{X})$. Usually, "safety margin", "failure function" and "limit state function" are used indiscriminately. The safe set is defined by $g(\mathbf{x}) > 0$ and the probability of non-failure is $P(M > 0)$ while the failure set is defined by $g(\mathbf{x}) < 0$ (or $g(\mathbf{x}) \leq 0$) and the probability of failure is $P(M < 0)$. The surface separating the failure set and the safe set is defined by $g(\mathbf{x}) = 0$ and it is called the *failure surface, limit state surface* or *limit state boundary.*

Correspondingly, for other events such as repair the sample space could be divided into a repair event and a non-repair event defined by the corresponding limit state function and event margin.

A2.2 Reliability Index

The non-failure probability or the reliability of a structural system is often expressed in terms of the reliability index. A system with one failure mode is considered here. If the probability calculations are based on level III methods (meaning that the joint distributions of all random parameters are used in the calculations) then the reliability index β is defined as

$$\beta = -\Phi^{-1}(P_F) \qquad (A2.1)$$

$$P_F = \int_F f_{\mathbf{x}}(\mathbf{x})d\mathbf{x} \qquad (A2.2)$$

where Φ is the standard normal distribution function, P_F is the probability of failure, F is the failure set and $f_{\mathbf{x}}(\mathbf{x})$ is the joint probability density function of the basic variables.

If the probability calculations are based on level II methods (meaning that the means and covariances of all random parameters are used in the calculations) several different definitions of reliability indices are available, see e.g. Madsen et al., 1986. In the programs described in chapter 6 the definition (A2.1) has been used.

Normally, the integral (A2.2) cannot be calculated analytically, therefore, the reliability index is usually calculated approximately. In the probability calculation program PROBAN-2 (see chapter 6) two approximate methods and a number of simulation methods are available. The approximate methods are the First Order Reliability Method (FORM) and the Second Order Reliability Method (SORM) which will be described here briefly. In the probability calculation program PARLSENSI (see chapter 6) FORM is used. The first two steps are the same for FORM and SORM.

1. The basic variables and the limit state function are transformed to a space where the probability (A2.2) is easier to compute and where the probability content of a given set is the same as in the basic space. Normally, the standard normal space is chosen as the transformed space. The transformation can be performed in different ways. For instance, in Madsen et al., 1986, the Rosenblatt transformation is described. This method is used in the programs PROBAN-2 and PARLSENSI. The Rosenblatt transformation is defined as

$$u_i = \Phi^{-1}(F_i(x_i \mid x_1, x_2, ..., x_{i-1})), \qquad i = 1, n \qquad (A2.3)$$

where u_i is the standard normal variable corresponding to x_i,
$F_i(x_i \mid x_1, x_2, ..., x_{i-1})$ is the distribution function of X_i conditional upon $X_1 = x_1, ..., X_{i-1} = x_{i-1}$ and n is the number of variables. In figure A2.1 the original space and the transformed space are shown in the case of two variables. The failure function $g_{\mathbf{u}}$ in the transformed space is defined from g as

$$g_{\mathbf{u}}(\mathbf{u}) = g(\mathbf{x}) \qquad (A2.4)$$

2. In the standard normal space the minimum distance from the origin to the failure surface is calculated. The corresponding point on the failure surface is called the design point. Calculation of the design point can be formulated as an optimization problem for which the derivatives of $g_{\mathbf{u}}$ are needed

$$\frac{\partial g_{\mathbf{u}}(\mathbf{u})}{\partial u_i} = \sum_{j=1}^{k} \frac{\partial g(\mathbf{x})}{\partial x_j} \frac{\partial x_j}{\partial u_i} \qquad (A2.5)$$

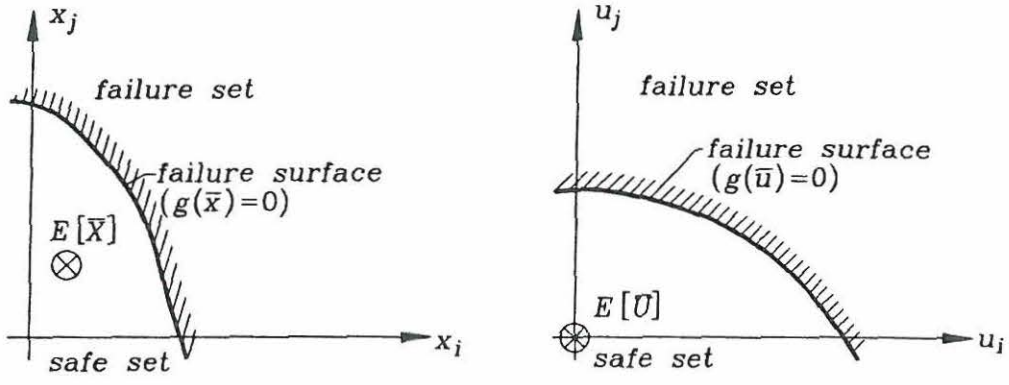

Figure A2.1 Basic space and standard normal space.

3a. If FORM is used the limit state function is approximated by a linear function, i.e. it is linearized at the design point. In this case the reliability index is equal to the distance from the origin to the design point in the u-space and the failure probability can be calculated as

$$P_F \approx \Phi(-\beta^{FORM}) \qquad (A2.6)$$

3b. If SORM is used the limit state function is approximated by a quadratic function at the design point. For a quadratic failure surface the integral (A2.2) can be calculated and the reliability index is defined by in (A2.1).

A2.3 Parallel- and Series Systems

Series Systems

If a structural system has more than one failure mode these failure modes can be considered as elements in a series system and the failure probability is equal to the unified probability content of the failure events, see figure A2.2

$$P_F = P(\cup_{i=1}^{k}\{g_i(\mathbf{x}) \leq 0\}) \qquad (A2.7)$$

where k is the number of failure modes.

Different upper and lower bounds on the failure probability can be calculated, see e.g. Madsen et al., 1986, but the problem can also be solved approximately by considering the complementary problem, i.e. a parallel system

$$P_F \approx 1 - P(\cap_{i=1}^{k}\{g_i(\mathbf{x}) > 0\}) \qquad (A2.8)$$

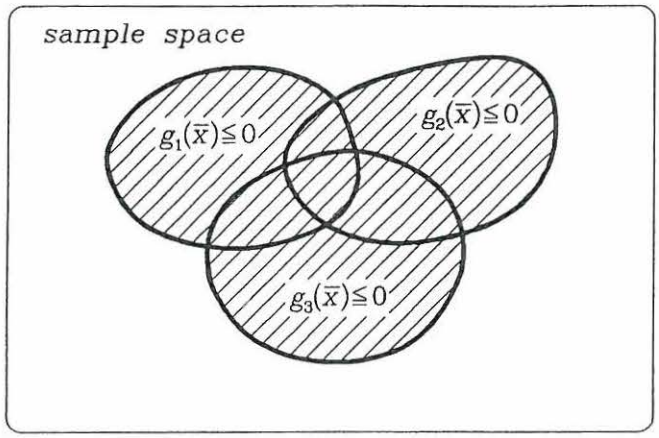

Figure A2.2 Probability content of a series system of events.

Parallel Systems
If a number of local failure modes acting together will cause failure of the whole system then the local failure modes can be considered as elements in a parallel system. The probability of system failure is equal to the common probability content of the local failure events, see figure A2.3

$$P_F = P(\cap_{i=1}^{k}\{g_i(\mathbf{x}) \leq 0\}) \qquad (A2.9)$$

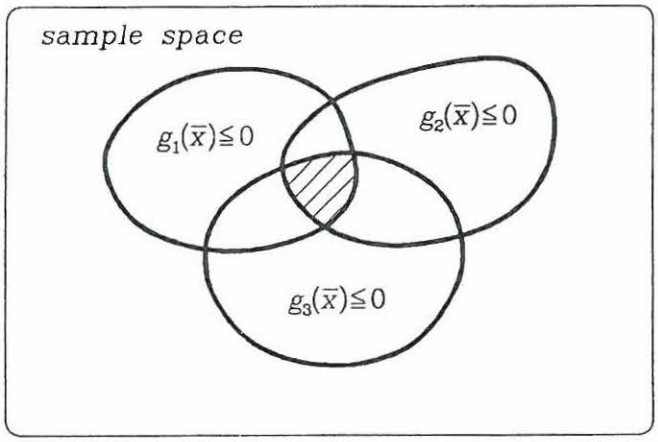

Figure A2.3 Probability content of a parallel system of events.

For parallel systems upper and lower bounds are available, see e.g. Thoft-Christensen and Murotsu, 1986. Using FORM and assuming that origo is not included in the failure set, the joint design point in the standard normal space is defined as the point closest to origo where all $g_i(\mathbf{u}) \leq 0$ ($\mathbf{u}^*$ in figure A2.4). Those elements for which

$g_i(\mathbf{u}) = 0$ at the joint design point are denoted active (elements no. 1 and 2 in figure A2.4) and those elements for which $g_i(\mathbf{u}) < 0$ at the joint design point are denoted inactive (element no. 3 in figure A2.4). To include the inactive elements in the calculations, consecutive joint design points are found for each inactive element under the restriction that for element no. i $g_i(\mathbf{u}) = 0$ and $g_j(\mathbf{u}) \leq 0$, $i \neq j$ ($\mathbf{u}_3^*$ in figure A2.4).

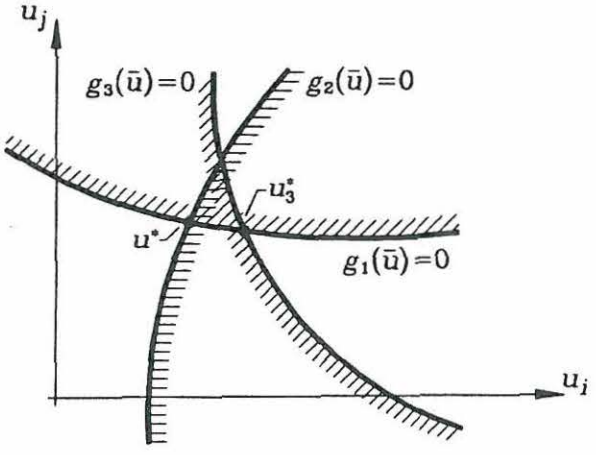

Figure A2.4 Parallel system with active and inactive elements.

If origo is included in the failure set, i.e. $g_i(\mathbf{0}) \leq 0$ for all elements, then individual design points are found for each active element defining active elements as the elements being part of the boundary of the failure set. In this case inactive elements will not influence the result and they are not included.

The probability can be calculated approximately using the k-dimensional standard normal distribution Φ_k

$$P_F \approx \Phi_k(-\overline{\beta^{FORM}}; R) \qquad (A2.10)$$

where $\overline{\beta^{FORM}}$ contains the reliability indices for the individual failure modes and the matrix $\mathbf{R}$ contains the correlation coefficients ρ_{ij} for the failure modes. The correlation coefficients ρ_{ij} are calculated using the unit vectors defined as

$$\alpha_i = -\frac{\nabla g_i(\mathbf{u}^*)}{|\nabla g_i(\mathbf{u}^*)|} \qquad (A2.11)$$

where $\mathbf{u}^*$ is the vector from the origin (= $E[\mathbf{U}]$) to the actual (joint) design point.

$$\rho_{ij} = \alpha_i{}^T \alpha_j \qquad (A2.12)$$

Further approximations can be made by not including the inactive elements in the calculations or by using individual design points for all elements.

In many real-life structural systems a combination of series and parallel systems would be necessary to model all the failure modes.

A2.4 Sensitivity Factors

Sensitivity factors of the reliability index are calculated in the programs PROBAN-2 and PARLSENSI and they are used in the optimization program PRODIM2. Considering a single element and using FORM, the sensitivity factor of the reliability index with regard to a certain parameter θ can be calculated as (see Madsen, 1988)

$$\frac{\partial \beta}{\partial \theta} \approx \frac{\partial \beta^{FORM}}{\partial \theta} = \frac{\frac{\partial}{\partial \theta} g(\mathbf{u}^*; \theta)}{\mid \nabla g(\mathbf{u}^*; \theta) \mid} \qquad (A2.13)$$

where θ is a deterministic variable or a statistical parameter of a stochastic variable.

For series systems and parallel systems several asymptotic methods are available for the calculation of sensitivity factors. In Madsen, 1988, an exact method for the calculation of $\frac{\partial \beta_S^{FORM}}{\partial \theta}$ for parallel systems is described including the effect of inactive components. The method can also be used for series systems considering the complementary problem, i.e. a parallel system.

A2.5 References

Madsen, H.O. (1988), *Sensitivity Factors for Parallel Systems*, Technical Note, Danish Engineering Academy, Denmark.

Madsen, H.O.; S. Krenk; N.C. Lind (1986), *Methods of Structural Safety*, Prentice-Hall.

Thoft-Christensen, Palle; Michael J. Baker (1982), *Structural Reliability Theory and Its Applications*, Springer-Verlag.

Thoft-Christensen, Palle; Yoshisada Murotsu (1986), *Application of Structural Systems Reliability Theory*, Springer-Verlag.

APPENDIX 3
INPUT TO PRODIM2

In this appendix the input to PRODIM2 is described and an example is given.

A3.1 Description of input

The input to PRODIM2 is given in a file whose default name is PROD.DAT. The input file is described line by line.

TITLE

In the first line a description of the actual problem is given.

INCBRAN INCELEM INACTV

INCBRAN — Parameter indicating which branches are used for estimating the failure and repair probability.
= 0 : All branches are used.
= 1 : Only the branch corresponding to no repair is used.
= 2 : Only branches with max one repair are used.

INCELEM — Parameter indicating which elements are included in parallel systems.
= 0 : All elements are included.
= 1 : No-failure elements are excluded.

INACTV — Parameter indicating whether inactive elements are linearized or not.
= 0 : Inactive elements are not included.
= 1 : Inactive elements are included.

TL BETAM RATE

TL — Lifetime of the structure.

BETAM — Minimum reliability index $\beta^{\min}$.

RATE — Real rate of interest.

TMIN TMAX NINSP

TMIN — Minimum inspection interval.

TMAX — Maximum inspection interval.

NINSP — Number of inspections.

MINSP

Number of inspections already performed.

LINSP(i) TINSP(i) i=1,MINSP (only if MINSP>0)

LINSP(i)	Result of inspection no. i. = 0 : No repair at the time TINSP(i). = 1 : Repair at the time TINSP(i).
TINSP(i)	Time at which inspection no. i was performed

CI0 CR0 CF0

CI0	Cost of one inspection.
CR0	Cost of one repair.
CF0	Cost of failure.

TDISTT(1)

Distribution of modelling uncertainty for stress contribution corresponding to water pressure on the ship side.

TDISTT(2)

Distribution of modelling uncertainty for stress contribution corresponding to the hull moment.

TDISTT(3)

Distribution of the yield stress (N/mm^2).

TDISTT(4)

Distribution of wave crest/trough (m).

TDISTT(5)

Distribution of hull moment (Nm).

TDISTT(6)

Distribution of modelling uncertainty for the actual longitudinal thickness (used in the repair criterion).

TDISTT(7)

Distribution of the corrosion starting time (years).

TDISTT(8)

Distribution of corrosion parameter A (A in μm).

TDISTT(9)

Distribution of corrosion parameter B.

The distributions are given as

N D P1 P2 P3

N	Number of the variable described (N = 1,9).
D	Number of distribution type.
D = 0	: fixed value (= $P1$)
D = 1	: normal distribution ($P1 = \mu, P2 = \sigma$)
D = 2	: Gumbel distribution ($P1 = \mu, P2 = \sigma$)
D = 3	: lognormal distribution ($P1 = \mu, P2 = \sigma, P3$ = lower bound)
D = -3	: lognormal distribution ($P1 = \beta, P2 = \alpha, P3$ = lower bound)
D = 4	: exponential distribution ($P1 = \sigma, P2$ = lower bound)
D = 5	: Weibull distribution ($P1 = \mu, P2 = \sigma, P3$ = lower bound)

DETVAR(1)

Deterministic value of the level above bottom (m).

DETVAR(2)

Deterministic value of the distance between longitudinals (m).

DETVAR(3)

Deterministic value of the panel thickness (mm).

DETVAR(4)

Deterministic value of the height of the longitudinal (mm).

DETVAR(5)

Deterministic value of the thickness of the longitudinal (mm).

DETVAR(6)

Deterministic value of the critical longitudinal thickness (mm).

EPSM MAXIT MAXLIN IPRINT PRINB IOPTME IFAIL

EPSM	Accuracy used in optimization algorithm.
MAXIT	Max number of iterations (in NLPQL). Max number of function calls (=MAXFUN in VMCWD).
MAXLIN	Max number of iterations in line search (=MAXFUN in NLPQL). Max number of function calls in a line search (in VMCWD).
IPRINT	Specification of output level. = 0 : No output from NLPQL/VMCWD and only final output from PRODIM2. = 1 : Only a final convergence analysis from NLPQL/VMCWD and final output from PRODIM2. = 2 : More detailed information.

= 3 : Detailed information.

IPRINB — Specification of calculations to be made.
= 0 : Optimization is performed, no beta as a function of time is determined.
= 1 : Optimization is performed, beta as a function of time is determined at the end of the optimization.
= 2 : Only beta as a function of time is determined.
= 3 : Only objective function is determined without any optimization.
= 4 : Beta as a function of time and objective function are determined without any optimization.

IOPTME — Specification of optimization method.
= 1 : NLPQL.
= 2 : VMCWD.

IFAIL — Only used in VMCWD.
= 0 : Gradients are checked (IPRINB = 0 or 1 is ignored).
= 1 : Optimization is performed

TCOMM

TCOMM — In order to be able to specify fixed values and start values it is possible to add a number of command lines to the lines specified above. The commands can be mixed and repeated but the first command word in each line has to be enclosed by ' '. PRODIM2 stops reading the input file when TCOMM = 'STOP'. The following commands can be used.

'TFIXED' IF TF — Inspection no. IF has to be performed at the time TF (T_{IF} = TF).

'IFIXED' IF T1...TIF — The first IF inspection intervals are fixed (t_1=T1,...,t_{IF} = TIF).

'TSTART' TS1...TSn — Initially the inspection times are equal to TS1,...,TSn (T_1 = TS1,...,T_n = TSn, n is the number of inspections).

'ISTART' TS1...TSn — Initially the inspection time intervals are equal to TS1,..., TSn (t_1 = TS1,...,t_n = TSn, n is the number of inspections).

'UMULT' NMULT — Only used in NLPQL.
Initially NMULT estimates of the Lagrangian multipliers are available. The remaining multipliers are assumed initially to be zero. The multipliers associated with the constraints are ordered in the following way:
1. Multipliers corresponding to equality constraints (here

equal to specified inspection times).
2. Multipliers corresponding to inequality constraints (here first the reliability constraint $\beta(T) \geq \beta^{\min}$, then $t^{\min} \leq T - \sum_{i=1}^{n} t_i$ and finally $T - \sum_{i=1}^{n} t_i \leq t^{\max}$).
3. Multipliers corresponding to the simple bounds (first the lower bounds and then the upper bounds).
After the line with 'UMULT' the following NMULT lines have to be specified:

IMULT(i) UMULT(i) (i = 1,NMULT)
IMULT(i) is the no. of the i'th multiplier. UMULT(i) is the initial estimate of multiplier no. IMULT(i).

'STOP' Input reading is stopped.

A3.2 Example of input file

```
Longitudinal no. 1, z = 1.8 m.
0 0 1                              INCBRAN INCELEM INACTV
20. 3. 0.04                        TL BETAM RATE
1. 19. 2                           TMIN TMAX NINSP
0                                  MINSP
1.  10. 100.                       CIN0 CR0 CF0
3 1.0 0.1 0.0001                   TDISTT(1)
3 1.0 0.1 0.0001                   TDISTT(2)
3 353. 35. 280.                    TDISTT(3)
5 .335 .372 0.                     TDISTT(4)
5 2.746D7 2.829D7 0.               TDISTT(5)
3 1.0 0.1 0.0001                   TDISTT(6)
1 9. 0.9                           TDISTT(7)
1 200.  40.                        TDISTT(8)
1 1.1   0.1                        TDISTT(9)
1.80                               DETVAR(1)
0.76                               DETVAR(2)
14.0                               DETVAR(3)
340.                               DETVAR(4)
15.                                DETVAR(5)
13.                                DETVAR(6)
1.D-6 20 5 3 0 2 1                 EPSM MAXIT MAXLIN IPRINT IPRINB IOPTME IFAI
'STOP'
```

A3.3 References

PRODIM, User's Manual (1988), A.S. Veritas Research Report No. 88-2030, Høvik, Norway.

APPENDIX 4
PROGRAM FOR CALCULATION OF TRAFFIC LOAD IN EACH GIRDER

The Fortran-program used in chapter 4 to calculate the traffic load in each girder is shown below.

```
      PROGRAM GIRMOM
*
*  Calculation of girder moment using live load moment distribution (LLMD),
*  girder influence line and truck distribution across each lane (two lanes,
*  span=80' and girder spacing=6').
*
      REAL MG(0:52), MY(15), MB(52), MT(52)
      DIMENSION FT(52), GR(11,10), DFR(11), DFL(8), FG(0:52),
     2 A(52), B(0:30,10), V1(10), FB(52), C(52), SD(15), FMTOT(5,300)
      PARAMETER (YY=5583., ST=1005.)
*
      OPEN (5,FILE='GIRMOM.DAT',STATUS='UNKNOWN')
      OPEN (3,FILE='GIRMOM.RES',STATUS='UNKNOWN')
      WRITE (3,'(//)')
      WRITE(3,*) 'A girder bridge with two lanes, span= 80 feet'
      WRITE(3,*) 'and 5 girders (spacing= 6 feet) is considered.'
      WRITE(3,*) 'The girder moment is calculated using the total'
      WRITE(3,*) 'live load distribution, girder influence line'
      WRITE(3,*) 'and truck distribution across each lane.'
      write(3,*)
      write(3,*) 'Total moment (kNm), mean = ',yy,'  st.dev. = ',st
      write(3,*)
*     write(3,*)'      Moment       f(m)           dF(m)           F(m)'
*     write(3,*)'      (kNm)'
*
*  Calculate distribution of total moment.
*
      EPS=SQRT(ALOG((ST/YY)**2+1))
      XI= ALOG(YY)-0.5*EPS**2
      FMM=0.0
      do 10 I=1,52
        MT(I)=250.*I
        FM=0.3989423/EPS/MT(I)*EXP(-.5*((ALOG(MT(I))-XI)/EPS)**2)
        DFM=FM*250.d0
        FMM=FMM+DFM
*       write(3,*)250*I,FM,DFM,FMM
        FT(I)=FMM
 10   continue
*
*  Read Truck Moment Ratio for each girder and probability (delta F) of
*  truck in the actual position (11 positions) for truck in right lane.
*
      DO 20 I=1,11
       READ(5,*) GR(I,1), GR(I,2), GR(I,3), GR(I,4), GR(I,5), DFR(I)
 20   CONTINUE
*
*  Read Truck Moment Ratio for each girder and probability (delta F) of
*  truck in the actual position (8 positions) for truck in left lane.
*
      DO 30 I=1,8
       READ(5,*) GR(I,6), GR(I,7), GR(I,8), GR(I,9), GR(I,10), DFL(I)
```

```
 30   CONTINUE
*
*  Calculations for truck in right or left lane.
*
      DO 200 L=1,10
       DO 32 I=1,30
        B(I,L)=0
32     CONTINUE
       DO 150 I=1,11
*
*  Calculation of moment values for girder no. L and truck position no. I.
*
        K=1
        FG(0)=0
        MG(0)=0
        DO 50 J=1,52
         MG(J)= GR(I,L)*MT(J)
         IF (L.GT.5) GOTO 35
         FG(J)= DFR(I)*FT(J)
         GOTO 40
 35      IF (I.GT.8) GOTO 40
         FG(J)= DFL(I)*FT(J)
*
*  Moment distribution values for moments equal to 250, 500, 750 kNm etc.
*
 40      IF (MG(J).LT.250*K) GOTO 50
         A(K)= FG(J-1)+(FG(J)-FG(J-1))*(250*K-MG(J-1))/(MG(J)-MG(J-1))
         K=K+1
 50     CONTINUE
        IF (K.GT.30) GOTO 100
        DO 90 J=K,30
         A(J)=FG(52)
 90     CONTINUE
*
*  The moment distributions for different truck positions are summed for
*  girder no. L.
*
100     DO 140 K=1,30
         IF (L.GT.5) GOTO 130
         B(K,L)=A(K)+B(K,L)
         GOTO 140
130      IF (I.GT.8) GOTO 140
         B(K,L)= A(K)+B(K,L)
140     CONTINUE
150    CONTINUE
200   CONTINUE
*
*  Calculation of mean and standard deviation for moment distribution for
*  each girder.
*
      DO 250 L=1,10
       B(0,L)=0
       MY(L)=0
       V1(L)=0
       DO 220 K=1,30
        MY(L)= 250*K*(B(K,L)-B(K-1,L))+MY(L)
        V1(L)= (250*K)**2*(B(K,L)-B(K-1,L))+V1(L)
220    CONTINUE
       SD(L)= SQRT(V1(L)-MY(L)**2)
250   CONTINUE
*
*   Output for trucks in right lane or left lane.
*
      WRITE (3,'(//)')
      WRITE(3,*)'************************************************************
     2******'
      WRITE(3,*) 'INPUT'
      WRITE (3,'(/)')
      WRITE(3,*)'Truck Moment Ratio and probability of truck in the actu
     2al position.'
      WRITE (3,'(/)')
      WRITE(3,'(10X,A,20X,A)') 'Right lane', 'Left lane'
```

```
      WRITE(3,*) ' G1   G2   G3   G4   G5   DF     G1   G2   G3   G4
     2   G5   DF  '
      DO 256 I=1,8
      WRITE(3,'(6F5.2,2X,6F5.2)') GR(I,1),GR(I,2),GR(I,3),GR(I,4),GR(I,5
     2),DFR(I),GR(I,6),GR(I,7),GR(I,8),GR(I,9),GR(I,10),DFL(I)
256   CONTINUE
      DO 257 I=9,11
      WRITE(3,'(6F5.2,2X,6F5.2)') GR(I,1),GR(I,2),GR(I,3),GR(I,4),GR(I,5
     2),DFR(I)
257   CONTINUE
      WRITE (3,'(//)')
      WRITE(3,*)'*************************************************
     2******'
      WRITE(3,*) 'OUTPUT'
      WRITE (3,'(/)')
      WRITE(3,*)'Moment distribution for each girder (incl. dynamic load
     2).'
      WRITE (3,'(/)')
      WRITE(3,*)'TRUCK IN RIGHT LANE'
      WRITE(3,*)' M(kNm)    F(MG1)     F(MG2)     F(MG3)     F(MG4)     F(MG5
     2)'
      DO 260 I=1,30
       WRITE(3,'(2X, I5.2, 5F10.5)') I*250, B(I,1), B(I,2), B(I,3),
     2 B(I,4), B(I,5)
260   CONTINUE
      WRITE (3,'(///)')
      WRITE(3,*)'TRUCK IN LEFT LANE'
      WRITE(3,*)' M(kNm)    F(MG1)     F(MG2)     F(MG3)     F(MG4)     F(MG5
     2)'
      DO 270 I=1,30
       WRITE (3,'(2X, I5.2, 5F10.5)') I*250, B(I,6), B(I,7), B(I,8),
     2 B(I,9), B(I,10)
270   CONTINUE
*
*  Calculations for trucks in both lanes: Moment distribution incl. dynamic
*  load for each girder.
*
      DO 850 L=1,5
       DO 300 I=1,30
        B(I,L)=0
300    CONTINUE
       K=1
       DO 800 J=1,11
        DO 750 I=1,8
         DFB= DFR(J)*DFL(I)
         GB= GR(J,L)+GR(I,L+5)
*
*  Calculation of moment values for girder no. L and truck positions J and I.
*
         M=1
         MB(0)=0
         FB(0)=0
         DO 400 N=1,52
          MB(N)= GB*MT(N)
          FB(N)= DFB*FT(N)
*
* Moment distribution values for moments equal to 250, 500, 750 kNm etc.
*
          IF (MB(N).LT.250*M) GOTO 400
          C(M)= FB(N-1)+(FB(N)-FB(N-1))*(250*M-MB(N-1))/(MB(N)-MB(N-1))
          M=M+1
400      CONTINUE
         IF (M.GT.30) GOTO 470
         DO 450 N=M,30
          C(N)=FB(52)
450      CONTINUE
*
*  The moment distributions for different truck positions are summed for
*  girder no. L.
```

```
*
470       DO 500 N=1,30
           B(N,L)= B(N,L)+C(N)
500       CONTINUE
          K=K+1
          IF (K.GT.88) GOTO 850
750      CONTINUE
800     CONTINUE
850    CONTINUE
*
*  Calculation of mean and standard deviation for moment distribution for
*  each girder.
*
       DO 900 L=1,5
        MY(L+10)= 0
        V1(L)= 0
        DO 880 K=1,30
         MY(L+10)= 250*K*(B(K,L)-B(K-1,L))+MY(L+10)
         V1(L)= (250*K)**2*(B(K,L)-B(K-1,L))+V1(L)
880     CONTINUE
        SD(L+10)= SQRT(V1(L)-MY(L+10)**2)
900    CONTINUE
*
*  Output for trucks in both lanes
*
       WRITE (3,'(///)')
       WRITE(3,*)'TRUCK IN BOTH LANES'
       WRITE(3,*)' M(kNm)    F(MG1)     F(MG2)     F(MG3)     F(MG4)     F(MG5
      2)'
       DO 910 I=1,30
        WRITE(3,'(2X, I5.2, 5F10.5)') I*250, B(I,1), B(I,2), B(I,3),
      2 B(I,4), B(I,5)
910    CONTINUE
       WRITE (3,'(///)')
       WRITE(3,*)'************************************************************
      2******'
*
*  Output of means and standard deviations.
*
       WRITE(3,*)'Mean and standard deviation for moment distributions'
       WRITE(3,*)'of each girder.'
       WRITE (3,'(/)')
       WRITE(3,*)'TRUCK IN RIGHT LANE'
       WRITE(3,*)'                G1         G2         G3         G4
      2       G5'
       WRITE(3,'(1X,A,4X,5F10.4)') 'Mean', MY(1), MY(2), MY(3), MY(4),
      2 MY(5)
       WRITE(3,'(1X,A,1X,5F10.4)') 'St.dev.', SD(1), SD(2), SD(3), SD(4),
      2 SD(5)
       WRITE (3,'(/)')
       WRITE(3,*)'TRUCK IN LEFT LANE'
       WRITE(3,*)'                G1         G2         G3         G4
      2       G5'
       WRITE(3,'(1X,A,4X,5F10.4)') 'Mean', MY(6), MY(7), MY(8), MY(9),
      2 MY(10)
       WRITE(3,'(1X,A,1X,5F10.4)') 'St.dev.', SD(6), SD(7), SD(8), SD(9),
      2 SD(10)
       WRITE (3,'(/)')
       WRITE(3,*)'TRUCK IN BOTH LANES'
       WRITE(3,*)'                G1         G2         G3         G4
      2       G5'
       WRITE(3,'(1X,A,4X,5F10.4)') 'Mean', MY(11), MY(12), MY(13),
      2 MY(14), MY(15)
       WRITE(3,'(1X,A,1X,5F10.4)') 'St.dev.', SD(11), SD(12), SD(13),
```

```
     2 SD(14), SD(15)
      WRITE(3,*)'************************************************************
     2******'
      WRITE (3,'(///)')
      WRITE(3,*)'Mean and standard deviation for shear distributions'
      WRITE(3,*)'of each girder.'
      WRITE (3,'(/)')
      WRITE(3,*)'TRUCK IN RIGHT LANE'
      WRITE(3,*)'                G1        G2        G3        G4
     2       G5'
      WRITE(3,'(1X,A,4X,5F10.4)') 'Mean', MY(1)/6.1, MY(2)/6.1,
     2 MY(3)/6.1, MY(4)/6.1, MY(5)/6.1
      WRITE(3,'(1X,A,1X,5F10.4)') 'St.dev.', SD(1)/6.1, SD(2)/6.1,
     2 SD(3)/6.1, SD(4)/6.1, SD(5)/6.1
      WRITE (3,'(/)')
      WRITE(3,*)'TRUCK IN LEFT LANE'
      WRITE(3,*)'                G1        G2        G3        G4
     2       G5'
      WRITE(3,'(1X,A,4X,5F10.4)') 'Mean', MY(6)/6.1, MY(7)/6.1,
     2 MY(8)/6.1, MY(9)/6.1, MY(10)/6.1
      WRITE(3,'(1X,A,1X,5F10.4)') 'St.dev.', SD(6)/6.1, SD(7)/6.1,
     2 SD(8)/6.1, SD(9)/6.1, SD(10)/6.1
      WRITE (3,'(/)')
      WRITE(3,*)'TRUCK IN BOTH LANES'
      WRITE(3,*)'                G1        G2        G3        G4
     2       G5'
      WRITE(3,'(1X,A,4X,5F10.4)') 'Mean', MY(11)/6.1, MY(12)/6.1,
     2 MY(13)/6.1, MY(14)/6.1, MY(15)/6.1
      WRITE(3,'(1X,A,1X,5F10.4)') 'St.dev.', SD(11)/6.1, SD(12)/6.1,
     2 SD(13)/6.1, SD(14)/6.1, SD(15)/6.1
      WRITE(3,*)'************************************************************
     2******'
*
*  Calculating of total density function for each girder
*
      DO 650 I=1,5
        EPSR=SQRT(ALOG((SD(I)/MY(I))**2+1))
        XIR= ALOG(MY(I))-0.5*EPSR**2
        EPSL=SQRT(ALOG((SD(5+I)/MY(5+I))**2+1))
        XIL= ALOG(MY(5+I))-0.5*EPSL**2
        EPSRL=SQRT(ALOG((SD(10+I)/MY(10+I))**2+1))
        XIRL= ALOG(MY(10+I))-0.5*EPSRL**2
        DO 600 J=1,300
          X=10.*J
          FMR=0.3989423/EPSR/X*EXP(-.5*((ALOG(X)-XIR)/EPSR)**2)
          FML=0.3989423/EPSL/X*EXP(-.5*((ALOG(X)-XIL)/EPSL)**2)
          FMRL=0.3989423/EPSRL/X*EXP(-.5*((ALOG(X)-XIRL)/EPSRL)**2)
          FMTOT(I,J)=0.66*FMR+0.33*FML+0.01*FMRL
 600    CONTINUE
 650  CONTINUE
*     WRITE(3,'(///)')
*     WRITE(3,*)'TOTAL MOMENT'
*     WRITE(3,*)' M(kNm)    f(MG1)     f(MG2)     f(MG3)     f(MG4)     f(MG5
*    2)'
*     DO 660 I=1,300
*       WRITE(3,'(2X, I5.2, 5F10.5)') I*10, FMTOT(1,I),FMTOT(2,I),
*    2  FMTOT(3,I),FMTOT(4,I),FMTOT(5,I)
*660  CONTINUE

      STOP
      END
```

STRUCTURAL RELIABILITY THEORY SERIES

PAPER NO. 80: A. M. Sommer, A. S. Nowak & P. Thoft-Christensen: *Inspection Strategies for Highway Steel Girder Bridges.* ISSN 0902-7513 R9102.

PAPER NO. 81: S. R. K. Nielsen: *Probability of Failure by Integral Equation Methods.* ISSN 0902-7513 R9037.

PAPER NO. 82: I. Enevoldsen & J. D. Sørensen: *Reliability-Based Optimization of Series Systems of Parallel Systems.* ISSN 0902-7513 R9039.

PAPER NO. 83: S. R. K. Nielsen & A. S. Cakmak: *Evaluation of Maximum Softening as a Damage Indicator for Reinforced Concrete under Seismic Excitation.* ISSN 0902-7513 R9048.

PAPER NO. 84: G. B. Pirzada: *Estimation of the Reliability of Plastic Slabs.* Ph.D.-Thesis. ISSN 0902-7513 R9049.

PAPER NO. 85: A. Johansen & P. Thoft-Christensen: *Estimation of the Reliability of Existing Structures - An Overview.* ISSN 0902-7513 R9140.

PAPER NO. 86: J. Almlund: *Life Cycle Model for Offshore Installations for Use in Prospect Evaluation.* Ph.D.-Thesis. ISSN 0902-7513 R9139.

PAPER NO. 87: I. Enevoldsen: *Reliability-Based Structural Optimization.* Ph.D.-Thesis. ISSN 0902-7513 R9106.

PAPER NO. 88: J. D. Sørensen & M. H. Faber: *Optimal Inspection and Repair Strategies.* ISSN 0902-7513 R9143.

PAPER NO. 89: M. Delmar & J. D. Sørensen: *Probabilistic Analysis in Economic Decision Making.* ISSN 0902-7513 R9153.

PAPER NO. 90: I. B. Kroon, M. H. Faber & J. D. Sørensen: *Decision Theory in Structural Engineering.* ISSN 0902-7513 R9218.

PAPER NO. 91: K. J. Mørk & S. R. K. Nielsen: *Program for Stochastic Analysis of Plane Reinforced Concrete Frames under Seismic Excitation.* ISSN 0902-7513 R9129.

PAPER NO. 92: S. R. K. Nielsen, H. U. Köylüoğlu & A. Ş. Çakmak: *One and Two-Dimensional Maximum Softening Damage Indicators for Reinforced Concrete Structures under Seismic Excitation.* ISSN 0902-7513 R9211.

PAPER NO. 93: L. Thesbjerg: *Optimal Vibration Control of Civil Engineering Structures.* Ph.D.-Thesis. ISSN 0902-7513 R9214.

PAPER NO. 94: H. U. Köylüoğlu, S. R. K. Nielsen & A. Ş. Çakmak: *Response of Stochastically Loaded Bernoulli-Euler Beams with Randomly Varying Bending Stiffness.* ISSN 0902-7513 R9228.

PAPER NO. 96: M. H. Faber, J. D. Sørensen & I. B. Kroon: *Optimal Inspection Strategies for Offshore Structural Systems.* ISSN 0902-7513 R9240.

STRUCTURAL RELIABILITY THEORY SERIES

PAPER NO. 97: M. H. Faber, J. D. Sørensen, R. Rackwitz, P. Thoft-Christensen & P. Bryla: *Reliability Analysis of an Offshore Structure A Case Study - I.* ISSN 0902-7513 R9241.

PAPER NO. 98: J. D. Sørensen, M. H. Faber, R. Rackwitz, P. Thoft-Christensen & G. Lebas: *Reliability Analysis of an Offshore Structure A Case Study - II .* ISSN 0902-7513 R9242.

PAPER NO. 99: K. J. Mørk: *Stochastic Response Analysis of 3D Reinforced Concrete Structures under Seismic Excitation.* ISSN 0902-7513 R9209.

PAPER NO. 100: P. Thoft-Christensen: *Risk-Based Optimization.* ISSN 0902-7513 R9219.

PAPER NO. 101: I. Enevoldsen: *Sensitivity Analysis of a Reliability-Based Optimal Solution.* ISSN 0902-7513 R9213.

PAPER NO. 102: I. Enevoldsen: *Reliability-Based Optimization as an Information Tool* ISSN 0902-7513 R9215.

PAPER NO. 103: A. M. Sommer: *Optimal Inspection and Maintenance Strategies for Structural Systems.* Ph.D.-Thesis. ISSN 0902-7513 R9309.

PAPER NO. 104: I. Enevoldsen, M. H. Faber, J. D. Sørensen: *Adaptive Response Surface Techniques in Reliability Estimation.* ISSN 0902-7513 R9243.

PAPER NO. 105: H. U. Köylüoğlu, A. Ş. Çakmak & S. R. K. Nielsen: *Linear Dynamic Analysis of SDOF Systems with Random Parameters Subject to Earthquake Excitations.* ISSN 0902-7513 R9244.

PAPER NO. 108: H. U. Köylüoğlu, S. R. K. Nielsen & R. Iwankiewicz: *Reliability of Non-Linear Oscillators Subject to Poisson Driven Impulses.* ISSN 0902-7513 R9235.

PAPER NO. 109: C. Pedersen & P. Thoft-Christensen: *Reliability Analysis of Prestressed Concrete Beams with Corroded Tendons.* ISSN 0902-7513 R9306.

PAPER NO. 113: J. D. Sørensen & I. Enevoldsen: *Sensitivity Weaknesses in Application of some Statistical Distribution in First Order Reliability Methods.* ISSN 0902-7513 R9302.

PAPER NO. 114: H. U. Köylüoğlu & S. R. K. Nielsen: *Stochastic Dynamics of Linear Structures with Random Stiffness Properties and Random Damping subject to Random Loading.* ISSN 0902-7513 R9308.

PAPER NO. 115: H. U. Köylüoğlu & S. R. K. Nielsen: *New Approximations for SORM Integrals.* ISSN 0902-7513 R9303.

Department of Building Technology and Structural Engineering
University of Aalborg, Sohngaardsholmsvej 57, DK 9000 Aalborg
Telephone: 45 98 15 85 22 Telefax: 45 98 14 82 43